BAW-1388, Rev. 1
July 1973

23,234

OCONEE 1
FUEL Ddensification REPORT

(Nonproprietary Version of BAW-1387)

— Revision 1 —

Babcock & Wilcox

DISCLAIMER

BAW 1388, Rev. 1

July 1973

OCONEE 1

FUEL Ddensification REPORT

— Revision 1 —

BABCOCK & WILCOX
Power Generation Group
Nuclear Power Generation Division
P.O. Box 1260
Lynchburg, Virginia 24505

Babcock & Wilcox
Power Generation Group
Nuclear Power Generation Division
Lynchburg, Virginia

Report BAW-1388, Rev. 1

July 1973

Oconee 1 Fuel Densification Report

Key Words: Fuel, Densification Effects

ABSTRACT

In July 1973, Babcock & Wilcox filed topical report BAW-10055 (Rev. 1), "Fuel Densification Report", which describes the methods to be used in analyzing fuel densification effects. The body of this report, with Appendix A, presents an analysis of effects on fuel for Oconee Nuclear Power Station, Unit 1, and supports the operation of Unit 1 at the rated power level of 2568 MWt. Appendix B answers the questions of the AEC Directorate of Licensing Regulatory Staff pursuant to their review of this report.

CONTENTS

List of Tables

Tables (Cont'd)

List of Figures

1. INTRODUCTION

This report documents the effects of hypothesized fuel densification for the Oconee 1 core as calculated in accordance with guidelines set forth in the AEC report of November 14, 1972. The application of these guidelines for the results presented in this report are discussed fully in revision 1 of topical report BAW-10055, "Fuel Densification Report."

The analysis of Oconee 1 is limited to an examination of the first fuel cycle. Although Babcock & Wilcox has no operating data on the fuel densification phenomenon, data to be released from pressurized water reactors (PWRs) now operating with prepressurized fuel are expected to allow relaxation of the current guidelines.

2. CONCLUSIONS

Based on the analysis performed for Oconee 1, which utilized the methods given in BAW-10055, Rev. 1 the following conclusions are made even if the fuel pellets should densify to 96.5% of theoretical density:

1. The cladding will not collapse because all B&W fuel rods are prepressurized.

2. The mechanical performance of B&W fuel rods will not be impaired.

3. The interim acceptance criteria for the emergency core cooling system (ECCS) will not be violated.

4. The reactor can be safely operated at the rated power level of 2568 MWt with only minor modifications to reactor protection system (RPS) setpoints. These modifications ensure that the thermal design criteria are not exceeded.

5. The modifications to the RPS are a reduction in the overpower trip setpoint, from 114 to 112% of rated power, and a minor reduction in allowable imbalance limits as shown in Figure 3.3-3.

3. RESULTS

3.1. Power Spike Model

The guidelines outlined in "Technical Report on Densification of Light Water Reactor Fuels," November 14, 1972, have been used to determine the maximum axial gap as a function of core height. The probability values (F_K) given in the same report (Table 4.2.A, column 4) have been used in calculating the power spike factor. This factor, as calculated in section 2 of BAW-10055, Rev. 1 is applicable to individual reactors. The maximum gap size versus axial position is shown in Figure 3.1-1, and the power spike factor versus axial position is shown in Figure 3.1-2. These figures also show the initial and final theoretical densities (TDI, TDF) used in the calculations. These data form the basis for the following analyses.

This section of the report covers four main topics: thermal analysis, nuclear analysis, safety analysis, and mechanical analysis. The thermal analysis section considers protection of the fuel melt and DNBR criteria. The nuclear analysis section considers thermal design criteria, imbalance trip limits, and core operational limits. The safety analysis section re-analyzes all postulated accidents analyzed in the Oconee FSAR assuming that densification occurs. The mechanical analysis section summarizes the input summary and results, cladding creep and collapse, cladding stresses, and fuel pellet irradiation swelling.

Figure 3.1-1. Maximum Gap Size Vs Axial Position

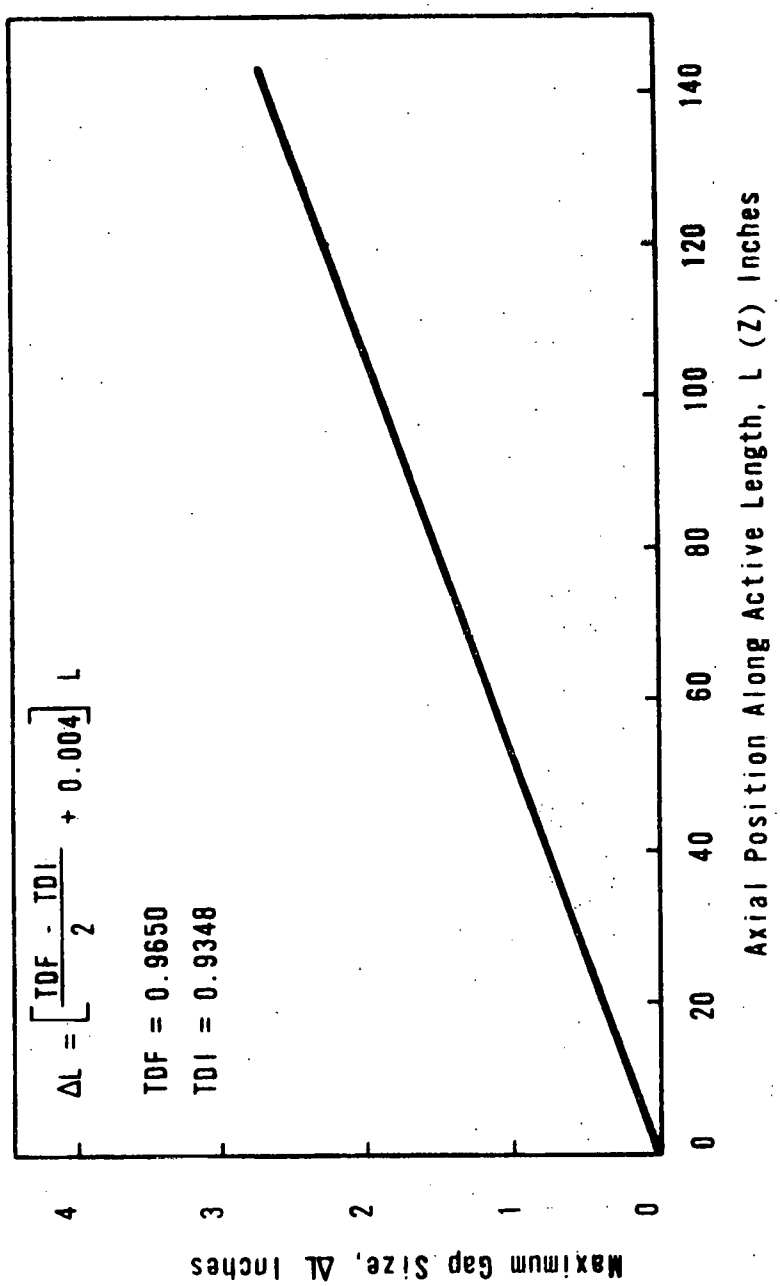

Figure 3.1-2. Power Spike Factor Vs Axial Position

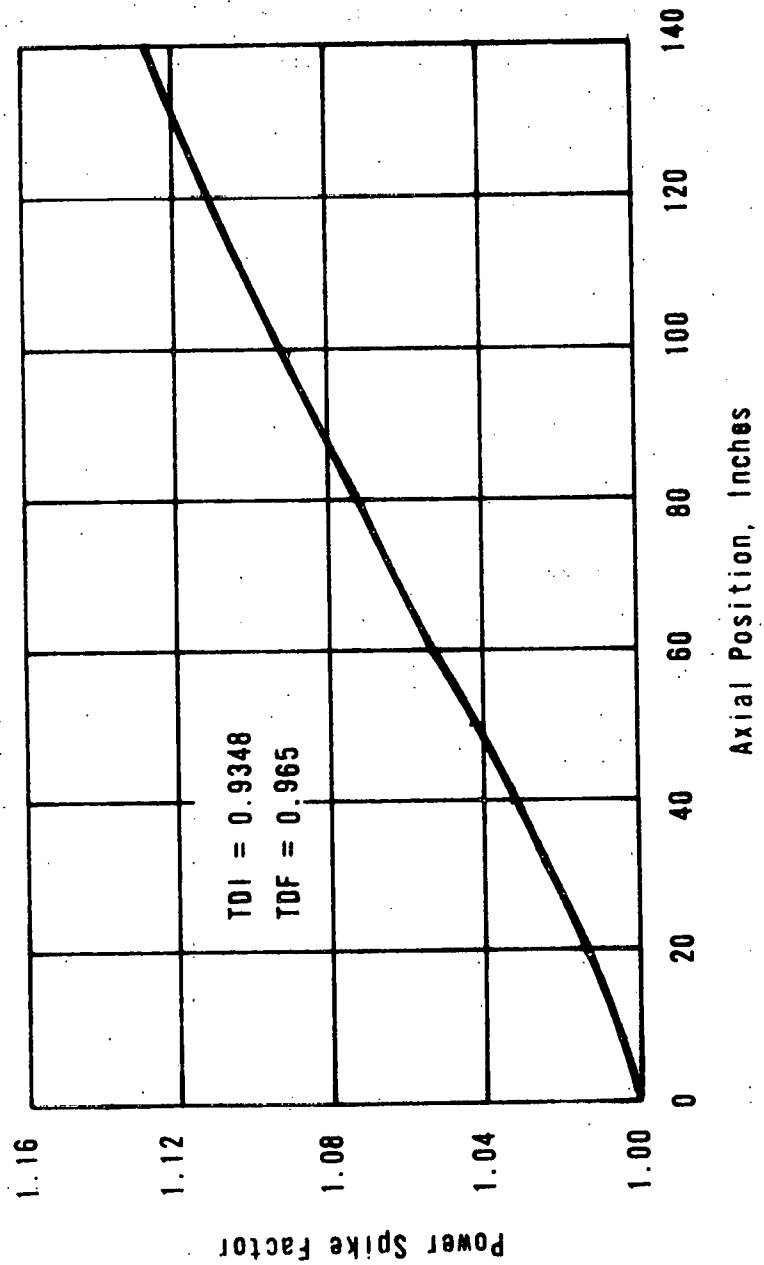

3.2. Thermal Analysis

3.2.1. Fuel Temperature Analysis

Utilizing the analysis established in BAW-10055, Rev 1., the fuel-to-cladding cold diametral gap after densification was calculated as 12.8 mils. This gap size and the TAFY fuel pin temperature and pressure code (BAW-10044) were used to perform a fuel temperature analysis. Average and maximum fuel temperatures for densified fuel at the beginning of life (BOL), at 100 days, and at the end of the first cycle of operation are compared in Tables 3.2-1 and 3.2-2 and in Figures 3.2-1 and 3.2-2. The gap heat transfer coefficients for these same times are compared in Figure 3.2-3.

3.2.2. DNBR Analysis

The thermal effects due to densification can be divided into two categories: (1) the result of the reduced stack height and (2) the combined result of the reduced stack height with the power spike superimposed. Thermal effects are then imposed on calculations of the minimum departure from nucleate boiling ratio (DNBR) used to set thermal design limits.

The reduced active length was calculated to be 141.8 inches, which represents a reduction of 2.17 inches from the nominal active length of 143.97 inches. The as-built information given in Appendix A was used in calculating this densified active length.

The axial flux shape that gave the maximum change in DNBR from the original design value was an outlet peak with a core offset of +11.8%. The spike magnitude and the maximum gap size used in the analysis are 1.125 and 2.62 inches. The results of the two effects are summarized in Table 3.2-3 in terms of percentage change in minimum hot channel DNBR and peaking margin.

3.2.3. Summary

This analysis assumes that densification and associated phenomena will affect the hot channel, which has the most limiting thermal-hydraulic characteristics in the core. In addition, the power spike is assumed to be located at the hot channel position that minimizes DNBR. The resultant 4.46% DNBR loss or 2.01% power peaking

margin reduction will be compensated so that the plant can function at rated power without violating the initial design criteria for DNBR and/or fuel melting. The allowable power shapes and the new offset limits are discussed in section 3.3.

Table 3.2-1. Fuel Temperature Comparison at Low Power Density

Density, % theor	Cold gap, mils	Time in life	kW/ft	Surface fuel temp, F	Avg fuel temp, F	Max fuel temp, F
96.5	12.8	BOL	5.6	904	1228	1584
96.5	12.8	End 100 days	5.6	920	1247	1605
96.5	12.8	End cycle 1	5.6	940	1271	1633

Table 3.2-2. Fuel Temperature Comparison at High Power Density

Density, % theor	Cold gap, mils	Time in life	kW/ft	Surface fuel temp, F	Avg fuel temp, F	Max fuel temp, F
96.5	12.8	BOL	17.6	1338	2741	4210
96.5	12.8	End 100 days	17.6	1362	2774	4242
96.5	12.8	End cycle 1	17.6	1389	2808	4274

Table 3.2-3. Effects of Fuel Densification on DNBR and Power Margin @ 114% 2568 MW(t)

	Densified active length			Densified active length and power spike		
Axial power shape	DNBR (W-3)	%Δ DNB	%Δ Margin	DNBR (W-3)	%Δ DNB	%Δ Margin
Outlet peak with +11.8% core offset	1.521	-1.62	-0.67	1.477	-4.46	-2.01

Figure 3.2-1. Maximum Fuel Temperature Vs Linear Heat Rate — Oconee 1

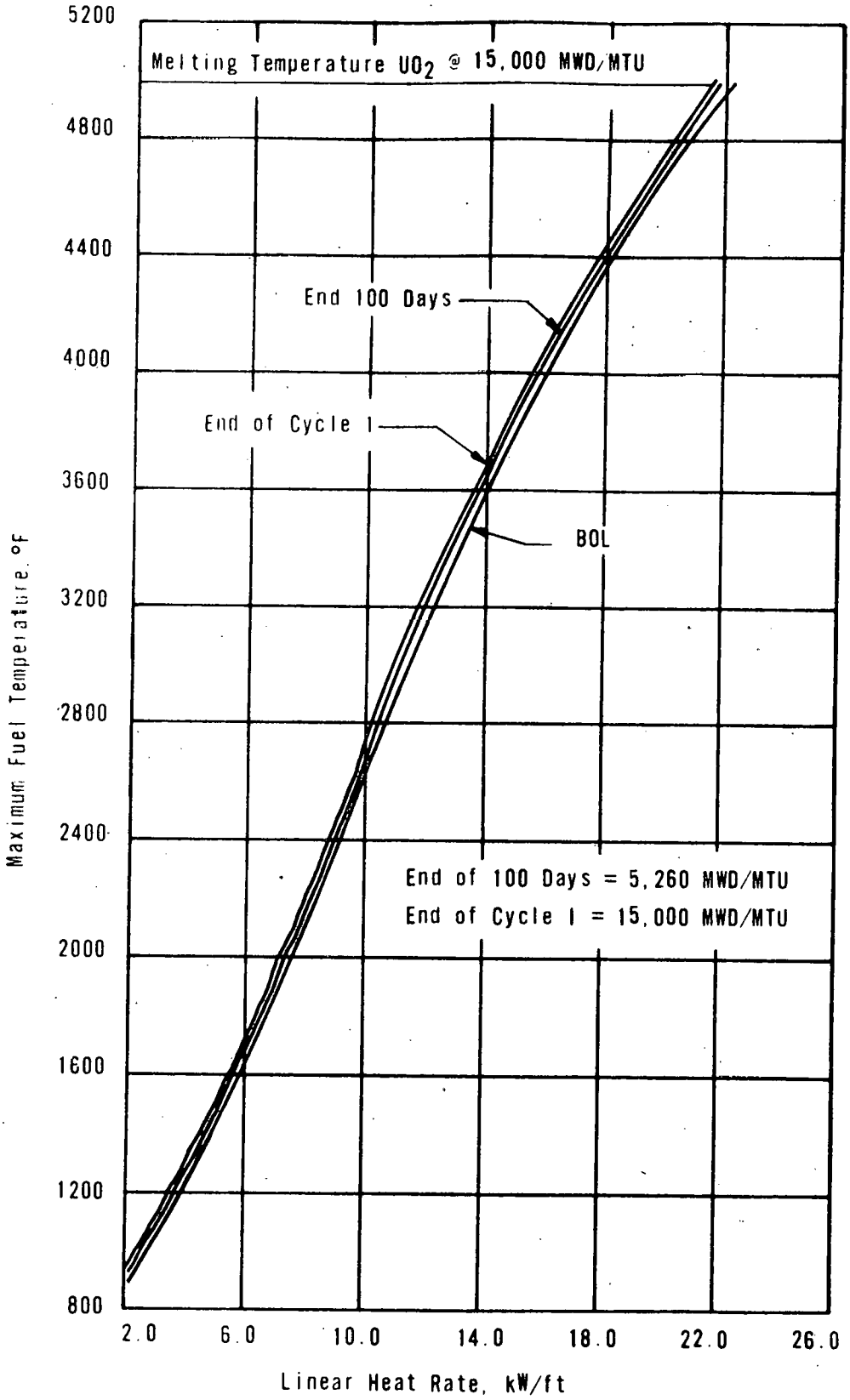

Figure 3.2-2. Average Fuel Temperature Vs Linear Heat Rate — Oconee 1

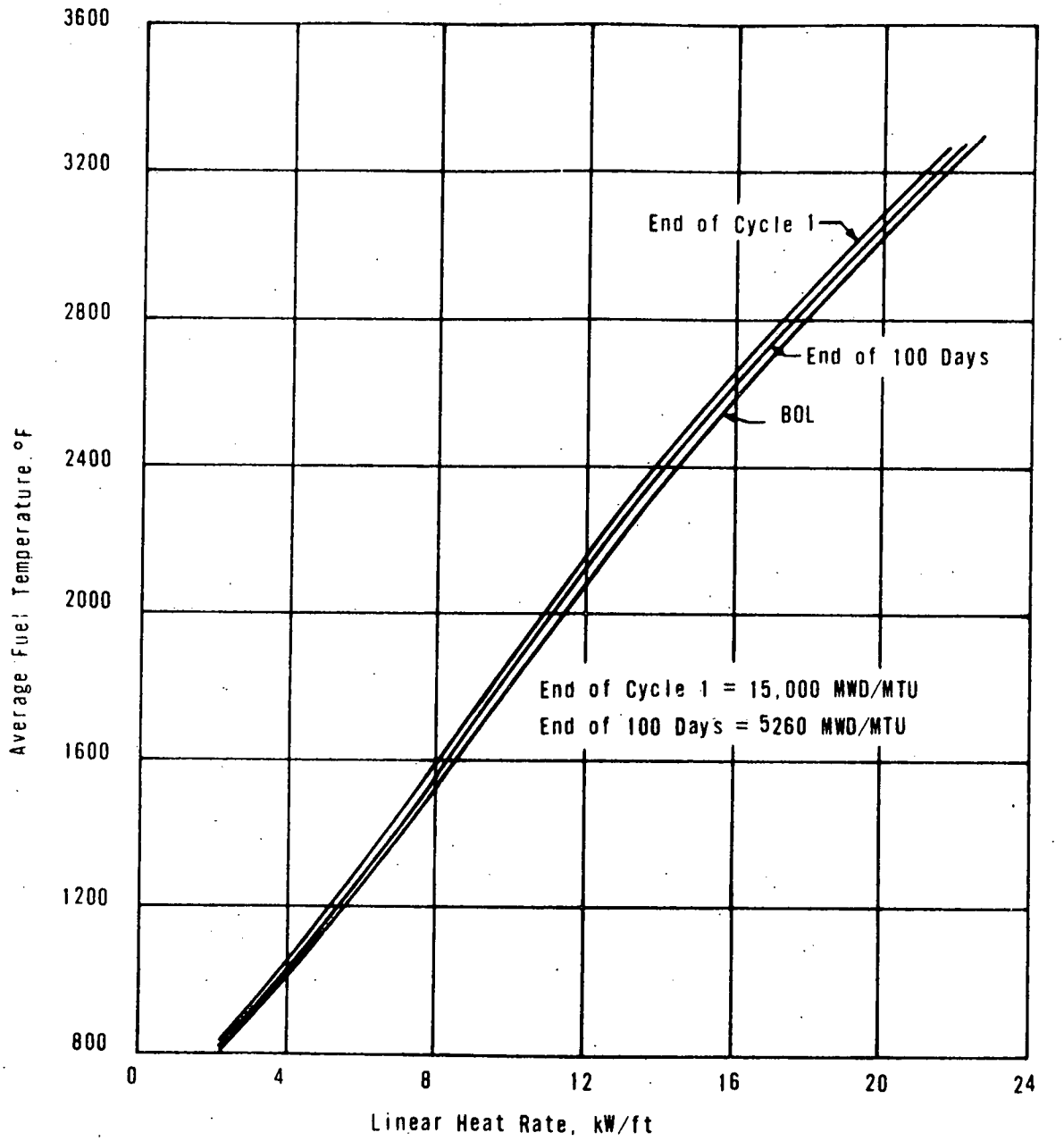

Figure 3.2-3 Gap Coefficient vs. Linear Heat Rate - Oconee 1

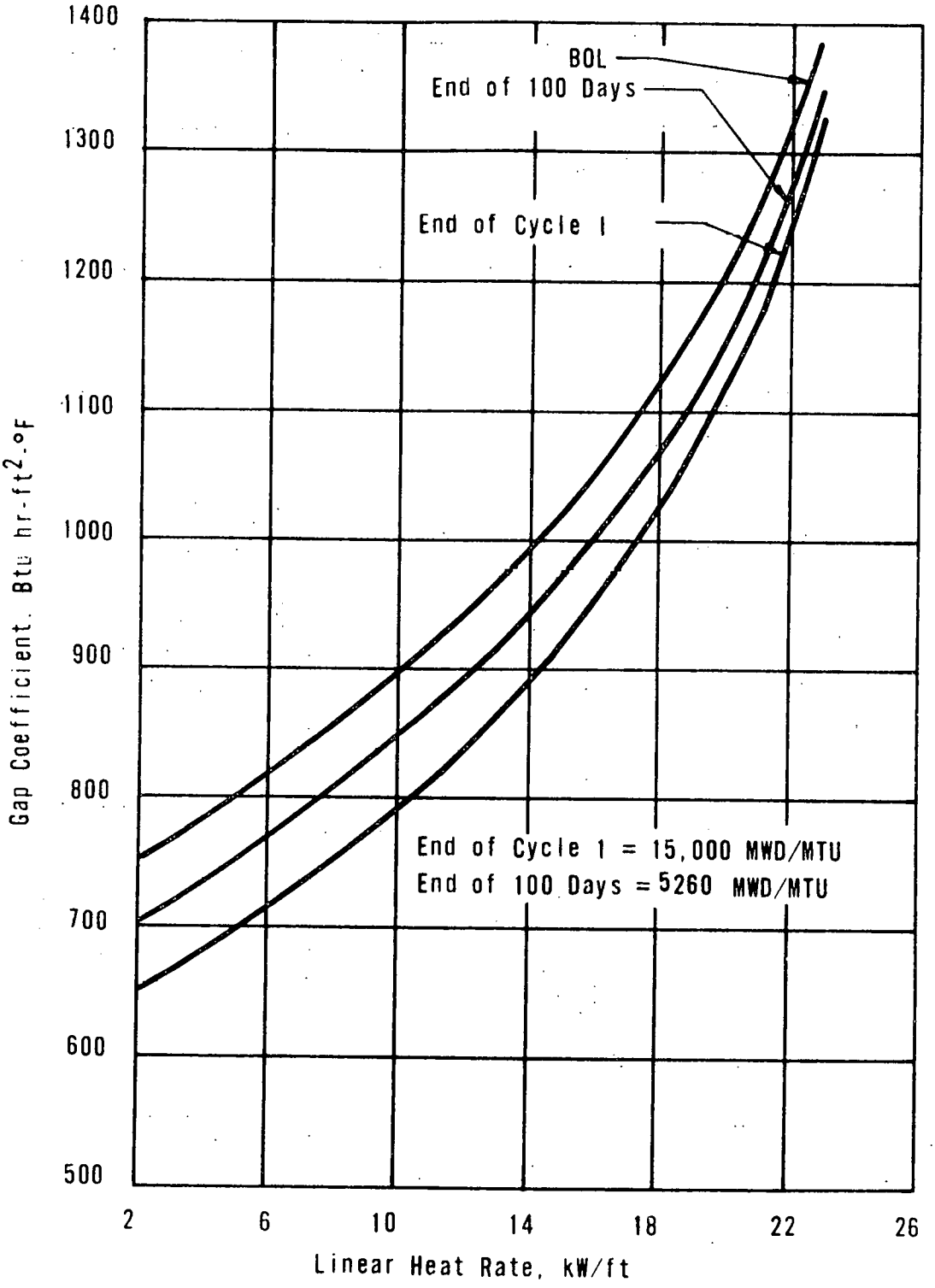

3.3. Nuclear Analysis

3.3.1. Reactor Protection System

The safe operation of a reactor core requires an extensive analysis of power distributions resulting from the various modes of plant operation. The primary considerations and results of this analysis are as follows:

1. Assurance that thermal criteria are not exceeded; i.e., specified minimum DNBRs and centerline fuel temperatures may not be violated.
2. Definition of imbalance limits to prevent adverse power peaks that would exceed the foregoing criteria.
3. Definition of core operational limits and recommended operating procedures to prevent unnecessary reactor trips.

The complete maneuvering study entails a combined nuclear-thermal analysis of the power distributions. This section describes the methods and criteria used in developing the RPS setpoints and in modifying the setpoints required to account for postulated densification effects.

3.3.2. Analysis of Power Distributions Before Densification

The three-dimensional PDQ07 code with thermal feedback effects is used to analyze power distributions. This analysis determines power distributions for all modes of reactor operation except accidents and other rapid transients. The design power transient (100-30% power and return to 100% at peak xenon) is analyzed throughout core life. The fuel cycle and transient analyses determine power distributions for normal equilibrium and transient conditions, respectively. The extremes of core operation, such as control rod bank insertion beyond normal limits and maloperation of axial power shaping rods, are also examined. The extreme control rod bank conditions define the limits for the imbalance protection system.

3.3.2.1. Correlation of Power Peaks to Thermal Design Criteria

The power peaks from PDQ cases are corrected for calculational uncertainty and are analyzed to determine the margin to the thermal criteria: centerline fuel melt and departure from nucleate boiling (DNB). The margin to centerline fuel melting is defined as

$$\text{Fuel melt margin} = \left(\frac{\text{Max allowable peak}}{\text{Max calculated peak}} - 1\right) 100\%.$$

The maximum allowable peak is defined as the pointwise power that yields centerline fuel melting:

$$\text{Max allowable peak} = \frac{22.2 \text{ kW/ft}}{5.656 \text{ kW/ft} \times 1.014 \times \text{FOP}}$$

where

22.2 kW/ft = fuel melt limit,

5.656 kW/ft = average heat rate at 2568 MWt,

1.014 = hot channel factor,

FOP = fraction of power.

The maximum calculated peak is the largest total peak from the PDQ power increased by a factor of 1.075 to account for calculational uncertainity.

The determination of DNB margin requires a more complex analysis. DNBR is a function of peak location, magnitude of the power peak component parts (radial and axial), and other core parameters. To arrive at true DNB conditions, each power distribution is analyzed explicitly. From the PDQ power distribution, the maximum calculated total peak is obtained and adjusted for uncertainty. The DNB margin is then defined as

$$\left(\frac{\text{Allowable total peak}}{\text{Max calculated total peak}} - 1\right) 100\%.$$

The basis for the allowable total peak is the reference design DNBR at design conditions, or a 1.30 DNBR associated with the protection system envelope, or a quality limit based on model applicability, whichever is most limiting.

3.3.2.2. Offset-Margin Relationship

Core offset, a measure of the axial power imbalance, is defined as the fraction of total core power in the top half of the core minus the fraction of total core power in the bottom half of the core:

$$\text{Offset} = \frac{\text{Power (top) - power (bottom)}}{\text{Power (top) + power (bottom)}}.$$

The relationship between hot channel power peaks (i.e., thermal margins) and core offset defines the protection system setpoints. Power imbalance is the primary signal to the protection system for flux shape protection. The maneuvering analysis defines the relationship between core imbalance and thermal margin.

Limiting offsets are determined to prevent the violation of thermal criteria for all operating conditions and power levels. To yield the imbalance trip envelope, the limiting offset values are corrected for potential instrumentation errors, imbalance detection bias, and calibration. The imbalance trip envelope defines the range of allowable operational imbalance and ensures that a 1.3 DNBR and/or the central fuel melting limit will not be exceeded. Figure 3.3-1 presents the trip setpoints based on these criteria. It is important to note that DNBR criteria define the positive imbalance slope, whereas centerline fuel melting is more limiting for the negative imbalance limits. The overpower trip setpoint shown in Figure 3.3-1 is controlling for overpower transients, whereas the solid horizontal line is the trip for loss of flow transients.

3.3.3. Analysis of Power Distributions With Densification Effects

Provision for possible fuel densification requires modification of the imbalance trip system for two reasons: (1) the fuel melt (kW/ft) criterion change, and (2) an additional power spike is included in the reactor power distributions. Since the power spike factor is a function of axial position, the appropriate power spike factor is used to increase each PDQ peak to account for potential densification.

The modified offset limits with fuel densification effects included are presented in Figure 3.3-2 and compared with the present limits. The primary differences between the two sets of calculated limits are as follows:

1. The DNBR loss of -4.46% results in a peaking margin loss of -2.01%

2. The central fuel melting limit changes from 22.2 kW/ft before densification to 21.8 kW/ft.*

3. A 2.21-inch decrease in fuel column length increases the nominal heat rate at 2568 MWt from 5.656 kW/ft before densification to 5.744 kW/ft.

4. The local power spike factor is applied to the calculated power distributions.

5. The overpower limit in the imbalance protection system is redefined as 112% of 2568 MWt. The effect of the reduced overpower limit is one-to-one for local heat rate and approximately two-to-one for DNBR.

The trip setpoints are obtained from the calculated offset limits by adjusting for potential electronic errors and offset measurement bias by the out-of-core detectors. The error-adjusted limits for densified fuel are shown in Figure 3.3-3. The imbalance trip points and overpower trip provide operating flexibility with assurance that thermal criteria are not exceeded. Furthermore, potential relaxation of the limits may be realized from the physics tests, in which the offset bias instrumentation behavior and the measured flow in the RC system will be determined.

3.3.3.1. ECCS Considerations

ECCS calculations that include fuel densification effects have shown that a peak fuel rod cladding temperature of 2291F is achieved with a linear heat rate of 19.8 kW/ft at 102% of 2568 MWt. The margins associated with 19.8 kW/ft have been re-examined for normal

- - - - -

*The 21.8 kW/ft central fuel melt limit was calculated for densified fuel for a maximum, first-cycle fuel pin burnup of 14,694 MWd/mtU. The code described in BAW-10044, "TAFY — Fuel Pin Temperature and Gas Pressure Analysis," was used for this calculation. A first-cycle burnup of 14,694 MWd/mtU includes a 10% uncertainity margin for first-cycle burnup.

equilibrium operation and maneuvering transients during the fuel cycle. The LOCA margin is defined as

$$\text{LOCA margin} = \left[\frac{\text{Limiting heat rate (19.8 kW/ft)}}{5.744\ \text{kW/ft} \times \text{calculated peak} \times 1.02} - 1\right] 100\%$$

where 5.744 kW/ft = average heat rate at 2568 MWt for densified fuel,

Calc peak = peak calculated with PDQ increased by a 1.075 uncertainty factor, 1.014 hot channel factor, and the power spike factor (Figure 3.1-2) as a function of axial position,

1.02 = 102% of 2568 MWt.

3.3.3.2. Normal Fuel Cycle Operation

Table 3.3-2 summarizes the fuel cycle calculations. The maximum total hot spot peak is presented with the corresponding peak linear power density (kW/ft). The LOCA margins represent the margin at the hot spot for a balanced core and normal control rod positions. After establishing equilibrium xenon, the LOCA margin exceeds 36% throughout the remainder of the rodded cycle; i.e., the peak linear power is 14.5 kW/ft compared to the 19.8 kW/ft limit. The margin increases throughout the fuel cycle except for the period from 285 to 310 days. At 310 days, the margin is calculated to be 31.2%. The decrease in margin at the end of the first cycle is due to the transient rod bank being fully withdrawn at 310 days to enable the reactor to meet end-of-life reactivity requirements.

3.3.3.3. Transient Data

A 100-30-100% power transient is the design transient for the core. The xenon override control rod bank (transient bank) is designed to recover from 30 to 100% power at maximum xenon, which occurs approximately 8 hours after the power reduction. Tables 3.3-3 through 3.3-8 summarize the calculated data for six transients at various times in core life. Power peaks result from the rod positions required to meet the design transient. After recovery to full power, control rods are inserted beyond their nominal insertion range to compensate for xenon undershoot. The largest operating power peaks occur at this time. In Table 3.3-3, the [ ]-hour peak is the largest operating

power peak. A hot spot heat rate of [ ] kW/ft occurs at this time, which gives the lowest operating LOCA margin of [ ]. This power peak is a result of bank 7 being fully inserted and bank 6 being inserted to approximately the midplane. Note that this peak is unrealistically conservative since 100 effective full power hours will be achieved during startup testing before the reactor is near full power. After 100 full power days, the maximum heat rates are below 16.4 kW/ft and the LOCA margins are in excess of 21%.

3.3.3.4. Quandrant Tilt

In the unlikely event of a quadrant power tilt during normal equilibrium operation and during design power transients, the primary concern is to ensure that the limiting heat rate of 19.8 kW/ft is not exceeded. The present technical specifications limit quadrant power tilt to 10% at rated power. The relationship of increased peaking and radial tilts has been investigated for various conditions and core designs. Figure 3.3-4 presents results for increased peaking as a function of quadrant tilt as indicated by the out-of-core detectors for dropped control rods and single and multiple control rods out of sequence. The magnitude of a radial tilt as indicated by out-of-core detectors depends on the relationship of the tilt axis and the out-of-core detectors. A maximum indication is obtained when the tilt axis is aligned with the out-of-core detectors. A minimum indication is obtained when the tilt axis is at an extreme angle from the out-of-core detector. An uncertainty of 23% is included in the tilt indication in Figure 3.3-4 to account for the potential difference between the nominal quadrant tilt and the minimum indication. Figure 3.3-4 is a plot of peaking increase as a function of tilt indication for a minimum indication by the out-of-core detectors. The data were determined with three-dimensional, thermal-hydraulic feedback analyses (PDQ-7), except for the dropped rod cases, which were determined from two-dimensional PDQ-7 analysis. The data are limited by a line with a slope of 1.84 $\frac{\Delta(\text{kW/ft, \%})}{\Delta(\text{Indic, \%})}$.

3.3.3.5. Rod Insertion Limits

A minimum LOCA margin of 18.4% is needed at 102% of 2568 MWt to accommodate a 10% quadrant tilt and not exceed LOCA criteria with densification effects included. A 5% quadrant tilt will

require a minimum LOCA margin of 9.2% at 102% of 2568 MWt to prevent exceeding LOCA criteria with densification effects included. Table 3.3-2 shows that early in core life under present operating conditions, the minimum LOCA margin is [ ] at the time of xenon undershoot. Since power peaks in a rodded core are primarily a function of rod insertion, the total power peak can be reduced by control rod insertion limits. Figure 3.3-5 is a plot of maximum heat rate as a function of rod index for equilibrium xenon and transient xenon conditions. Rod index is defined as the sum of the percentage insertions of banks 6 and 7. The figure indicates a range of control rod indices which yield lower peaking conditions. When the core is at power, the selection of a control rod operating band between rod indices of 52 and 117% will result in lower peaks. Utilizing the foregoing control operating band, the maximum heat rate at 102% of 2568 MWt, with all densification effects and a 7.5% uncertainty factor, is 17.82 kW/ft. This rate yields a LOCA margin of 11.1%.

The inclusion of a rod index range for power operation will yield a minimum LOCA margin of 11.1%, which is sufficient to accommodate a 5% quadrant tilt. Furthermore, maintaining the rods within the 52 to 117% index range will lead to larger margins during the early part of core life. The rod index limitation would be required only for operation above 90% power. Below the 90% power level, the LOCA margins are large enough to handle a 5% tilt without rod index restriction. Further, restrictions on a rod index could be removed after the first 100 days of full-power operation. Table 3.3-4 indicates that even for the normal rod index of 141.7%, the LOCA margin is in excess of the required 9.2%.

3.3.4. Summary

Fuel densification and associated design limit changes have produced modifications to the RPS and operational changes. The power peaking margin loss of 2.01% from the DNB analysis, the lower fuel melting limits, and the additional power spike factor have been compensated by a 2% reduction in design overpower and by more stringent offset limits. The revised RPS allows operation at 100% power with assurance that thermal criteria, with all densification effects included, are not exceeded. The modifications are summarized and compared with the previous system in Table 3.3-1.

Table 3.3-1. Modifications to Reactor Protection System Setpoints and Design Parameters

A. Imbalance System

Parameter	Previous system	Modified system (densification)
Fuel melt limit, kW/ft	22.2	21.8
DNB peaking margin penalty, %	--	-2.01
Nominal heat rate, kW/ft	5.66	5.74
Overpower, % of 2568 MWt	114	112
Offset limits at rated power		
Positive offset	+39	+26
Negative offset	-65	-62
Trip setpoints at rated power		
Positive imbalance	+12	+8
Negative imbalance	-30	-32
Spike factor	None	1.00 to 1.125
Nuclear power peak uncertainty	1.075	1.075

B. ECCS Considerations

The normal operating power peaks incorporating a power spike factor for densification result in heat rates at 102% of 2568 MWt, which are less than the limiting value of 19.8 kW/ft. The peak heat rate without rod index limits is [ ] kW/ft.

C. Radial Tilt

For power levels above 90% of 2568 MWt, an operating rod index range from 52 to 117% will yield a minimum LOCA margin of 11.1%. This value contains sufficient margin to accommodate a 5% quadrant power tilt. The peak heat rate with rod index limits is 17.82 kW/ft.

Table 3.3-2. Oconee 1 — Nominal Rod Positions Fuel Cycle Data, Equilibrium Steady State

Time, days	Offset, %
0	+5.80
4	+3.18
25	+1.61
50	-3.96
100	+3.43
150	-8.48
200	+1.11
250	-8.43
285	+2.63
310	+8.31

Table 3.3-3. Four-Day Design Transient Data, Transient Bank 1

Time, h	Offset, %
96	+3.32
104	+6.88
104.5	-15.2
105	-13.7
106	+0.1
107[a]	-12.1
108[a]	-10.5
109[b]	-9.64
110	-5.73
111	-3.98
112	-2.24

[a] Bank 7 = 100% inserted and bank 6 = 45.8% inserted.

[b] Bank 7 = 100% inserted and bank 6 = 41.7% inserted.

Table 3.3-4. 100-Day Design Transient Data, Transient Bank 1

Time, h	Offset, %
2400	-4.60
2408	-2.28
2408.5	-16.3
2409	-5.96
2410	+1.20
2411[a]	-11.3
2412	-14.4
2413	-11.3

[a]Bank 7 = 100% and bank 6 = 41.7%.

Table 3.3-5. 100-Day Design Transient Data, Transient Bank 2

Time, h	Offset, %
2400	-4.34
2408	-1.40
2408.5	+2.96
2409	-2.38
2410	+4.02
2411	-0.60
2412	-10.1
2413[a]	-12.9
2414	-11.0
2415	-11.9
2416	-12.5
2417	-12.8

[a] Bank 7 = 100% and bank 6 = 54%.

Table 3.3-6. 200-Day Design Transient Data, Transient Bank 2

Time, h	Offset, %
4800	-5.24
4808	-9.50
4808.5	-1.42
4809	+1.48
4810	+4.02
4811	-5.82
4812	-12.5
4813	-16.1
4814	-17.8
4815	-17.0
4820[a]	-21.8
4822	-21.0
4828	-19.0
4836	-8.6
4844	-4.8

[a]Bank 7 = 100% and bank 6 = 45.8%.

Table 3.3-7. 200-Day Design Transient Data, Transient Bank 3

Time, h	Offset, σ_0
4800	-3.21
4808	-1.91
4808.5	-11.8
4809	-6.04
4810	+2.34
4811	+0.11
4812	-6.95
4813	-9.21
4814	-11.4
4815	-11.0
4816	-11.9
4818	-14.4
4820	-17.3
4822[a]	-16.5
4824	-16.1
4828	-12.3
4832	-7.03
4836	-1.35
4844	+1.65

[a] Bank 7 = 100% and bank 6 = 42%.

Table 3.3-8. 285-Day Design Transient Data, Transient Bank 3

Time, h	Offset, %
6840	-8.89
6848	-9.01
6848.5	-6.93
6849	+1.67
6850	+2.29
6851	-2.91
6852	-11.5
6853	-13.5
6854	-13.2
6855	-12.5
6856	-13.1
6858	-15.4
6860	-19.1
6862	-20.3
6864[a]	-19.2
6868	-15.5
6872	-10.4
6876	-6.35
6884	-3.15
6892	-1.71
6900	-4.28
6908	-6.91

[a] Bank 7 = 100% and bank 6 = 42%.

Figure 3.3-1. Trip Setpoints Vs Axial Imbalance Without Densification Effects

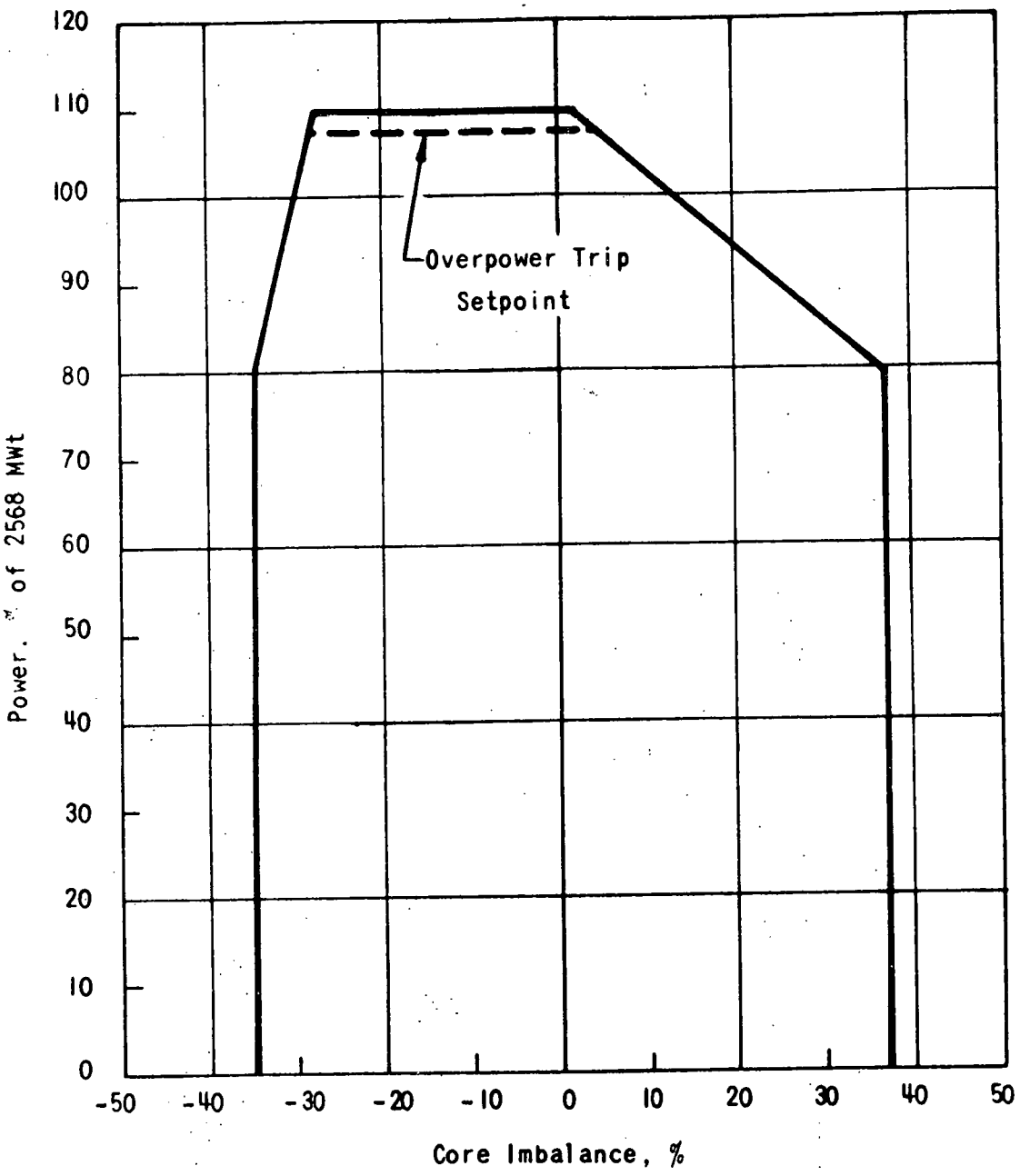

Figure 3.3-2. Calculated Offset Limits Vs Power

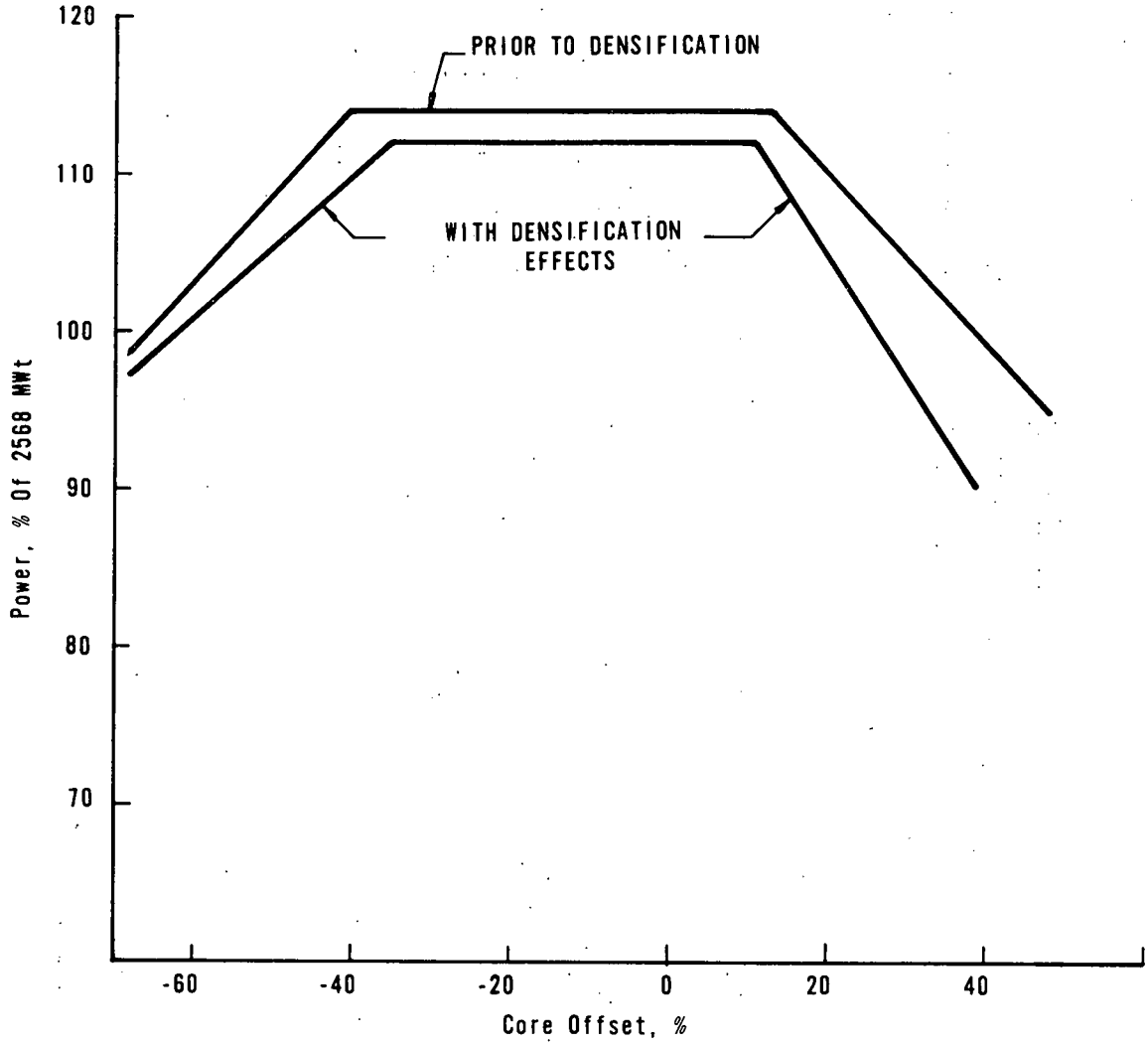

Figure 3.3-3. Trip Setpoints Vs Axial Imbalance With Densification Effects

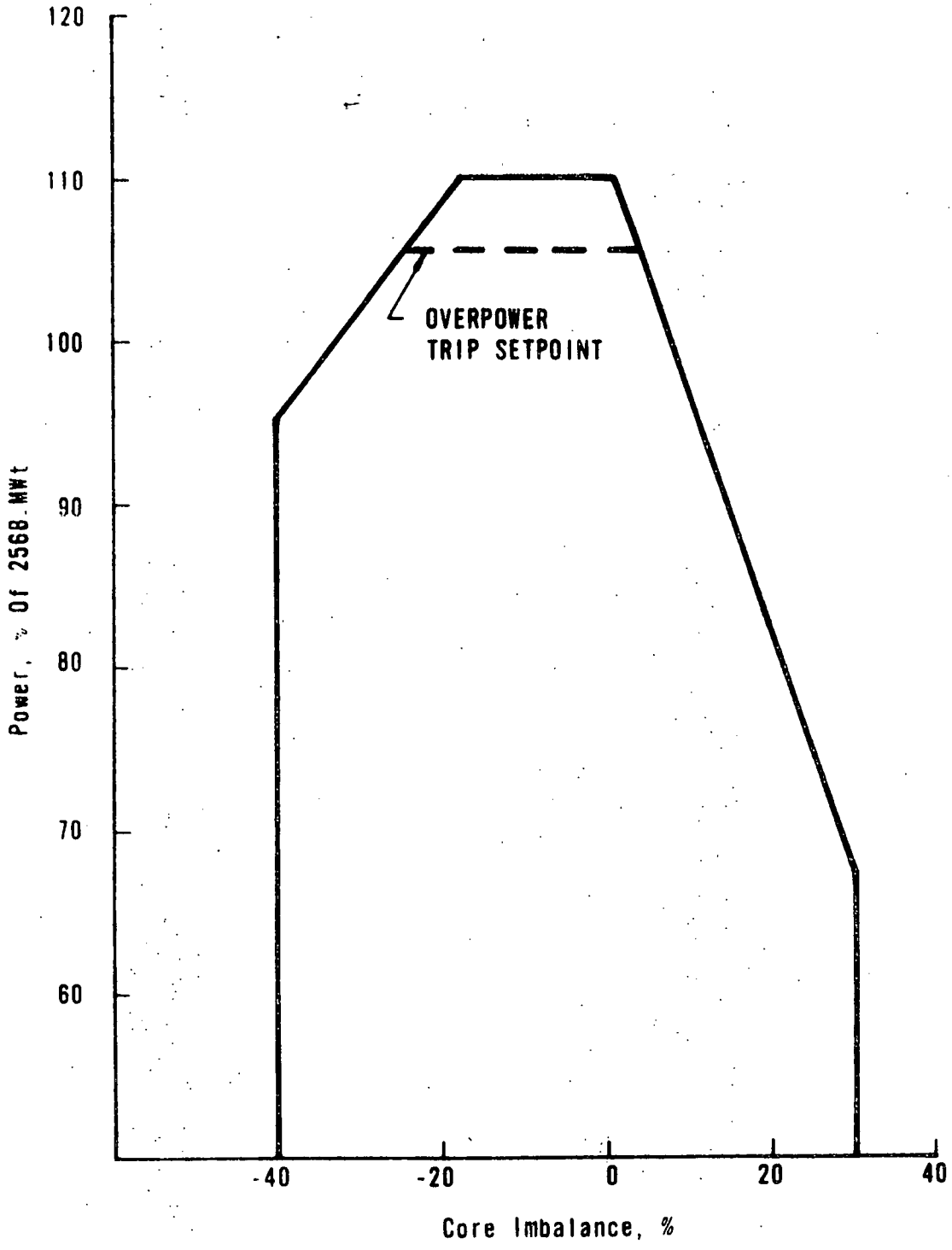

Figure 3.3-4. Percentage Change in Peak Power Vs Indicated Tilt

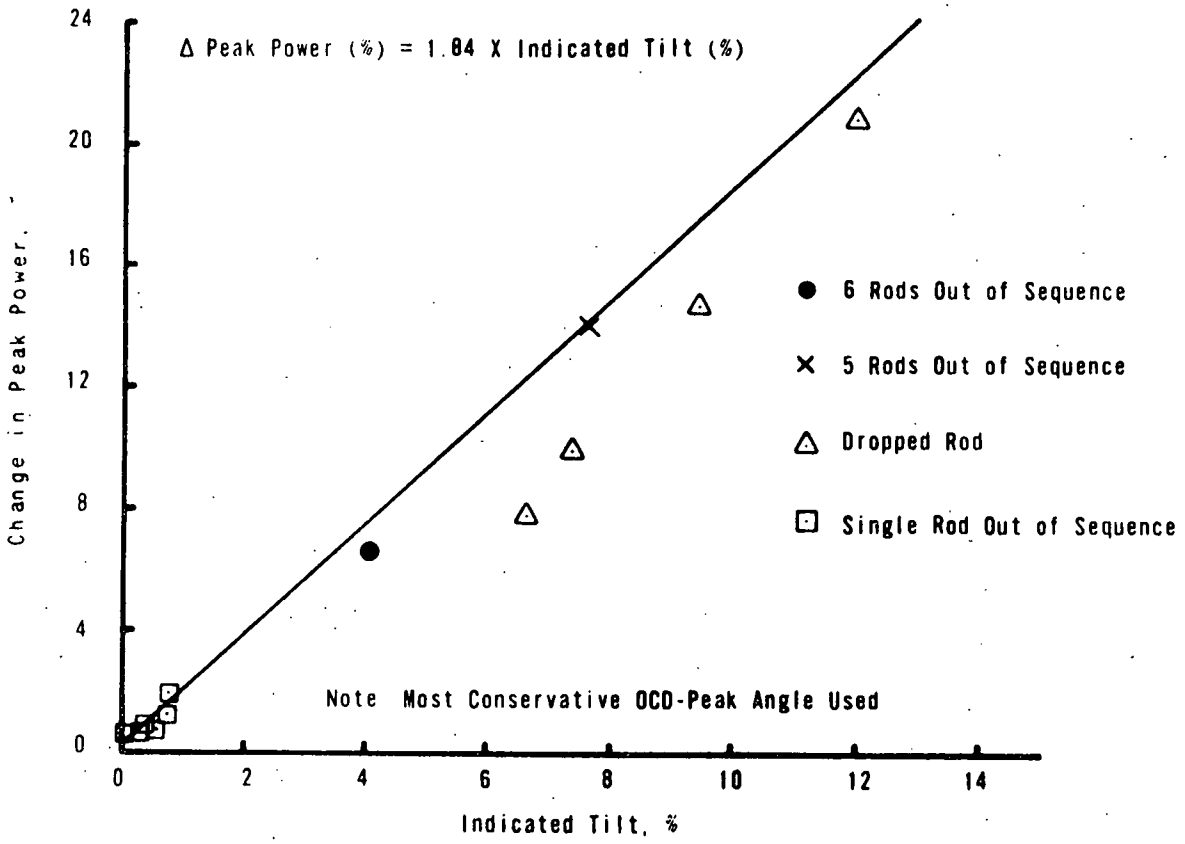

Figure 3.3-5. Maximum kW/ft Vs Rod Index for Equilibrium and Transient Xenon Conditions at 102% of 2568 MWt (BOL) and LOCA Limit of 19.8 kW/ft

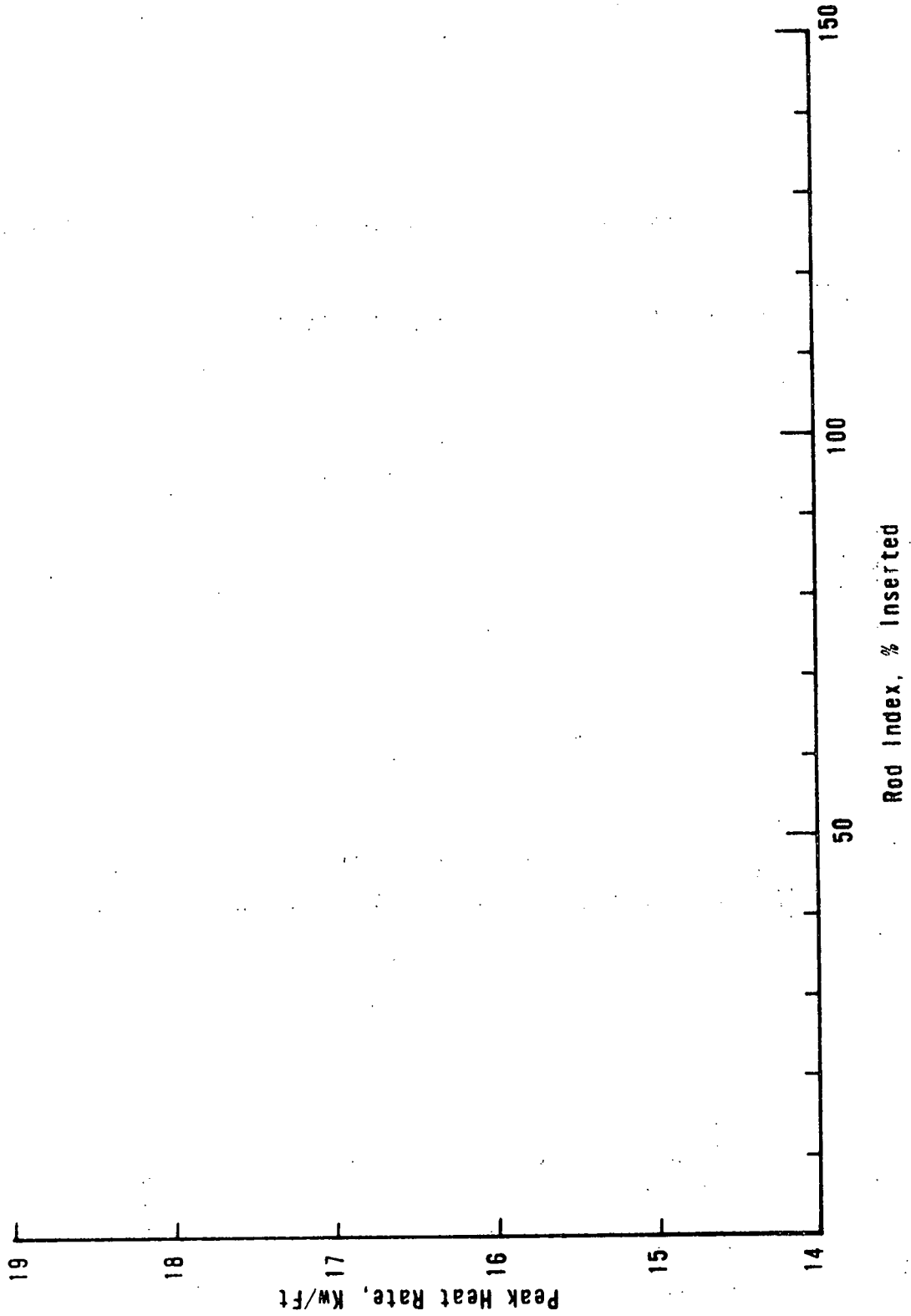

3.4. Safety Analysis

3.4.1. General Safety Analysis

3.4.1.1. Introduction

The significant effects of fuel densification are an increase in maximum fuel temperature and a slight increase in average heat flux due to shrinkage of the pellet stack length. In addition, spikes in the neutron power can occur due to gaps in the fuel. These combined effects will lead to a slightly decreased initial DNBR for the accident calculations presented in the Oconee SAR. For overpower transients, such as a rod withdrawal, the effects are offset by a reduction in the overpower trip setpoint. The parameters used in the analysis are the same as those used in the SAR analysis. The changes in fuel geometry and higher fuel temperature will lead to slightly more negative values of the moderator and Doppler coefficients; however, to maintain conservatism the original values were used. All calculations were made for BOL conditions.

3.4.1.2. Reactivity Insertion Transients

The rod withdrawal from zero power was not recalculated since for all combinations of parameters, including the simultaneous withdrawal of all rods in the core, the peak thermal power attained during the transient is always less than 100%. The rod withdrawal from rated power was calculated for two rod withdrawal rates: 1.4×10^{-4} $\Delta k/k/s$, which corresponds to the maximum single group withdrawal rate and 7.25×10^{-4} $\Delta k/k/s$, which corresponds to an all-rods withdrawal. The single group withdrawal gave a peak thermal power of 106%, and the all-rods withdrawal gave a peak thermal power of 103%. Both of these values are well below the 112% design thermal power level; therefore, the 1.3 limit on DNBR is maintained for this transient.

The startup of an inactive loop was not considered in the analysis since the maximum thermal power achieved during the transient is much less than 100% and occurs after full flow is reached. The rod drop accident results in an initial decrease in power which is followed by a return to 100% power. Since it has been shown previously that neither the withdrawal nor the drop of a single control element will perturb the flux shape sufficiently to exceed design conditions

at 112%, such occurrences still do not present any thermal problems. The moderator dilution accident results in reactivity insertion rates that are very slow, and the accident is terminated by the high-pressure trip well before power reaches the 112% design thermal power level. Therefore, the 1.3 limit on DNBR is maintained.

Ejection of the most reactive control rod at BOL with densified fuel was analyzed. The results show that this accident is no more severe than the equivalent accident presented in the Oconee SAR. The ejection of a 0.5% $\Delta k/k$ rod (maximum worth that occurs at rated power) results in a peak neutron power of 320% and a peak thermal power of 119.5%. The comparable values presented in the SAR are 277 and 126%, respectively. A comparison of the values shows that a rod ejection with densified fuel is less severe because of the increased time constant of the fuel heat transfer, which results in a slightly lower peak thermal power. Appendix B provides additional information on this subject.

Secondary system accidents resulting in a power increase occur at or near end of life (EOL) when a highly negative moderator coefficient exists. Since more DNB margin exists at EOL, these secondary accidents, such as a steam line break, are not expected to cause thermal limits that are more severe than those presented in the SAR. The SAR analysis of secondary system accidents, such as tube ruptures and loss of electric power, is unchanged since the thermal power remains the same or decreases during the transients and, therefore, does not increase the potential for reaching design limits.

3.4.1.3. Loss of Coolant Flow

The loss-of-coolant flow accident has been analyzed under initial conditions that represent the most conservative that can occur in the core with densified fuel. The case considered is a balanced power peak case with the power spike placed at the point of minimum DNBR. The other parameters normally considered in the coastdown calculations remain unchanged from the FSAR values. Figure 3.4-1 shows power, flow and the calculated average heat flux for a four-pump coastdown initiated from 102%. Figure 3.4-2 shows

the calculated DNBR and film coefficient as a function of time. The gap conductance used for this calculation was 850 Btu/h-ft^2-F. The fuel and cladding temperature is not shown since there was no variation in these parameters, because the DNBR for this accident did not go below the criterion value of 1.3. It is therefore concluded that no fuel damage will occur.

3.4.2. LOCA Analysis

3.4.2.1. Introduction

Topical report BAW-10034 established the 8.55-ft^2 split break at the pump discharge as the worst break location and size in the RC system. This analysis assumed that the axial power peaked 3 feet from the bottom of the core and was shown to result in a higher cladding temperature than that obtained when the power peaks at higher elevations in the core.

As shown in Table 3.3-2, the highest linear heat rate for equilibrium operation is on the order of 16 kW/ft. Higher peak heat rates can occur during maneuvering transients. The highest of these occurs during the 4-day transient at 5.5 feet from the bottom of the core. The peak linear heat rate was placed at the 5.5 foot level for this analysis. An axial peaking factor of 1.786 was used and the radial varied until the limiting cladding temperature ($\tilde{=}$ 2300F) was reached. This procedure was accomplished to establish the reference case relative to which LOCA margin could be determined.

3.4.2.2. Initial Conditions

The normal design basis transient is defined as a 100-30-100% transient consisting of operation at 100% power, reduction in power to 30% power, operation at 30% power for about 8 hours, and a return to 100% power. The return to 100% power is made at the time of maximum xenon, at a rate of power change of 10% per minute.

The return to 100% power for a condition of maximum xenon causes a rapid depletion of xenon, and control rods must be inserted with a resultant increase in the axial peaking factor. The highest values of power peaking occur at "xenon undershoot," which requires the greatest rod insertion. Further, the largest peaking factors occur near the beginning of core life.

An axial peaking factor of 1.786 was used in the LOCA analysis. This is the largest value for the design basis transient and includes the usual factors for calculational uncertainty. The maximum axial power occurs at 5.5 feet above the bottom of the core, or 0.5 feet below the core midplane. Instead of imposing a power spike at the 5.5-foot elevation due to fuel densification, the local power spike was replaced by an equivalent radial multiplier over the entire fuel pin. This approach leads to a higher calculated peak cladding temperature of approximately 10F.

When these adverse peaks occurred, it was further assumed that the fuel changed to 96.5% of theoretical density with a decrease of 1.8% in pellet stack height. Rather than change the stack height in the THETA1-B model, the radial peaking factor was increased by 1.018 to provide an increase in linear heat rate. The diametral gap between the fuel and the cladding was increased with a corresponding increase in fuel temperatures.

3.4.2.3. Analysis

Results from CRAFT were input into the THETA1-B code to determine the peak cladding temperature. The THETA model utilized 13 axial segments divided into eight 12-inch-long, two 16-inch-long, one 8-inch-long, and two 4-inch-long regions. The B&W carryout rate fraction was used in the REFLOOD code to determine the FLECHT heat transfer coefficients.

3.4.2.4. Results

The maximum linear heat rates accounting for fuel densification up to 96.5% TD for BOL and EOL were calculated according to procedures similar to those found in part 4, Appendix A, of the AEC Interim Acceptance Criteria for Emergency Core Cooling Systems for Light Water Power Reactors, dated June 29, 1971, as amended December 18, 1971. The results are as follows:

	Maximum linear heat rate, kW/ft	Maximum cladding temp, F
BOL	19.80	2291
EOL (40,000 MWd/t)	18.50	2280

The kW/ft values associated with the interim acceptance criterion of 2300F peak cladding temperature were used to show the conservatism of the operating power distribution (Tables 3.3-1 through 3.3-8). The results demonstrate that the operating power distributions, with all densification effects included, yield linear heat rates that are below the allowable peak values listed above.

Figure 3.4-1. Oconee Scram and Coastdown Curves With 0.62 Trip Delay Time for Four-Pump Coastdown

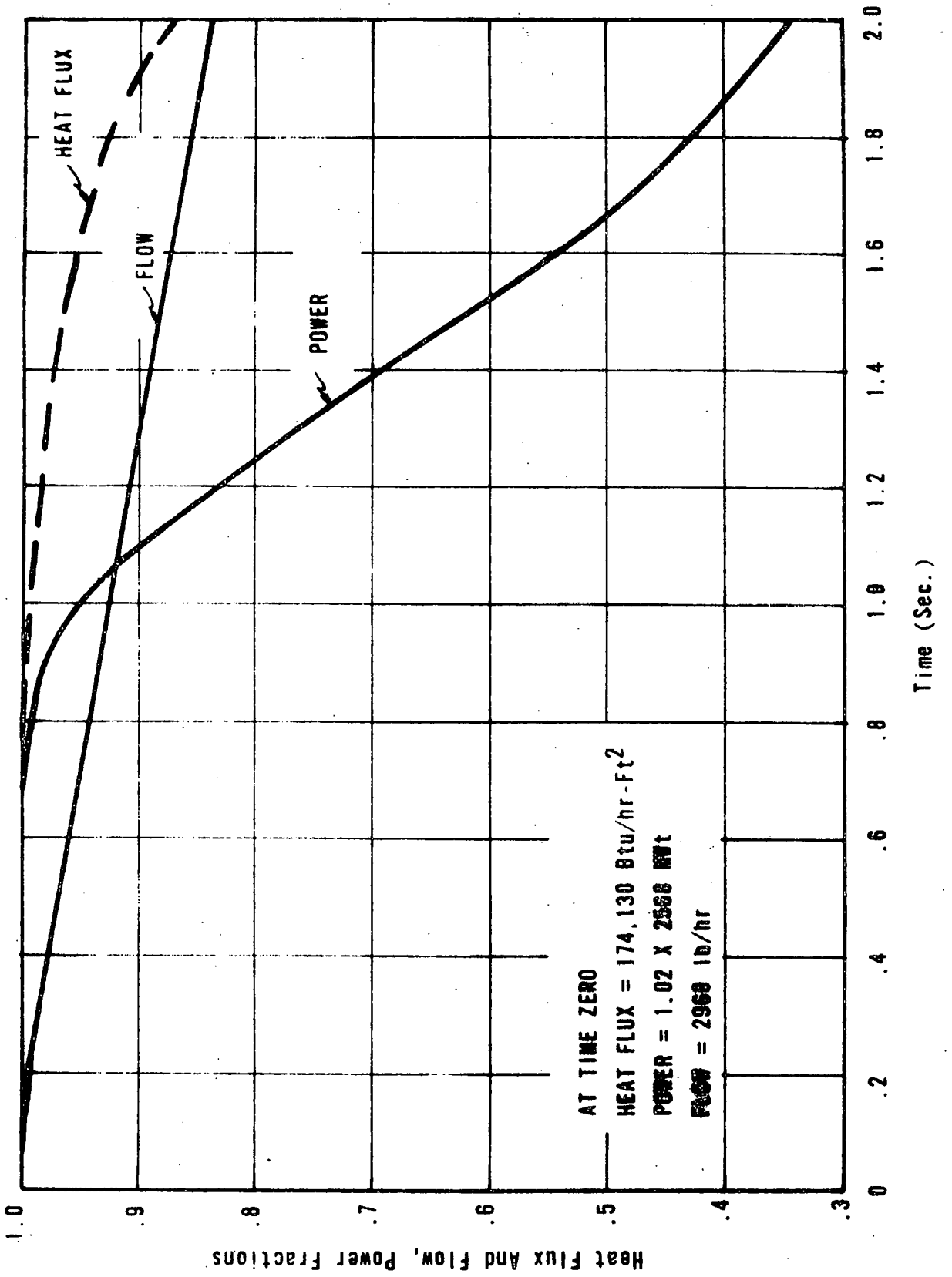

Figure 3.4-2. DNBR and Film Coefficient Vs Time for Four-Pump Coastdown

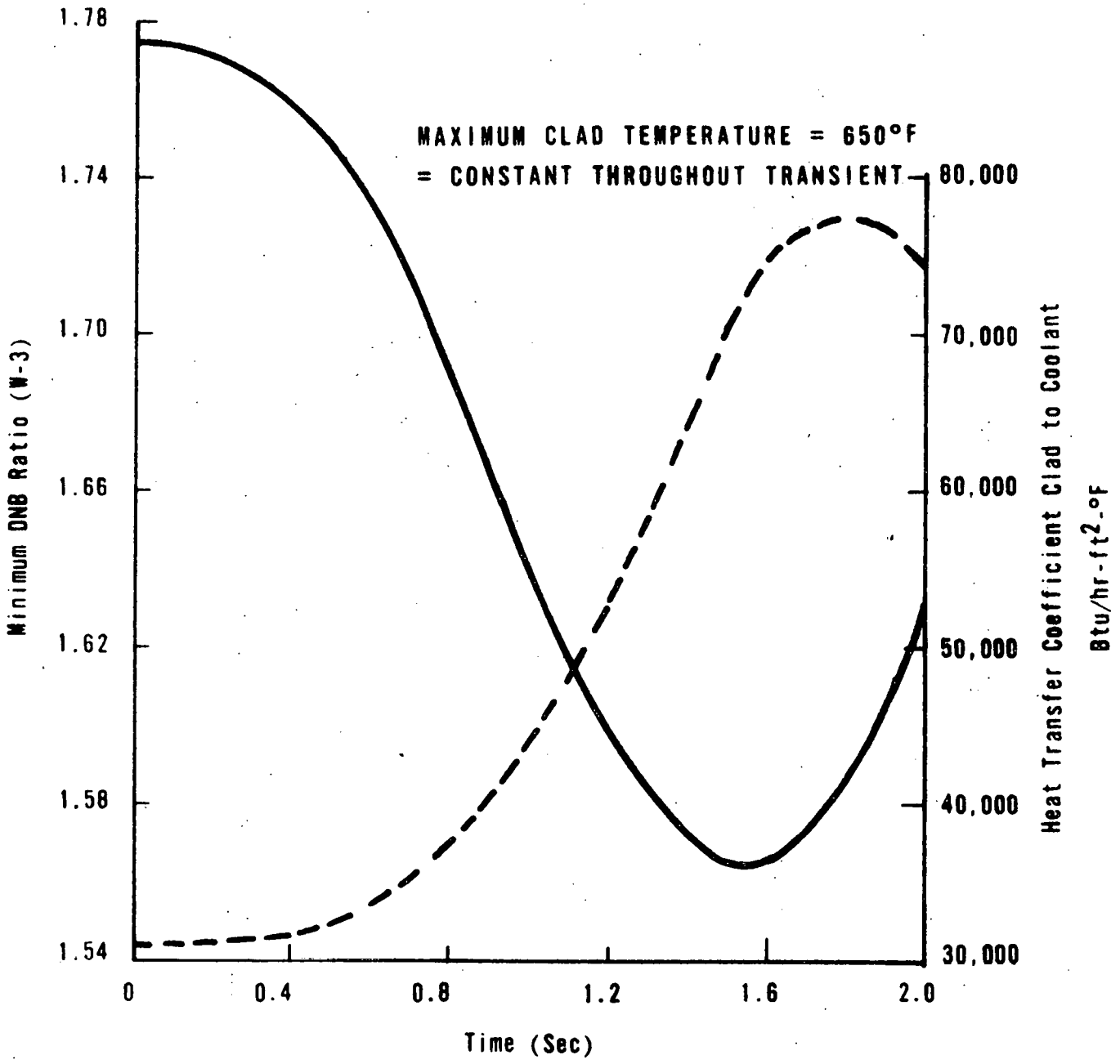

3.5. Mechanical Analysis of Oconee 1 Fuel

3.5.1. Cladding Collapse

Input Summary

1. Pellet OD, in. 0.36998
2. Cladding ID, in. [ ]
3. Pellet density (batch 3) [ ]
4. Pre-densif. int. press. (cold), psia [ ]
5. Post-densif. int. press. (cold), psia [ ]
6. Cladding ovality, in. [ ]
7. Cladding wall thkns, in. 0.0262
8. Rod time-temp-press. history:

Time, h	Cladding temp, F	Internal press., psia
0-600	639	
600-1,200	639	
1,200-2,400	639	
2,400-4,800	631	
4,800-6,000	642	
6,000-6,840	634	
6,840-7,440	638	
7,440-8,640	642	
8,640-9,840	639	
9,840-11,040	635	
11,040-12,240	626	
12,240-14,280	624	
14,280-14,880	623	
14,880-16,080	621	
16,080-17,280	621	
17,280-18,480	621	
18,480-19,680	622	
19,680-21,720	621	
21,720-22,320	622	

9. Post-densif. pellet OD in. [ ]
10. Fast flux level 6.94×10^{13}

Results

Predicted time-to-collapse: [ ] h when fission gas release is ignored.

3.5.2. Cladding Stress

Input Summary

1.	Min int. press. (cold) after densif., psia	[ ]
2.	Cladding temp.	As described in BAW-10055 Rev 1

Results

1. Table 3.5-1 lists cladding maximum stress calculated at various times in life. In no case does stress exceed yield.
2. Cumulative fatigue damage after three cycles is less than 0.9.

3.5.3. Fuel Pellet Irradiation Swelling

Input Summary

1.	Density (mean + 2σ local)	[ ]
2.	Initial pellet dia, in.	0.36998
3.	Cladding ID, in.	[ ]
4.	Max local three-cycle burnup, MWd/mtU	42,000
5.	Pellet dia after densif., in.	[ ]
6.	Peak local heat rate, kW/ft	22

Results

Circumferential plastic strain less than 1% after three cycles.

3.5.4. Revision Input to Creep-Collapse Calculations

The application of the creep model to fuel rods in a specific reactor was performed using input from the worst-case rod. The method for selecting this input is described as follows:

1. An initial gap between the pellet and the cladding is calculated on the basis of as-built dimensions. The mean as-built pellet OD is combined with the mean as-built cladding ID minus two standard deviations to determine a minimum BOL gap. These dimensions result in fuel pellets with low thermal expansion and fission-gas release, and therefore a rod with a high pressure differential.

2. Initial pellet density is the mean as-built density for fuel assemblies operated for three cycles. When the pellet densifies to 96.5%, a change in stack and pellet dimensions produces a change in rod internal pressure. The use of the minimum diametral gap in the foregoing step produces a minimum gap volume that contains backfill gas. The increase in void volume due to pellet shrinkage will in this case have the greatest effect on BOL pressure.

3. The internal rod pressure before densification is assumed to be the lowest allowable pressure for backfill gas. (All B&W fuel will be prepressurized.)

4. Rod length, end cap dimensions, and internal spacer arrangement and dimensions are assumed to be at values that will minimize the rod internal void volume.

5. Combining steps 1 through 4, the BOL cold rod internal pressure is calculated by the equation

$$\text{BOL press.} = \text{backfill press.} \times \frac{\text{Rod void volume before densification}}{\text{Rod void volume after densification}} .$$

The increase in void volume is based on pellet dimensional changes calculated in accordance with the AEC report of November 14, 1972.

6. Cladding ovality at BOL is the mean as-built ovality plus two standard deviations.

7. The wall thickness at BOL is the mean as-built thickness minus two standard deviations.

8. For each plant, the radial × local peaking histories of three-cycle assemblies are examined to determine a conservative worst-case rod peaking history. For each time increment (varying from 25 to 100 days), the maximum peak for any three-cycle assembly is assumed to be the peak for that increment. Thus, the final assembly peaking history represents a combination of peaks from many assemblies. Rod peaking history is obtained by applying a rod-peak/assembly-peak ratio [ ] to the assembly history. A [ ] uncertainty factor is also applied. The resultant peaking versus time history is used as input to the cladding temperature model. After relating the history to burnup, it is also used as input to the

TAFY code (along with the rod geometry and pressure described above) to compute the rod internal pressure versus time curve.

9. The cladding OD temperature along a gap in the pellet stack drops to the coolant temperature within about 1/8 inch. The temperature increase across the cladding wall has been calculated to be 3F due to radiating from pellets at the boundary. Therefore, the assumed maximum cladding temperature for any gap is the coolant temperature corresponding to the peaks described in step 8 plus 3F.

Table 3.5-1. Cladding Circumferential Stress

Case	Ext press., psia	Int press., psia	Cladding temp, F	Bending + membrane stress, psi	Total stress, psi	Yield strength, psi	Ultimate strength, psi
1	2200	460	532	-22500	-22500	48000	57000
	2500	460	532	-27600	-27600	48000	57000
2	2200	580	650	-20800	-20800	45000	50000
	2500	580	650	-25700	-25700	45000	50000
3	2200	600	650	-20500	-20500	45000	50000
	2500	600	650	-25400	-25400	45000	50000
4	2200	580	723	-21000	-24900	42000	44000
	2500	580	723	-26100	-30000	42000	44000
5	2200	600	733	-20700	-25100	41500	43500
	2500	600	733	-25700	-30200	41500	43500
6	2200	460	532	-22500	-22500	48000	57000
	2500	460	532	-27600	-27600	48000	57000
9	2200	580	704	-20900	-23800	43000	46000
	2500	580	704	-26000	-28900	43000	46000
10	2200	600	711	-20600	-23900	43000	46000
	2500	600	711	-25600	-28900	43000	46000
11	2200	460	535	-22500	-22800	48000	57000
	2500	460	535	-27600	-27800	48000	57000
12	1725	400	425	-16300	-16300	50000	62500

APPENDIX A

Summary of Statistical Analysis for Oconee 1 As-Built Data

In keeping with the guidelines given in "Technical Report on Densification of Light Water Reactor Fuels," November 14, 1972, as-built data on the UO_2 fuel pellets have been utilized in the densification analysis. The results for fuel pellet diameter and density are given in Table A-1.

The standard deviations for the local pellet diameters and densities (σ_L) were pooled to give a representative value for the core.

Table A-1. Summary of Statistical Analysis for Oconee 1 As-Built Fuel Pellet Data

APPENDIX B

Answers to Questions Contained in Letter to Duke Power from R.C. DeYoung dated March 14, 1973

The AEC issued a list of questions to Duke Power Company on March 14, 1973 as a culmination of the Staff review of effects of postulated fuel densification on the design and operation of the Oconee 1 nuclear station. These questions are addressed in this appendix to facilitate referral to the answers.

Question 1

Provide the values for the following physical properties and dimensions of the Oconee Unit 1 fuel pins:

1. Fuel pellet length, diameter, dished end volume and chamfer volume.
2. Fuel pellet density.
3. Clad inside and outside diameter, initial ovality, and wall thickness.

For each of these parameters, provide the nominal value, the specified value and tolerances, and the average value (as built) with standard deviation as well as maximum and minimum measured values.

Describe the method of measuring that was used, the frequency of measuring samples, and the production step at which the measurements are performed in the production process of the fuel assembly. If any of these parameters is measured at different times in the production process, e.g., at the fuel pellet manufacturer and at B&W, with identical or different measuring techniques compare the results and discuss any differences.

Response

1.2. Fuel Pellet As-Built Data

In general, the fuel pellet vendor is the source of information. All vendor measurements are taken at the end of the pelletizing process.

1.2.1. Acceptance Criteria

The fuel pellet vendor is required to sample every production lot for pellet length, average diameter and density based on a variables sampling plan. The acceptable quality level (AQL), lot tolerance percent defective (LTPD), consumer's risk (CR) and producers risk (PR) are specified. These, in conjunction with the tolerance limits, determine the sample size and the acceptability of the pellet lot.

The fuel pellet vendor is also required to sample every production lot for dish dimensions based on an attributes sampling based on specified AQL, LTPD, CR, and PR. Again these parameters and the tolerances determine the acceptance criteria for the pellet lot.

1.2.2. Commercial Nuclear Fuel Plant Overcheck

B&W's Commercial Nuclear Fuel Plant performed over-checks on pellet length, average diameters, density and dish dimensions utilizing attributes sampling. These results are compared with vendor quality control data before acceptance for fuel assembly production.

1.2.3. Method of Measurement

The vendors quality control program requires:

1. Pellet length will be measured with a disc micrometer with a minimum graduation of 0.001 in.

2. Pellet average diameter is measured at each end and at the midpoint with a micrometer of minimum graduation of 0.001 in. The three measurements taken along the pellet length are spaced 120° apart radially. Average diameter is calculated by adding the two end measurements to twice the midpoint measurement and dividing by four.

3. Pellet dish depth and diameter are measured by attributes-type sampling employing a bench-type indicating dish depth gage with a minimum graduation of 0.0001 in. and an optical comparator readable to 0.001 in. for diameter.

4. Pellet density is calculated from average diameter and length and weight. Weight is measured to a graduation of 0.01 gram. A correction factor is applied for the dished ends.

1.3. Details of Inspection of Oconee 1 Cladding

The cladding vendor was required to perform 100% inspection for ID, OD, and minimum wall thickness dimensions with a scanning instrument covering at least 720°/ft. The specification requires all traces to be within the given tolerance limits before the cladding is acceptable for fuel assembly production.

Available vendor traces on Oconee 1 cladding include 300 traces from 6 lots. In addition, B&W's Commercail Nuclear Fuel Plant performs an ID and OD overcheck at a frequency of 10 tubes/1000. ID was measured at both ends, and OD was measured at the ends and middle of the cladding tubes.

Question 2

In order to assess the B&W evaluation model, TAFY, for stored energy, fuel pellet to clad gap conductance, and clad temperature of a fuel pin for Oconee Unit 1, a detailed description of the following items is required. Where applicable, equations and empirical formulations should be provided.

2.1. Question 2(a)

The amount and composition of the sorbed gases assumed to be present in the fuel including the analytical methods used to describe the release rate of the sorbed gases.

Response

The content of the sorbed gas in the fuel is assumed to be air and is considered to be completely released into the gap at beginning of life. The sorbed gas is accounted for in the gap conductance determination. The initial concentration of sorbed gas is 0.02 cc/gm

2.2. Question 2(b)

The amount and content of the gas in the gap between fuel pellet and clad.

Response

The backfill gas is 100% He. Oconee 1 fuel rods were prepressurized to [ ]

2.3. Question 2(c)

Description of gas mixture conductivity model for the gas in the fuel pellet-clad gap, and the thermal expansion model for the fuel pellet and the clad. Discuss how the fuel cracking is treated.

Response

The gas conductivity mixture model used in TAFY is called GSMIX and it is a sub routine of the main code. The GSMIX sub routine was obtained from Argonne National Laboratory and detailed explanation can be found in the following reference: Holmes, J.T. and Baerns, M.G., "Evaluation of Physical Properties of Gases and Multicomponent Gas Mixtures", Report number ANL-6951, Argonne National Laboratory, November 1964.

The TAFY-3 input to GSMIX is the gm-moles of sorbed gas, the gm-moles of residual air, the gm-moles of He backfill, and the gm-moles of fission gas released. The mass of sorbed gas, residual air, and He backfill gas will remain constant with lifetime, however, the relative concentration of the mixture will change with lifetime since the initial

mixture is being diluted with fission gas throughout burnup. The constituents tha make up the fission gas are 15.8% krypton and 84.2% xenon.

Thermal Expansion of Fuel and Clad

Fuel

The thermal expansion of the fuel in the axial and radial directions are considered separately in TAFY-3.

The axial or longitudinal fuel swelling is a function of the mean sectional temperature and the mean coefficient of expansion. The mean section temperature is calculated by the following equation:

$$\bar{T}_a = \frac{T_{max} - T_s}{2}$$

where:

T_{max} = maximum centerline fuel temperature for the axial segment.

T_s = fuel pellet surface temperature.

The mean coefficient of axial expansion (α_a) is temperature dependent and is calculated as follows:

$$\text{if } \bar{T}_a \leq 1950°F$$

$$\alpha_a = 5.699 \times 10^{-6} \quad (2)$$

$$\text{and if } \bar{T}_a > 1950°F$$

$$\alpha_a = 4.005 \times 10^{-6} + 8.575 \times 10^{-10} \bar{T}_a \quad (3)$$

The longitudinal differential expansion for each segment can be calculated and summed to attain the total stack differential expansion using the following equation:

$$\Delta L_f = \sum_{i=1}^{n} \alpha_{a_i} (\bar{T}_{a_i} - T_o) L_i \qquad (4)$$

T_o = initial ambient temperature

L_i = initial segment length @ ambient conditions

ΔL_f = total axial differential expansion of fuel due to thermal effects.

n = total number of axial segments

The pellet radial thermal expansion is also a function of a mean coefficient of linear expansion as given in equations 2 and 3. The equivalent temperature (Tr) is based on the following equation.

$$\bar{T}_r = \frac{\sum_{i=1}^{n} \left[\frac{(T_i - T_{i-1})}{2} \right] (R_{i-1}^2 - R_i^2)}{(R_{max}^2 - R_{min}^2)} \qquad (5)$$

where:

T_i = fuel temperature at i th radial segment

T_{i-1} = fuel temperature at i-1 radial segment

R_{i-1} = radius of 1-1 segment

R_i = radius of i th segment

R_{max} = radius of pellet O.D.

R_{min} = radius of central void. If central void doesn't exist $R_{min} = 0.0$

n = total number of radial segments

The total radial expansion of the fuel due to thermal growth can be written as:

$$\Delta R_f = \alpha_r \ (R_{max} - R_{min}) \ (\bar{T}_r - T_o) \qquad (6)$$

where: $\alpha_r = \alpha_a$

Both of the values for longitudinal and radial thermal growth will vary throughout the lifetime of the fuel since the fuel temperature will vary with lifetime.

Clad

The thermal expansion of the clad in the radial and longitudinal direction are considered separately in TAFY-3.

The longitudinal clad growth is a function of the mean clad temperature and the mean coefficient of linear expansion which is:

$$\alpha_c = 3.1346 \times 10^{-6} + 3.878 \times 10^{-10} \ \bar{T}_c \qquad (7)$$

where:

α_c = coefficient of mean expansion

$\bar{T}_c$ = numerical average of the temperature of the cladding's inner and outer surfaces.

The total axial elongation due to thermal expansion is given by:

$$\Delta L_c = \sum_{i=1}^{n} \alpha_{ci} \ (\bar{T}_{ci} - T_o) \ L_i \qquad (8)$$

where:

T_o = initial ambient temperature

L_i = initial segment length @ ambient conditions

ΔL_c = total axial elongation due to thermal expansion

The clad radial expansion due to thermal effects is assumed to be adequately described by a "thin cylinder" approximation. For thermal expansion the inner cladding radius is computed by:

$$Ric = Ric_o \left[1 + \alpha_c \quad (\bar{T}_c - T_o) \right]$$

where:

Ric_o = inner clad radius @ ambient conditions

α_c = mean coefficient of linear expansion (see equation 8)

T_o = ambient temperature

$\bar{T}_c$ = numerical average of the temperature of the cladding's inner and outer surfaces.

The value of cladding axial and radial thermal expansion will vary directly as the mean cladding temperature varies with lifetime.

Fuel pellet cracking is not treated explicitly by the B&W fuel pin temperature and pressure code TAFY. Fuel pellet cracking, however, is implicit in the empirical data used to formulate the various models contained within TAFY.

2.4. Question 2(d)

A listing of input values used for the TAFY code, including fuel and clad surface roughness and the fuel pin plenum volume.

Response

The AEC model used to predict the fuel pellet geometry and fuel pin internal pressure utilizes the following equations to determine the densified diameter.

$$D_f = D_i - \frac{(\rho_f - \bar{\rho}_i + 2\sigma)\, D_i}{3} \qquad (1)$$

where:

D_f = final densified diameter of the fuel (0.36523)

D_i = nominal value of fuel pellet diameter (0.36998)

ρ_f = final density at which densification is complete (96.5% T.D.)

$\bar{\rho}_i$ = [ ] as built data

2σ = [ ] T.D.

The densified stack length is given by:

$$L_f = L_i - \frac{(\bar{\rho}_f - \bar{\rho}_i)\, L_i}{2} \qquad (2)$$

where:

L_f = final densified stack length, (141.8 in.)

L_i = initial nominal stack length from as-built data, (143.97 in) (143.97)

The total initial void volume is calculated by the following equation. The first term represents the volume in the gap, the second term represents the total plenum volume, and the last term is the dish void volume.

$$V_i = \frac{L_i \pi}{4} (D_c^2 - D_i^2) + [\quad] + \frac{L_i \pi D_i^2}{4} [\quad] \qquad (3)$$

where:

V_i = the initial void volume present in the fuel rod [ ]

D_c = the statistical diameter of the clad I.D. [ ]

The final void volume is given by:

$$V_f = L_f \frac{\pi}{4} (D_c^2 - D_f^2) + [\quad] + \Delta L \frac{\pi}{4} (D_i^2) + \left[L_f \frac{\pi}{4} D_f^2 [\quad] \right] \tag{4}$$

where:

V_f = final total void volume after densification [ ]

$\Delta L = L_i - L_f$

Knowing the initial pre-pressurization level and the initial and final void volumes, the final internal pin pressure can be calculated from:

$$P_f = \frac{P_i V_i}{V_f} \tag{5}$$

where:

P_f = final internal pin pressure after densification [ ]

P_i = initial total pre-pressurization level [ ]

The remaining terms unaffected by densification which are input to TAFY-3 are given below:

Film coefficient = 5000 Btu/hr-ft^2-°F

Coolant Temperature= 582°F

Sorbed Gas = 0.02 cc/gm

Roughness = [ ] (fuel/clad) RHR 10^{-6} in.

2.5. Question 2(e)

A listing of the following parameters calculated with TAFY; hot gap size, fuel pellet diameter, conductivity of gas mixture, temperature jump distance, gap conductance and the contribution of each of the additive terms in the gap conductance. The information should be provided as a function of linear heat generation rate (kW/ft) and as a function of fuel burnup.

Response

The following tables give the requested parameters as calculated with TAFY for densified and undensified fuel.

Table 2-1. Without Densification [ ] Nominal Cold Diametrical Gap)

Linear Heat Rate (Kw/ft)	Burnup (MWD/MTU)	Hot Gap (Mils)	Hot Fuel Pellet Dia. (in)	Conductivity Of Gas (Btu/hr-ft °F)	Temperature Jump Distance (in)
5.6	BOL			0.127733	0.3317×10^{-5}
5.6	End cycle 1			0.095218	0.2011×10^{-5}
20.1	BOL			0.139597	0.2029×10^{-5}
20.1	End cycle 1			0.104022	0.3795×10^{-5}

Table 2-2. With Densification [ ] Diametrical Gap)

5.6	BOl			0.127778	0.5107×10^{-5}
5.6	End cycle 1			0.108418	0.3829×10^{-5}
20.1	BOL			0.148057	0.6382×10^{-5}
20.1	End cycle 1			0.125849	0.4793×10^{-5}

Provided in the two tables below are the individual contrubutions of each additive term in the conductance equation for no densification effects and with densification effect. These results pertain to the Oconee 1 plant and they were obtained from TAFY-3.

Table 2-3. Without Densification

Linear Heat Rate (kw/ft)	Burnup	H_{total} (Btu/hr-ft^2°F)	H_{gas} (Btu/hr-ft^2°F)	H_{solid} (Btu/hr-ft^2°F)	$H_{radiation}$ (Btu/hr-ft^2°F)
5.6	BOL	1364.0	1302.0	60.0	2.0
5.6	End cycle 1	1128.0	1061.0	65.0	2.0
20.1	BOL	3505.0	3347.0	155.0	3.0
20.1	End cycle 1	3235.0	3037.0	195.0	3.0

Table 2-4. With Densification

5.6	BOL	798.0	758.0	38.0	2.0
5.6	End cycle 1	700.0	660.0	37.0	3.0
20.1	BOL	1189.0	1147.0	37.0	5.0
20.1	End cycle 1	1114.0	1069.0	40.0	5.0

2.6. Question 2(f)

Provide comparison of TAFY with fuel performance data. Of interest is comparison with gaps of approximately the size assumed after densification.

Response

The TAFY computer code was developed as an accurate model for the calculation of fuel temperatures within a cylindrical fuel rod. In this endeavor a realistic approach has been taken with regard to the indivdual components of this model. Where little data was available for a particular area of concern a conservative approach was taken. Thus, the complete model should be capable of predicting fuel temperatures in a realistic but generally conservative manner. The ultimate evaluation of the complete model should be its ability to reproduce fuel performance data available in the published literature.

TAFY has been compared to published data with respect to two performance criteria: 1) measured fuel centerline temperatures 2) measured

or "inferred" gap conductances.

Tabular and graphical comparisons of TAFY with data from four sources are presented:

1. "Microscopic, Autoradiographic and Fuel/Sheath Heat Transfer Studies on UO_2 Fuel Elements", A.S. Bain, Chalk River, June 1966, AECL-2588

2. "In-Pile Determination of UO_2 Thermal Conductivity Density Effects and Gap Conductance", G. Kjaerheim and E. Rolstad, December 1967, HPR-80.

3. "In-Pile Measurement of UO_2 Thermal Conductivity", M.G. Balfour, J.A. Christensen and H.M. Ferrari, March 1966, WCAP-2923.

4. "Densification Considerations in BWR Fuel Design and Performance", D.C. Ditmore and R.B. Elkins, December 1972, NEDM-10735.

For each investigation, the pertinent physical parameters have been listed followed by the tabulation of experimental results and the corresponding TAFY prediction. Also included is a separate figure for each reference graphically presenting the tabulated results.

The results of measured centerline temperatures as reported by Cohen, Lustman, and Eichenberg (WAPD-228) were not selected for this comparison due to the extremely low heat rates involved (less than 6 kw/ft). Any comparison with published data in this power range would be of limited value in light of present peak heat rates.

The fuel-to-clad diametral gaps considered in these investigations ranged from 0 to 33 mils, which brackets the gaps encountered in the B&W fuel products, with and without the assumption of densification.

Due to the inherent uncertainties in "measuring" gap conductance the measured fuel centerline temperatures of HPR-80 and WCAP-2923 were selected as the most appropriate indication of TAFY's ability to reproduce published data. The composite of the TAFY comparison with these two sources is shown in Figure 2-1. As seen in this Figure, TAFY has been shown to be capable of predicting measured centerline temperatures in a realistic but generally conservative manner.

Figure 2-1. TAFY Comparison With Published Data

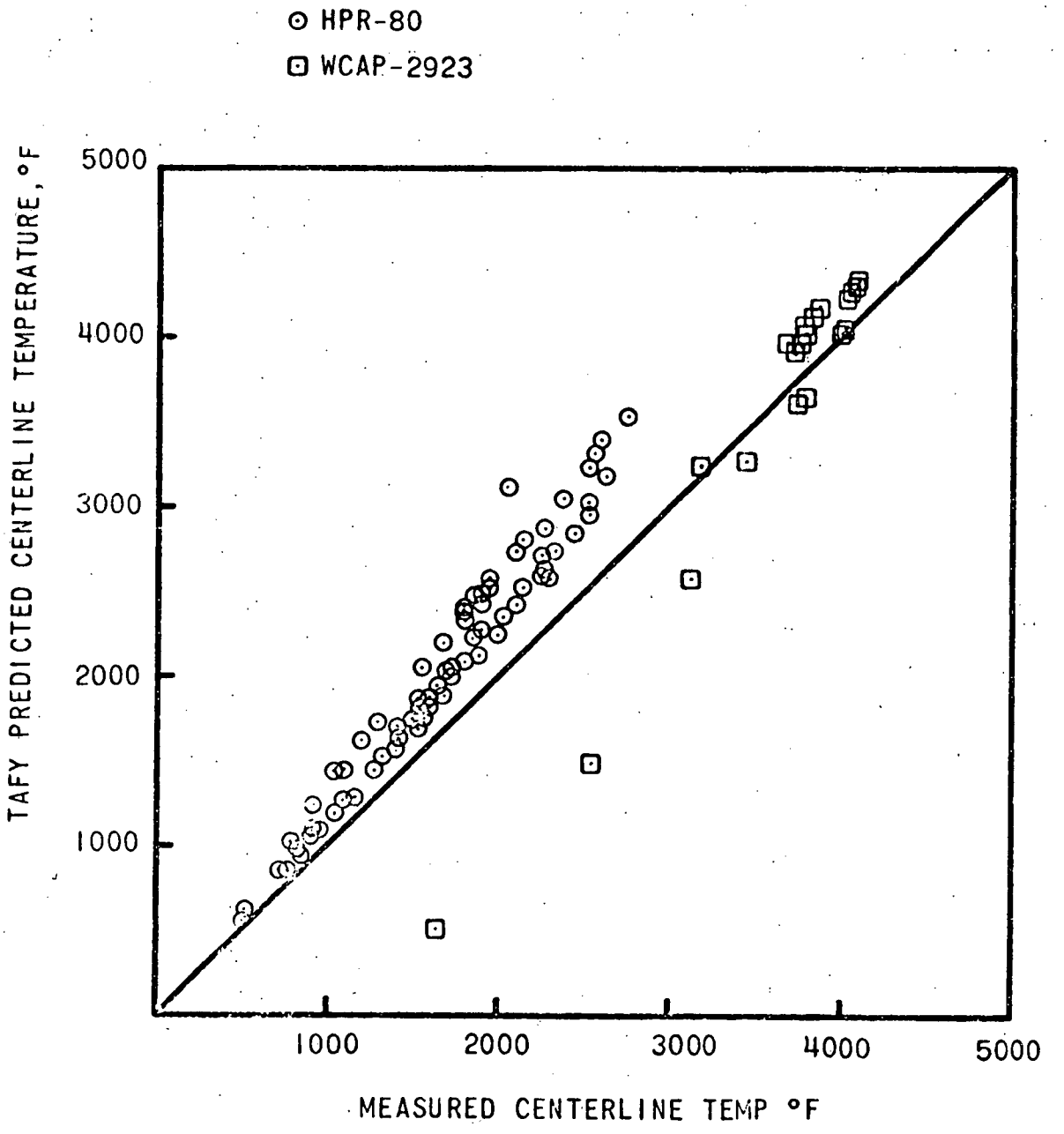

1. Comparison of TAFY with published data source 1, "Microscopic, Autoradiographic and Fuel/Sheath Heat Transfer Stuides on UO_2 Fuel Elements"

TAFY predictions of gap conductance are compared to gap conductances inferred from measured melt radii. The experiment represents a wide range of fuel-to-clad diametral gaps, fuel clad interface atmospheres and clad materials. The two tests were the Hydraulic Rabbit Test (coolant temperature = 50F and pressure = 100 psia) and the X-23201, S-23303, X-23401 Loop Tests (coolant temperature = 482F and pressure = 1420 psia). The specific conditions for the various elements are tabulated on the following page for the two tests.

Table 2-5. Test Data

ELEMENT NO.	CLAD MATERIAL	FILL GAS	U-235 WT. %	DENSITY % T.D.	CLAD I.D. IN.	CLAD O.D. IN.	FUEL LENGTH IN.	TEST APPARATUS
E-4, E-14	S.S.	AR.	1.0	97.8	.669	.721	2.76	PHASE 13 HYDRAULIC RABBIT
E-17 – E-31	S.S.	AR.	1.5	97.8	.669	.721	2.76	"
E-34 – E-45; E-47	S.S.	AR.	2.2	97.35	.669	.721	2.76	"
E-46, E-48	S.S.	HE.	2.2	97.35	.669	.721	2.76	"
E-49 E-59	ZR-4	AR.	2.75	97.2	.669	.721	2.76	"
M-9, M-10	ZR-2	AR.	2.0	96.0	.669	.719	3.01	X-23400 HYDRAULIC RABBIT
M-11, M-12	ZR-2	VAC.	2.0	96.0	.669	.719	3.01	"
M-15, M-16	ZR-2	AR.	2.75	96.0	.669	.719	3.01	"
M-17, M-18	ZR-2	VAC.	2.75	96.0	.669	.719	3.01	"
SR, SS	S.S.	AR.	3.99	95.3	.670	.722	2.76	PHASE 10 HYDRAULIC RABBIT
VC, VD	S.S.	VAC.	3.99	95.8	.666	.686	2.76	"
VE, VF	S.S.	AR.	3.99	95.8	.666	.686	2.76	"
VG, VH	S.S.	VAC.	4.82	96.7	.666	.686	2.76	"
VI, VJ	S.S.	AR.	4.82	96.7	.666	.686	2.76	"
FAO	ZR-2	AR.	1.5	95.8	.720	.794	6.0	X-23301 X-23303 X-23401
FAT	AR-2	AR.	1.5	95.9	.720	.794	6.0	"
FAP	ZR-2	AR.	1.5	95.5	.720	.794	6.0	"
FAW	ZR-2	AR.	1.5	95.5	.720	.794	6.0	"
FAR	ZR-2	AR.	1.5	95.7	.720	.794	6.0	"
FAX	ZR-2	AR.	1.5	95.7	.720	.794	6.0	"
FAS	ZR-2	AR.	1.5	96.0	.720	.794	6.0	"
FAY	ZR-2	AR.	1.5	96.1	.720	.794	6.0	"
FAN	ZR-2	AR.	1.5	95.7	.720	.794	6.0	"
FAZ	ZR-2	AR.	1.5	96.1	.720	.794	6.0	"
FAE	ZR-2	AR.	1.5	95.9	.7397	.800	6.0	"
FAF	ZR-2	VAC.	1.5	96.9	.7397	.800	6.0	"
FAT	ZR-2	AR.	1.5	96.2	.7401	.800	6.0	"
FAK	ZR-2	VAC.	1.5	96.2	.7397	.800	6.0	"

Table 2-6. TAFY Comparison With Phase 13 Hydraulic Rabbit Test Results

ELEMENT NO.	DIA. GAP (IN)	HEAT RATE (KW/FT)	GAP CONDUCTANCE TAFY (BTU/HR-FT^2-F)	GAP CONDUCTANCE EXPERIMENT (BTU/HR-FT^2-F)
E-4	.033	15.4	187	125
E-12	.033	15.1	170	117
E-17	.020	21.6	355	248
E-18	.026	21.3	263	236
E-20	.033	19.8	199	185
E-21	.020	21.0	335	233
E-22	.033	20.3	202	199
E-23	.020	21.3	345	254
E-24	.033	20.6	205	199
E-26	.026	20.1	245	217
E-28	.033	19.6	197	188
E-29	.026	20.1	245	217
E-31	.026	19.7	238	203
E-34	.026	25.0	327	336
E-36	.033	26.6	265	308
E-37	.020	26.1	499	444
E-38	.033	25.5	253	294
E-39	.020	26.3	507	520
E-41	.020	27.7	562	493
E-42	.026	27.3	377	402
E-43	.013	28.5	1055	749
E-44	.033	26.7	266	314
E-45	.026	25.5	337	395
E-46	.026	25.4	392	486
E-47	.026	25.4	266	361
E-48	.026	25.5	394	486
E-49	.006	35.9	1667	2325
E-52	.006	35.6	1655	2149
E-53	.020	33.7	862	1075
E-54	.020	33.7	862	1013
E-55	.020	34.0	883	978
E-56	.020	33	876	1145
E-57	.006	34.8	1655	1762
E-58	.020	33.1	822	942
E-59	.006	35.3	1655	1762

Table 2-7. TAFY Comparison with X-23301, X-23303, X-23401 Loop Test Results

ELEMENT NO.	DIA. GAP IN.	HEAT RATE KW/FT	TAFY (BOL) BTU/HR-FT^2-F	TAFY (8000 MWD/MT) BTU/HR-FT^2-F	EXPERIMENT BTU/HR-FT^2-F
FAP	.015	20.5	580	477	481
FAW	.029	20.5	254	207	276
FAR	.015	20.5	580	477	490
FAX	.029	18.6	228	183	257
FAS	.015	17.6	456	373	370
FAY	.029	15.6	198	149	231
FAN	.015	22.0	658	541	528
FAZ	.029	22.0	281	231	317
FAO	.015	17.4	449	366	352
FAT	.029	18.6	228	183	234

Table 2-8. TAFY Comparison with X-23400 Hydraulic Rabbit Test Results

ELEMENT NO.	DIA. GAP IN.	HEAT RATE KW/FT	TAFY BTU/HR-FT^2-F	EXPERIMENT BTU/HR-FT^2-F
M-9	.004	35.9	1584	3259
M-10	.004	33.0	1571	3523
M-11	.004	33.0	1651	7222
M-12	.004	33.0	1642	4404
M-15	.004	39.5	1591	2378
M-16	.004	39.5	1578	2114
M-17	.004	39.5	1669	3347
M-18	.004	39.5	1656	21490

Table 2-9. TAFY Comparison with Phase 10 Hydraulic Rabbit Test Results

ELEMENT NO.	DIA. GAP IN.	HEAT RATE KW/FT	TAFY BTU/HR-FT^2-F	EXPERIMENT BTU/HR-FT^2-F
SR	.003	33	2220	2290
SS	.003	33	2215	2290
VC	.0039	33.8	1870	2079
VD	.0039	33.8	1870	2079
VE	.0039	33.6	1812	1585
VF	.0039	33.5	1810	1585
VG	.0039	37.2	1859	2889
VH	.0039	37.0	1856	2008
VI	.0039	38.0	1794	1585
VJ	.0039	37.8	1791	1585

Figure 2-2. TAFY Comparison With Published Data

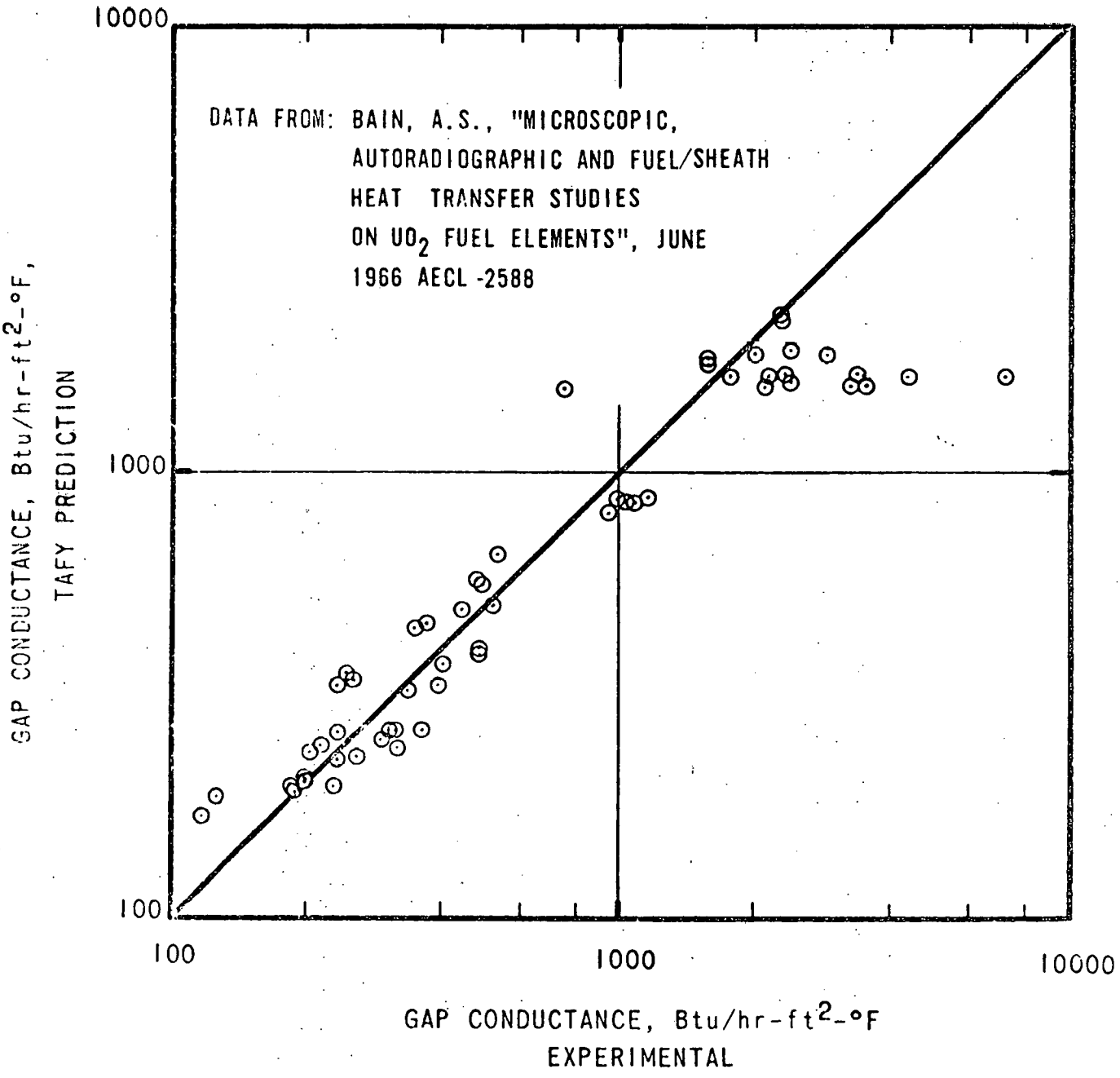

2. Comparison of TAFY with published data source 2, "In-Pile Determination of UO_2 Thermal Conductivity, Density Effects and Gap Conductance

Table 2-10. Test Data*

Fuel Rod	Thermocouple	Diametral Gap (IN)	Density (% T.D.)
HBA	11TF-1	.00189	98
HBB	11TF-2	.00205	96
HBC	11TF-3	.00650	96
HCA	21TF-1	.00185	98
HCC	21TF-2	.00661	96
HCD	21TF-3	.00228	96

* The following conditions were constant for all the fuel rod samples:

Pellet stack ht, in.	67.5
Clad material	Zr-2
Clad surface roughness, μin.	157.5
Pellet roughness, μin.	49.2
Clad surface temperature, F	473

Table 2-11. TAFY Comparison With Halden Test Results

HEAT RATE	CENTERLINE TEMPERATURE		GAP CONDUCTANCE	
	TAFY	HALDEN	TAFY	HALDEN
KW/FT	(F)	(F)	BTU/HR-FT^2-F	BTU/HR-FT^2-F
Fuel Rod HBA - Thermocouple 11TF-1				
2.90	870	734	710	1370
3.81	980	824	750	1430
4.72	1110	932	820	1500
8.23	1640	1418	1060	1780
8.99	1750	1499	1130	1860
9.30	1810	1580	1140	1870
9.45	1880	1580	1150	1880
9.45	1880	1544	1150	1880
10.06	1950	1652	1210	1920
11.80	2260	1994	1350	2060
13.47	2590	2228	1500	2150
15.54	3030	2516	1500	2200
Fuel Rod HBB - Thermocouple 11TF-2				
0.76	560	518	---	---
2.90	860	752	670	1330
3.66	960	842	720	1380
4.63	1100	968	770	1450
5.79	1290	1168	850	1540
8.08	1700	1436	1020	1730
8.84	1820	1544	1080	1790
9.20	1890	1670	1110	1820
9.30	1900	1634	1120	1830
9.30	1900	1688	1120	1830
9.75	2000	1724	1160	1870
11.58	2350	2012	1320	2020
13.26	2710	2246	1460	2160
15.39	3180	2624	1500	2200
Fuel Rod HBC - Thermocouple 11TF-3				
0.76	620	518	---	---
2.59	1020	788	250	590
3.66	1250	932	280	610
4.63	1450	1098	310	630
5.79	1730	1310	330	650
7.99	2210	1670	400	710
8.75	2380	1796	430	740
8.99	2430	1904	440	750
9.20	2490	1850	440	750
9.20	2490	1904	440	750
9.60	2570	1940	450	770
11.34	2380	2264	510	840
14.94	3540	2750	720	1080

Table 2-11. TAFY Comparison With Halden Test Results (Cont'd)

Fuel Rod HCA - Thermocouple 21TF-1

HEAT RATE	CENTERLINE TEMPERATURE		GAP CONDUCTANCE	
	TAFY	HALDEN	TAFY	HALDEN
(KW/FT)	(F)	(F)	BTU/HR-FT^2-F	BTU/HR-FT^2-F
4.72	1100	950	840	1530
5.49	1190	1040	890	1600
5.94	1270	1112	920	1630
7.22	1460	1274	1000	1720
8.84	1700	1526	1130	1850
9.20	1760	1562	1160	1880
10.06	1900	1670	1220	1950
10.97	2100	1814	1300	2020
11.13	2120	1868	1310	2030
12.50	2380	2111	1420	2140
13.56	2630	2264	1480	2190
14.69	2950	2516	1480	2180

Fuel Rod HCC - Thermocouple 21TF-2

4.48	1450	1049	280	640
5.33	1620	1184	310	670
5.70	1710	1292	320	680
7.16	2050	1562	360	720
8.53	2320	1796	410	770
8.84	2400	1841	420	770
9.39	2530	1940	430	800
9.60	2570	1940	440	810
10.52	2740	2102	470	830
10.82	2810	2156	480	850
12.10	3060	2372	520	890
12.50	3120	2466	540	910
13.11	3240	2534	570	930
13.56	3310	2543	600	960
14.17	3400	2606	630	990

Fuel Rod HCD - Thermocouple 21TF-3

4.57	1070	887	750	1370
5.39	1200	1040	800	1430
5.79	1280	1148	830	1460
7.01	1520	1328	910	1550
7.32	1570	1400	930	1580
8.69	1850	1562	1030	1680
8.99	1900	1634	1060	1710
9.66	2010	1706	1110	1770
9.75	2050	1724	1120	1780
10.73	2240	1841	1180	1850
10.97	2270	1904	1200	1880
12.25	2530	2138	1300	1990
12.65	2600	2246	1340	2020
13.32	2740	2318	1390	2070
13.78	2840	2444	1430	2090
14.33	2950	2534	1470	2090

Figure 2-3. TAFY Comparison With Published Data

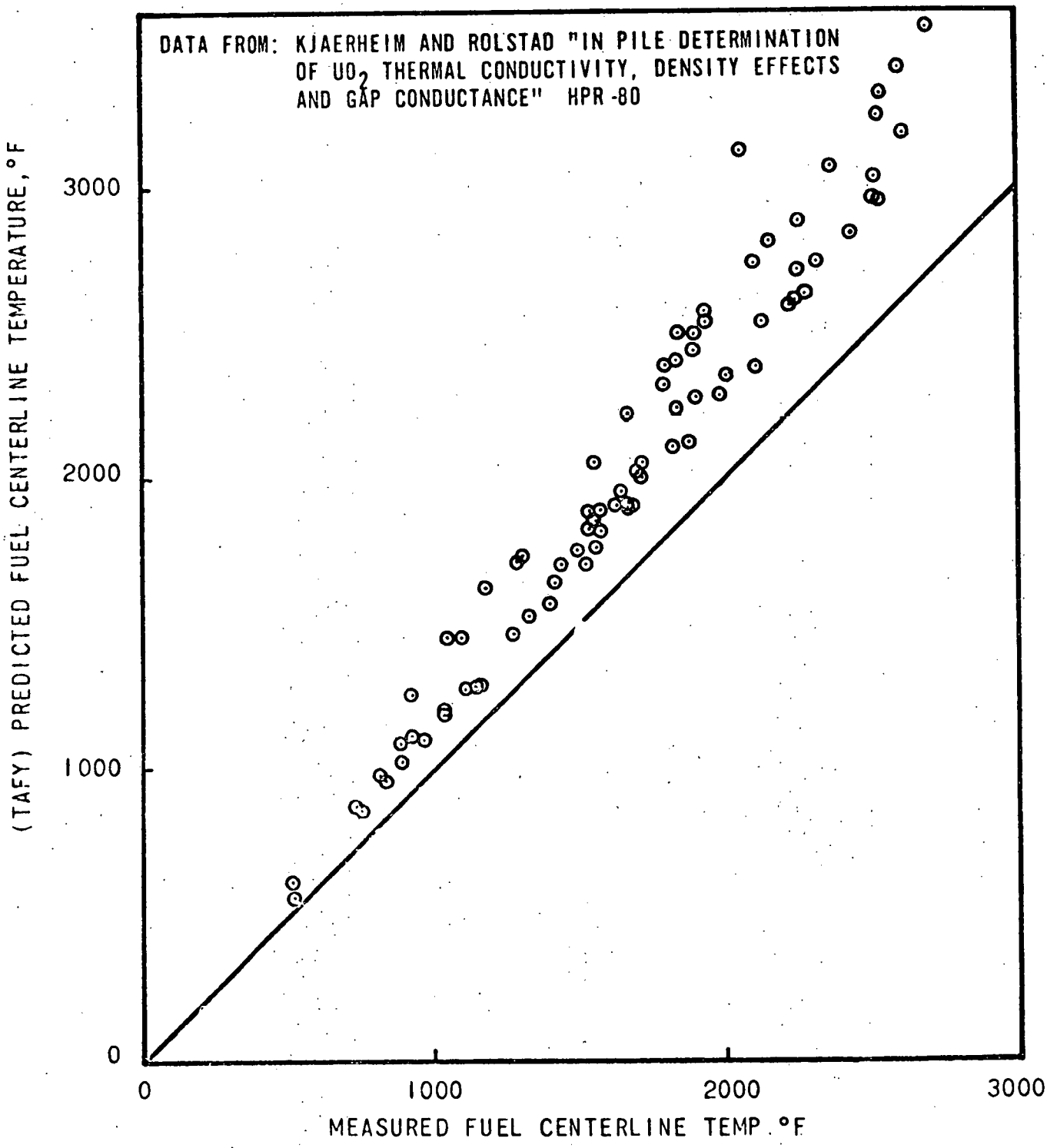

3. Comparison of TAFY with published data source 3, "In-Pile Measurement of UO_2 Thermal Conductivity"

Table 2-12. Test Data

Capsule I

Average heat rate	22 KW/FT
Fuel Density	95% T.D.
Enrichment	.64 w/o U-235
Fuel OD	1.25 in.
Fuel ID	0.068 in.
Clad ID	1.2745 in.
Fuel-to-Clad Dia. Gap	.0245 in.
Pellet and Clad Roughness	70 μin.
Clad Material	348 SS
Fuel-Clad Atmos.	1 atm He.

Capsule II

Average heat rate	23.6 KW/FT
Fuel Density	95% T.D.
Enrichment	.82 w/o U-235
Fuel OD	1.25 in.
Fuel ID	0.068 in.
Clad ID	1.2745 in.
Fuel-to-Clad Dia. Gap	.0245 in.
Pellet and Clad Roughness	70 μin.
Clad Material	348 SS
Fuel-Clad Atmos.	1 atm He.

Table 2-13. TAFY Comparison With Test Results

Capsule I:

Time (Hours)	$\dot{q}'$ KW/FT	T (°C)	T (F) (Experiment)	T (F) TAFY
6.5	16.2	1750	3180	3230
8.0	21.2	2030	3690	3962
9.5	20.8	2050	3720	3905
12.5	21.2	2070	3760	3962
16.5	21.7	2089	3790	4029
18.0	21.95	2095	3800	4064
20.5	22.34	2113	3840	4115
24.5	22.92	2131	3870	4193

Capsule II:

Time (Hours)	$\dot{q}'$ KW/FT	T (°C)	T (F) (Experiment)	T (F) TAFY
1.5	2.16	894	1640	523
2.5	8.23	1399	2550	1503
3.5	13.35	1720	3130	2584
5.0	16.61	1904	3460	3272
6.0	18.96	2073	3760	3614
7.0	19.20	2098	3790	3649
8.5	21.79	2209	4010	4013
9.5	21.95	2215	4020	4034
10.5	23.62	2239	4060	4253
11.5	23.71	2245	4070	4265
13.5	23.99	2250	4080	4299
15.5	24.23	2260	4100	4330
19.5	24.69			
23.5	25.21			
27.5	25.73			
29.5	25.97			

Figure 2-4. TAFY Comparison With Published Data

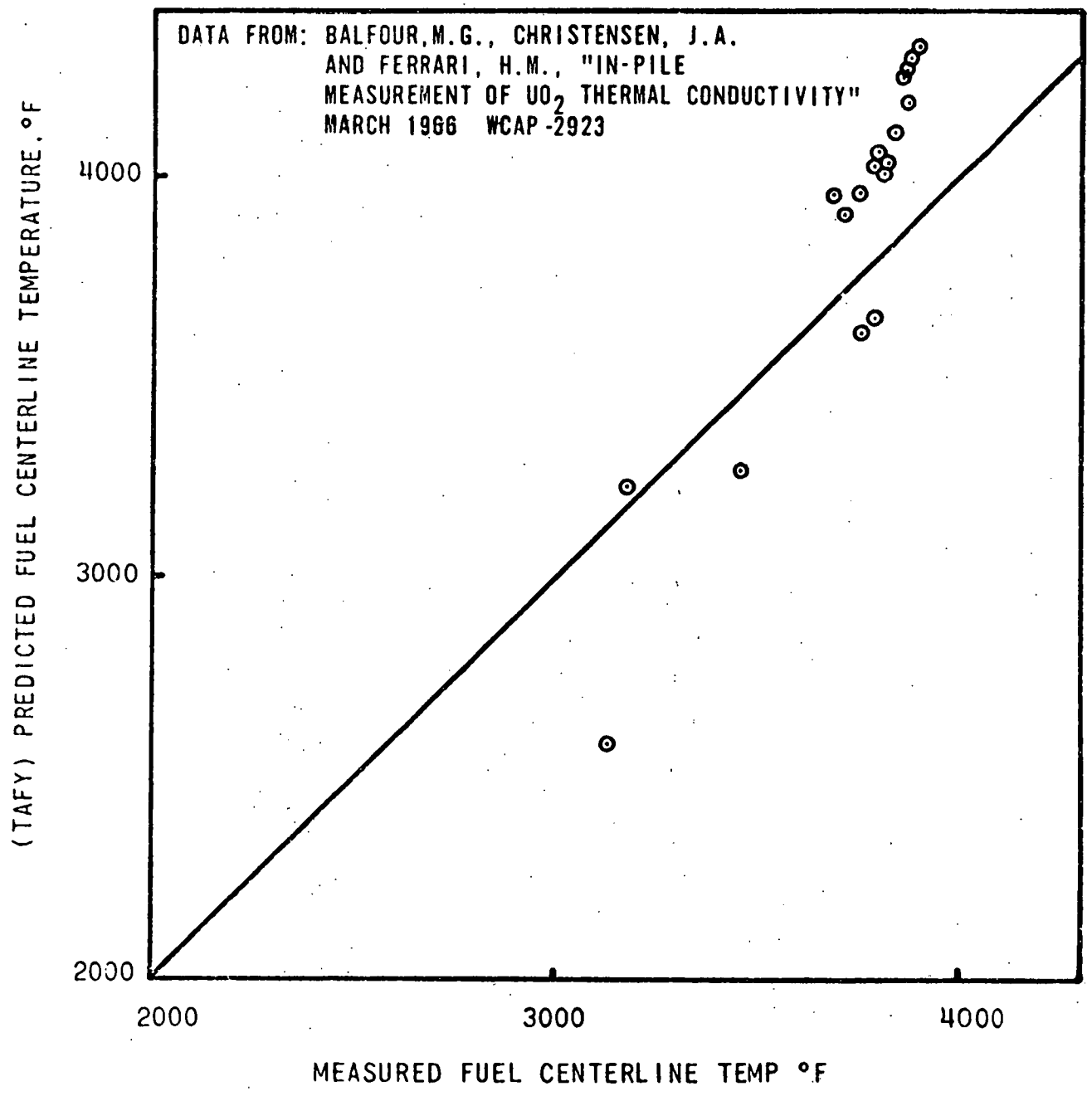

4. Comparison of TAFY with published data source 4, "Densification Considerations in BWR Fuel Design and Performance".

Table 2-14. G.E. Test Data

	Element	
	DP4	AEG
Pellet Diameter	.489 in	.488 in.
Clad O.D.	.565 in.	.544 in.
Clad I.D.	.505 in.	.5038 in.
Pellet Density	95% T.D.	95% T.D.
Enrichment	2.5 wt % U-235	2.5 wt % U-235
Atmosphere	1 atm He	1 atm He
Fuel Surface Roughness	39 μ in.	39 μ in.
Clad Surface Roughness	20 μ in.	20 μ in.
Coolant Pressure	1050 psi	1050 psi
Coolant Temperature	590 °F	590 °F
Fuel Length	30 in.	30 in

Table 2-15. TAFY Prediction of G.E. Test Data Results

Rod AEG - (Beginning-of-Life):

Heat Rate	Gap Conductance (BTU/HR-FT^2-F)	
(KW/FT)	W/Zr-2 Clad	W/SS Clad
10	435	478
11	446	485
12	460	494
13	473	503
14	488	514
15	506	526
16	525	540
17	547	557
18	572	575
19	599	597
20	630	620
21	663	647
22	716	688
23	773	736
24	837	789

Sorbed Gas Content = 0.05 cc/gm

Table 2-15. TAFY Prediction of G.E. Test Data Results (Cont'd)

Rod DP-4:

Heat Rate KW/FT	Gap Conductance (BTU/HR-FT^2-F) BOL Sorbed Gas Content 0.0 cc/gm	BOL Sorbed Gas Content 0.05 cc/gm	8000 MWD/MT Sorbed Gas 0.0 cc/gm
10	684	436	223
11	694	448	236
12	707	461	249
13	721	474	265
14	736	490	282
15	754	507	300
16	774	526	321
17	796	549	343
18	821	573	368
19	850	601	393
20	881	631	436
21	916	668	477
22	955	723	521
23	1017	782	569
24	1091	847	622

Table 2-5. TAFY Comparison With Published Data

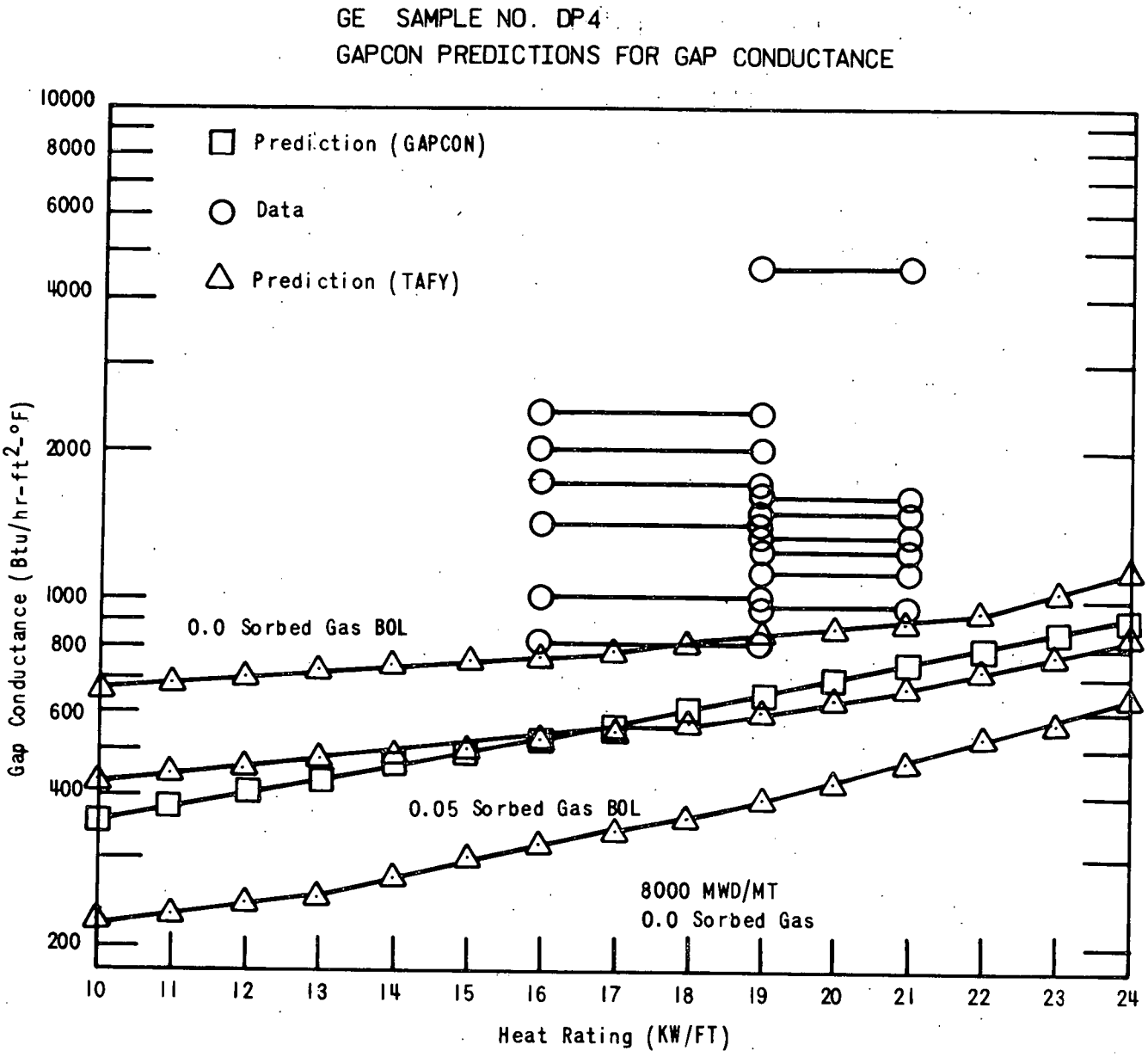

Table 2-6. TAFY Comparison With Published Data

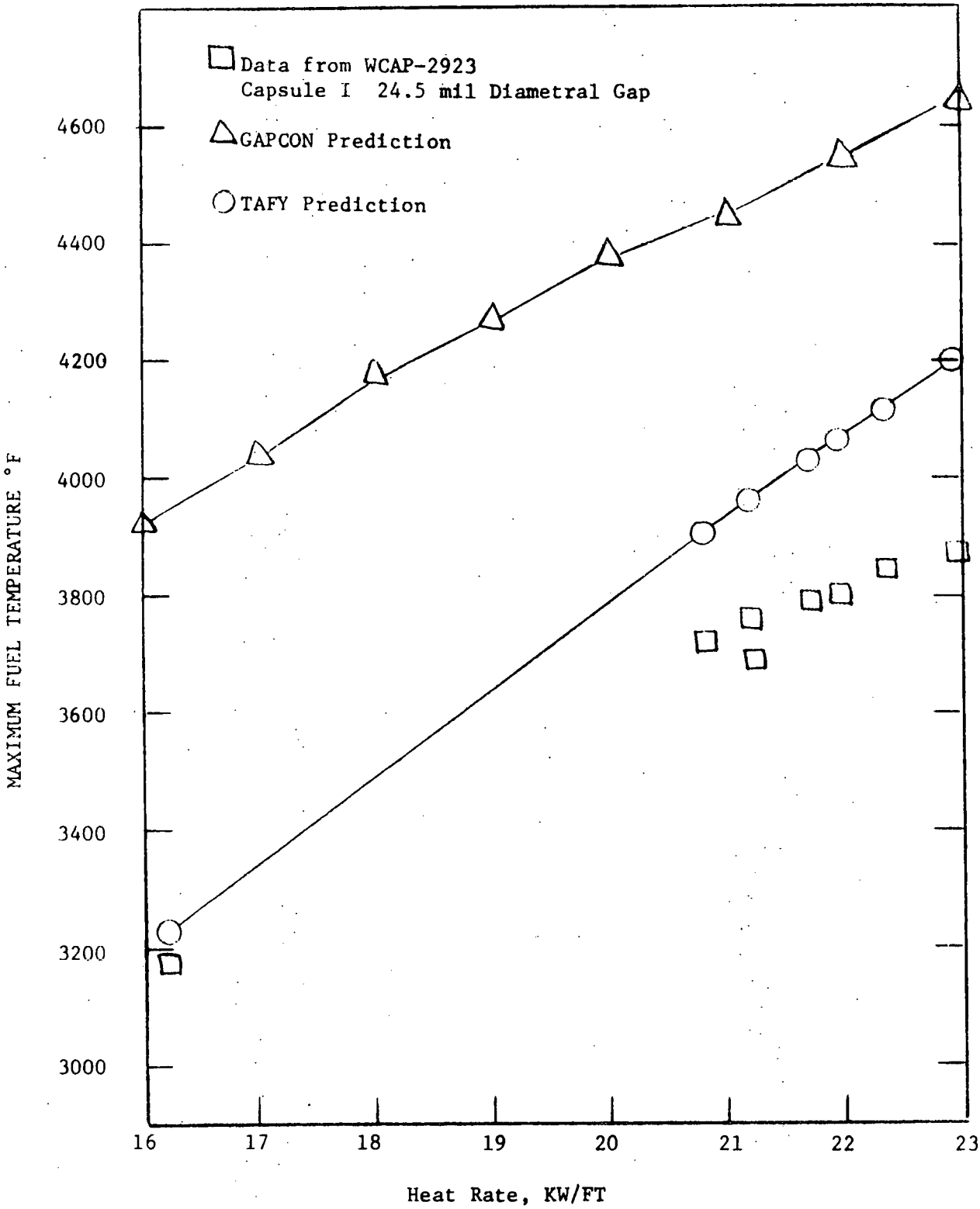

Question 3

Provide additional information on the fuel cladding creep tests that were performed in the BAWTR and that form the basis for the B&W clad creep model, CRECϕL (ed. B&W collapse model), which is used to calculate the expected collapse time for the Oconee Unit 1 fuel cladding. The requested information should include:

3.2. Question 3(b)

Physical dimensions of samples including measured outside diameter, ovality, and thickness.

Response

OD = 0.430 ± <0.001

Initial ovality = <0.0005

Thickness = 0.0265 ± <0.0005

Figure 3-1. Typical Tubing Profilometer Trace

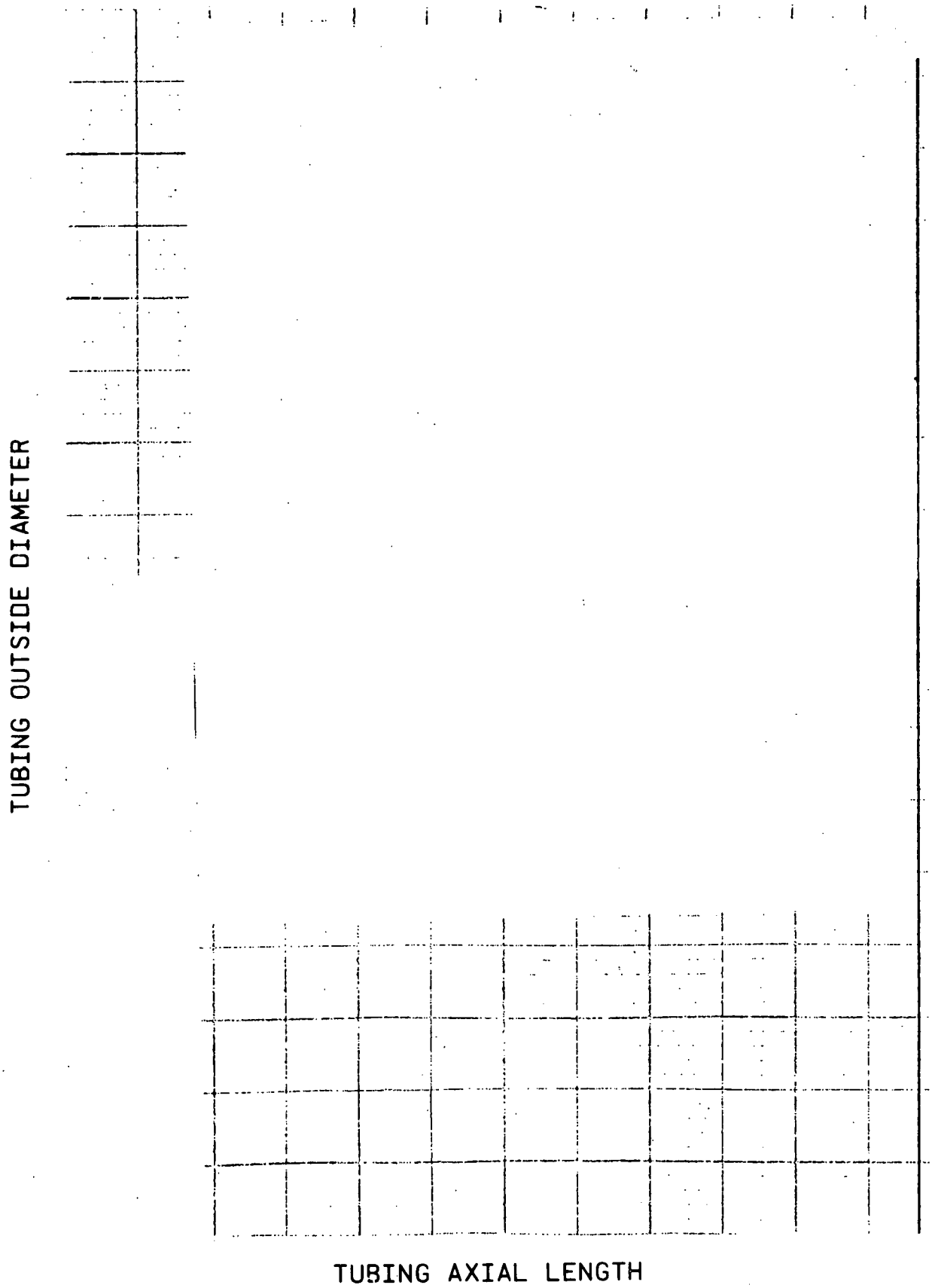

Figure 3-2. Typical Tubing Profilometer Trace

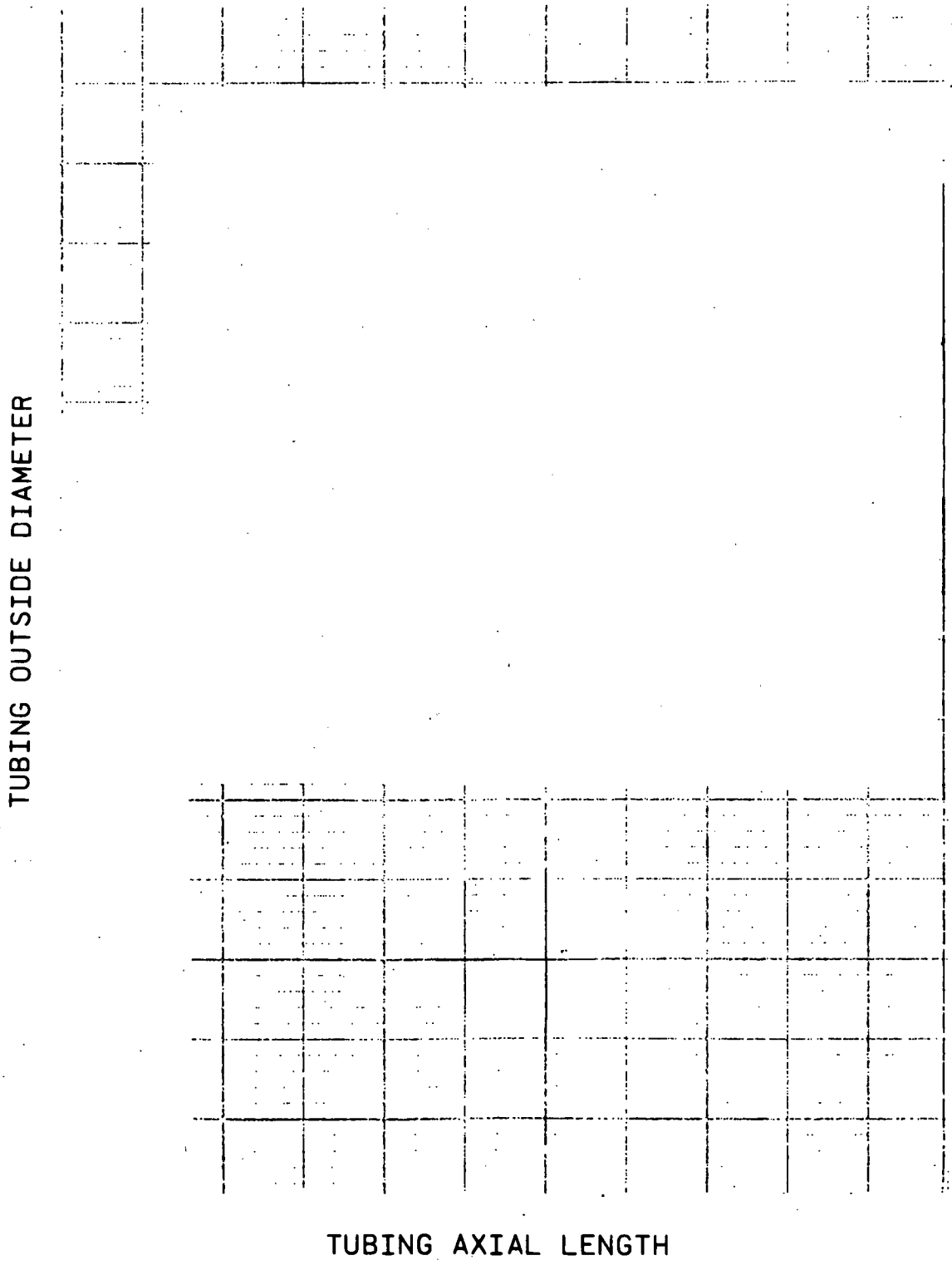

Figure 3-3. Typical Tubing Profilometer Trace

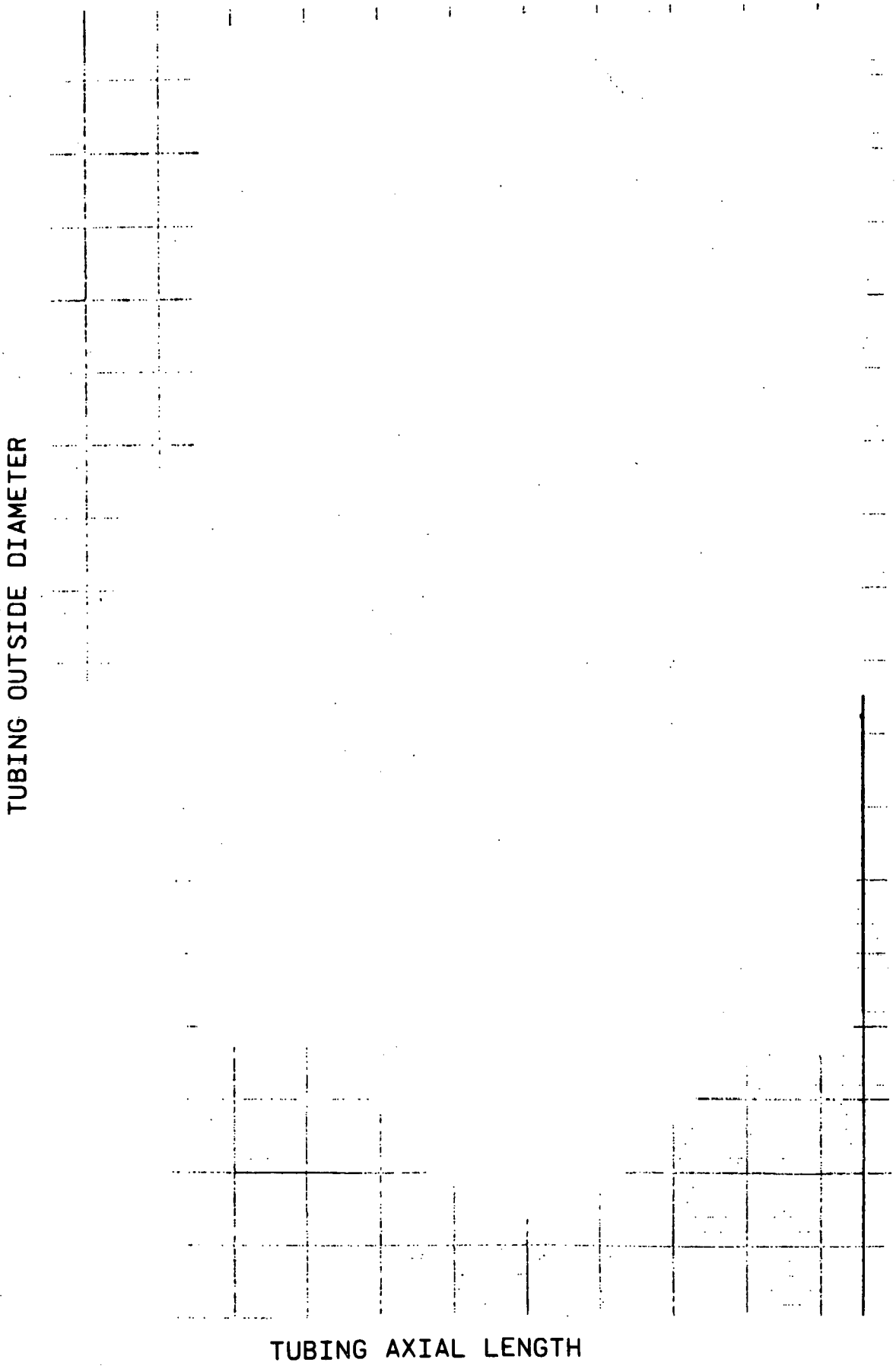

Question 4

In order to assess the B&W collapse model, CRECϕL (ed. B&W collapse model), that is used to calculate expected collapse time for the fuel pins in Oconee Unit 1, the following additional information is required:

4.1. Question 4(a)

The equation used to calculate collapse ovality and a justification for not using the creeprate of irradiated fuel in that calculation.

Response

$$\sigma_\Theta^{(i)} = \sigma_\Theta^{(i-1)} - \frac{12\,qr}{h^3\,(1-\Psi)} \cdot Z\,\Delta w_o^{(i)} + \frac{12\,\Delta M^{(i)} I}{h^3} \cdot Z$$

$$+ \frac{\Delta N_I^{(i)}}{h} - \frac{E}{I-\nu^2} \cdot (\Delta\varepsilon_\Theta^{(i)} + \nu\Delta\varepsilon_x^{(i)})$$

$$w_o^{(i)} = w_o^{(i-1)} + \Delta w_o^{(i)}$$

Refer to GAMD-9623 for a derivation and an explanation of terms. When the effective von Mises stress reaches the material yield strength, collapse is assumed to have occurred. The $w_o^{(i)}$ at this point is defined as the collapse ovality. CRECØL is utilized only to calculate the ovality at which the cladding becomes unstable, given a certain temperature and differentail pressure. Since irradiation effects on physical properties (i.e., yield strength) are ignored, collapse ovality becomes a function of geometry only.

4.2. Question 4(b)

A detailed description and justification for the extrapolation of BAWTR test data to the collapse time by use of the Larson Miller Parameter (LMP) including specific literature eferences to this method of extrapolation.

Response

In WAPD-TM-585, Figures 121, 122 and 123 depict a series of curves of hoop stress versus LMP for a variety of textures and geometries. For the range of pressure from 2000-3000 psi, these curves are appropriately linear and they can be extrapolated to 1000 psi. The B&W data was extrapolated over essentially the same range.

4.3. Question 4(c)

A justification for not including in the cladding stress analysis

such axial forces as cuased by pellet hangup, rod interference on grid plates, and rod bending at the spacer grids.

Response

Axial force due to pellet hangup will be accommodated by the flexible spacers located at both ends of the fuel rod.

All B&W fuel assemblies have sufficient gaps between the fuel rods and the upper end fitting to accommodate all differential growth between rods and guide tubes. This is true for both operating and refueling conditions.

B&W spacer grids have been designed to permit fuel rod axial slip at forces less than those necessary to cause significant bow in the fuel rods.

4.4. Question 4(d)

A comparison of CRECØL (ed. B&W collapse model) calculated critical ovality and collapse time with experimental clad performance data.

Response

Experimental specimens could only be observed during measurement periods, so it is impossible to determine the exact collapse ovality. However, the equations used in CRECØL to calculate when stress reaches the instability criterion include conservative assumptions. These lead to conservative collapse ovality predictions, as demonstrated by experimental data from unirradiated specimens at both 2250 and 2475 psi differential pressure. One specimen at 2250 psi had [ ] mils ovality without collapsing. Specimens at 2475 psi exhibited [ ], and [ ] mils ovality without collapse vs. the CRECØL prediction of about [ ] mils.

Experimental data were used to prepare Figure 3.3-3 in BAW-10054, so experimental collapse-times for specimens are implied directly from the curve (time-to-collapse is defined as the time it takes to reach the conservative CRECØL collapse ovality).

4.5. Question 4(e)

A discussion of how flow induced fuel pin vibrations could affect the fuel pin collapse time.

Response

As described in the Rancho Seco FSAR, mid-span fuel rod deflections due to flow-induced vibration have been experimentally determined to be less than [ ] mil. This experimentation is applicable to all B&W fuel assemblies. The stresses imposed on the cladding due to this deflection are insignificant.

4.6. Question 4(f)

A discussion of the clad temperature used in the CRECØL (ed. B&W collapse model) calculation.

Response

Cladding OD temperature along gap in the pellet stack drops to the coolant temperature within about 1/8". Temperature increase across the cladding wall has been calculated to be 3 degrees due to heat radiating from pellets at the boundary. Therefore, the assumed maximum cladding temperature for any gap is the hot-channel coolant temperature corresponding to the peaks described in item 5d, step 6, plus 3 degrees.

4.7. Question 4(g)

A comparison of the B&W CRECØL code and the CRECØL code described in USAEC Report GAMD 9623, GGA, 1969. The comparison should identify any changes made to result in the present B&W version.

Response

1. A subroutine "ZIRC" was added for Zircaloy-4 material properties based on BAW-3765-6, except for Poisson's ratio from WCAP-3629-41 and creep rate from AECL-2528.
2. A subroutine "PØLY" was added to evaluate the material properties in 1.
3. A creep rate evaluation change was made in "CREEP" to handle the different form of the AECL-2528 Zircaloy creep equation from the Hastelloy and stainless equations already in CRECØL.
4. In subroutine "RSTRESS", the initial time increment was increased to improve run time. This had no effect on the 5% change-in-ovality limit per time increment.

Question 5

In order to perform an independent staff evaluation of the clad integrity for Oconee Unit 1, the following information is requested:

5.1. Question 5(a)

Detailed discussion of the 0.9 value for the usage factor and of the damage categories included in the analysis.

Response

The 0.9 usage factor is allowable cumulative fatigue factor, not that predicted to occur in Oconee 1. The actual factor is calculated (based on Miner's rule) for bending, thermal and hoop stresses which occur during fluctuations in reactor power.

5.2. Question 5(b)

Collapse time calculated with CRECØL (ed. B&W collapse model) with a comparison to one cycle and three cycle operating times.

Response

Predicted time-to-collapse is [ ] hours when fission-gas buildup is ignored. One cycle operating time is 7440 hours and three cycle time is 22,320 hours.

5.3. Question 5(c)

A list of operating conditions and physical properties including:

maximum operating time
maximum external fuel pin pressure
clad temperature
clad outside diameter
clad thickness
initial ovality
yield stress vs. temperature and fast flux
elastic modulus vs. temperature
Poisson ratio vs. temperature
internal fuel pin pressure vs. time
fast flux

Response

1. Maximum operating time - 22,320 hours
2. External fuel pin pressure - 2200 psia
3. Cladding temperature and rod internal pressure vs. time -

4. Cladding OD - [ ] in. mean, σ = [ ] in.
5. Cladding thickness - [ ] in. mean, σ = [ ] in.
6. Cladding initial ovality - [ ] in. mean, σ [ ] inches.
7. Fast flux - 6.94×10^{13} - nvt (> 1 mev)
8. Yield stress elastic modulus, and Poisson's ratio as a function of temperature.

Temperature - F	σy - psi x 10^{-3}	E - psi x 10^{-6}	ν
500			.265
525			.264
550			.262
575			.260
600			.258
625			.256
650			.255
675			.253
700			.251
725			.250
750			.248

9. Yield stress as a function of fast fluence - (See following page).

5.4. Question 5(d)

Discussion of the assumptions for the internal fuel pin pressure vs. time, including the cold and hot BOL pressure with and without fuel densification.

Response

1. An initial gap between the pellet and cladding is calculated on the basis of as-built dimensions. Mean as-built pellet OD is combined with mean as-built cladding I.D. minus two standard deviations to determine a minimum BOL gap. These dimensions result in fuel pellets with low thermal expansion and fission-gas release, and therefore a rod with a high pressure differential.
2. Initial pellet density equals the mean as-built density for 3-cycle fuel assemblies. When the pellet densifies to 96.5%, a change in stack and pellet dimensions produces a change in rod internal pressure. The use of the minimum diametral gap in the above step produces a minimum gap volume which can contain backfill gas. The increase is void volume due to pellet shrinkage will therefore in this case have the greatest effect on BOL pressure.
3. Internal rod pressure preceeding densification is assumed

to be the lowest allowable under the tolerance for backfill gas (all B&W fuel will be prepressurized).

4. Rod length, end cap dimensions, and internal spacer arrangement and dimensions are all assumed to be such that rod internal void volume is a minimum.

5. Combining steps 1 to 4, BOL cold rod internal pressure is calculated by the equation:

$$\text{BOL PRESSURE} = \text{BACKFILL PRESSURE} \times \frac{\text{Rod Void Volume Before Densification}}{\text{Rod Void Volume After Densification}}$$

The increase in void volume is based on pellet dimensional changes calculated in accordance with the AEC technical report of November 14, 1972.

6. For each plant, the radial x local peaking histories of 3-cycle assemblies are examined to determine a conservative worst-case rod peaking history. For each time increment (varying from 25 to 100 days) the maximum peak for any 3-cycle assembly is assumed to be the peak for that increment. Thus the final "assembly" peaking history represents a combination of peaks from many assemblies. Rod peaking history is obtained by applying a rod-peak/assembly-peak ratio [ ] to the assembly history. A [ ] uncertainty factor is also applied. After relating the history to burnup, the resulting peaking-burnup history is used as input to the TAFY code (along with the rod geometry and pressure described above) to compute the rod internal pressure versus time history.

Hot BOL pressure calculated by the above steps represents a minimum value for the densified case. For Oconee 1, this pressure is [ ] psia. For the non-densified case, hot BOL internal pressure is [ ] psia, based on a cold BOL backfill pressure of [ ] psia and a high power rod.

Question 6

In order to assess the B&W evaluation of transients and accidents, provide a complete and consistent set of design values and operating parameters for conditions with and without fuel densification. Where applicable, appropriate information in the Final Safety Evaluation Report, FSAR, for Oconee Unit 1 should be referenced. The information requested should include:

a. Core wide radial power map (see Figure 6-1).

b. Radial local peak for hot assembly (See 6.6).

c. Axial flux shape (see Figures 6-3 and 6-4).

d. Local flux distribution in hot assembly (see Figure 6-2)

e. Mass inlet velocity to hot assembly (with and without one vent valve assumed open). (See 6.4).

f. Loss coefficients for spacer grids and upper and lower end fittings (see 6.4).

Response

Thermal-hydraulic information for the Oconee 1 plant is provided as per requested for fuel densification and without densification. This particular section addresses steady-state conditions. Transient and accident conditions are addressed in answers to other questions.

6.1. Core Operating Conditions

a. The reactor vessel inlet temperatures are given below:

	Nominal	Maximum
100% power	554F*	556F
114% power	550.6F	552.6F

b. The nominal outlet pressure is 2200* psia and the minimum outlet pressure is 2135 psia.

*Values given in the Oconee 1 FSAR.

6.2. Core Design

6.2.1. Fuel Assembly Information

a. There are 177* fuel assemblies in the core.

b. There are 208* fuel rods/assembly with an outside diameter of 0.430* in. and an inside diameter of 0.377* in.

c. There are 16* control rod guide tubes/assembly with dimensions of 0.530* in. OD x 0.016* in. wall thickness and one instrument tube/assembly with dimensions of 0.493* in. OD x 0.441* in. ID.

d. The fuel rod pitch is 0.568*in.

6.2.2. Fuel

a. The undensified active fuel length is 144* in.

b. The active length of the fuel with densification is 141.8 in.

c. The cladding is Zircaloy-4 (cold worked) with a thickness of 0.0265 in.

d. The undensified pellet is 0.370* in. diameter and 0.700 in. long and the densified pellet is [ ] in. in diameter.

e. Unit 1 core 1 is 93.5%* of theoretical density (specified).

6.3. Power Distribution

a. The design core radial power map is shown in Figure 6-1.

b. The maximum fuel assembly local rod power peaking distribution is shown in Figure 6-2.

c. The percentage of the power generated in the fuel is 97.3%*

d. The percentage of power generated in non-fuel regions is 2.7%*.

*Values given in the Oconee 1 FSAR.

6.4. Fluid Flow

a. Coolant Flows and Mass Velocities

	Vent valves closed	One vent valve open
Total reactor vessel coolant flow (lbm/h)	131.32* (10^6)	132.60 (10^6)
Effective core-coolant flow (lbm/h)	124.23* (10^6)	118.52 (10^6)
Average mass velocity at the core inlet (lbm/h-ft^2)	2.53 (10^6)	2.41 (10^6)
Inlet mass velocity to the hot assembly (lbm/h-ft^2)	2.235 (10^6)	2.13 (10^6)

b. The core flow area (effective for heat transfer) is 49.19* ft^2.

c. The loss coefficient for each spacer grid is [ ], for the lower end fitting it is [ ], and for the upper end fitting it is [ ]. These form loss coefficients are based on a flow area of [ ] in.^{2}/assembly.

6.5. Hot Channel Factors

a. The hot channel factor on average pin power (F_q) is 1.011. It is applied on the enthalpy rise for the entire channel. The hot channel factor on local surface heat flux (F''_q) is 1.014. This value is applied locally on the calculated local surface heat flux.

b. Flow area is reduced in the hot channel by a flow area reduction factor (F_A) of 0.98. This value is applied over the entire length of the channel.

c. Flow is reduced in the hot bundle by a flow maldistribution factor which is 95% of the nominal isothermal bundle flow.

*Values given in the Oconee 1 FSAR.

d. The energy mixing coefficient α is 0.02.

6.6. Core Peaking Conditions

The reference design 1.5 cosine symmetrical axial power shape was used as a base case to determine if other axial power shapes in any way magnified the variation in DNBR. A 1.78 radial-local nuclear peaking factor ($F\Delta h$) associated with a 1.5 cosine axial flux shape establish the maximum design condition resulting in the 1.55 DNBR at 114% of 2568 MW(t).

The results indicate that outlet peaks with the spike showed an overall larger degradation in DNBR than the densified 1.5 cosine axial power shape and its associated power spike. B&W utilized a conservative 1.83 ($P/\overline{P}$) outlet axial power shape in conjunction with a 1.49 ($P/\overline{P}$) radial-local peak to maintain the reference design DNBR of 1.55 at 114% of 2568 MW(t).

This set of peaking conditions maximizes the DNBR penalty associated with fuel densification and preempts the necessity of a reevaluation of all DNBR data for the power/imbalance/flow trip system. The penalty determined in this manner was used to modify the power/imbalance/flow system as indicated in section 3.3.4. The 1.83 ($P/\overline{P}$) outlet axial power shape shown in Figure 6-4 is precluded during normal operation as described in the Technical Specifications and as such is not a design criterion.

The 1.5 axial power shape in conjunction with a 1.783 radial shape peaking combination is used for transient and accident analyses. This particular shape results in a more conservative DNBR than any other shape that exists during normal operation. This shape is shown in Figure 6-3.

For LOCA analysis, the design bases axial power shape was a 1.786 peaking 0.5 feet below the core midplane. This shape and peak in conjunction with the calculated radial factor is the most conservative for the LOCA peak clad temperature analysis and could occur momentarily during the period of xenon undershoot following a design basis (100-30-100%) transient. This peaking factor and associated radial are within the

DNBR limiting criteria statement in the previous paragraph. The reason is that in LOCA analysis, the important parameter is peak cladding temperature; whereas for DNBR protection, the important parameter is not only heat flux and flux shape, but also the integration of heat input up the channel and the resultant enthalpy rise.

A graph of power spiking versus axial length is given in Figure 6-5.

The non-densified DNBR at design overpower is 1.55 and with densification and the spike utilizing the 1.83 axial power shape, the DNBR is 1.48. The reduction in overpower limit indicated in section 3.3.4 raised the 1.48 DNBR back to the design 1.55.

6.7. Heat Flux Conditions

The following data is based on the above peaking conditions so that a meaningful comparison between non-densified and densified fuel can be made.

Non-Densified Conditions

a. The heat transfer surface area/fuel pin is 1.351 ft^2.

b. The average heat flux (q_s'') is 171,470 Btu/h-ft^2.

c. The maximum heat flux at the minimum DNBR is 457,774 Btu/h-ft^2.

$[q_s''$ (MDNBR) $- \bar{q}_s''$ x 1.55 x 1.49 x 1.14 x 1.014]

Axial $(P/\bar{P})$ at MDNBR = 1.55

$(P/\bar{P})$ radial-local = 1.49

Max overpower = 114% of 2568 MWt*

Hot channel factor on local surface heat flux = 1.014*

d. The average power density in the core is 83.38 kW/liter, and the average linear heat rate is 5.66 kW/ft.

e. The maximum clad exterior surface temperature at 100% power is 650.0F for a pressure of 2135 psia.

*Values given in the Oconee 1 FSAR.

Densified Conditions

a. The heat transfer surface area/fuel pin is 1.3302 ft^2.

b. The average heat flux is 174,131 Btu/h-ft^2.

c. The maximum heat flux is 521,860 Btu/h-ft^2.

[q''_s (max) = $\bar{q}''_s$ x 1.74 x 1.49 x 1.14 x 1.014]

Axial $(P/\bar{P})$ at MDNBR with power spike = 1.74

$(P/\bar{P})$ radial local = 1.49

Max overpower = 114% of 2568 MWt*

Hot channel factor on local surface heat flux = 1.014*

d. Average volumetric power density in the core is 83.38 kW/liter and the average linear heat rate is 5.74 kW/ft. This assumes all fuel pins have the densified active length which is conservative.

e. The maximum clad exterior surface temperature 100% power is 650F for a pressure of 2135 psia.

*Values given in the Oconee 1 FSAR.

Figure 6-1. Typical Radial Power Distribution

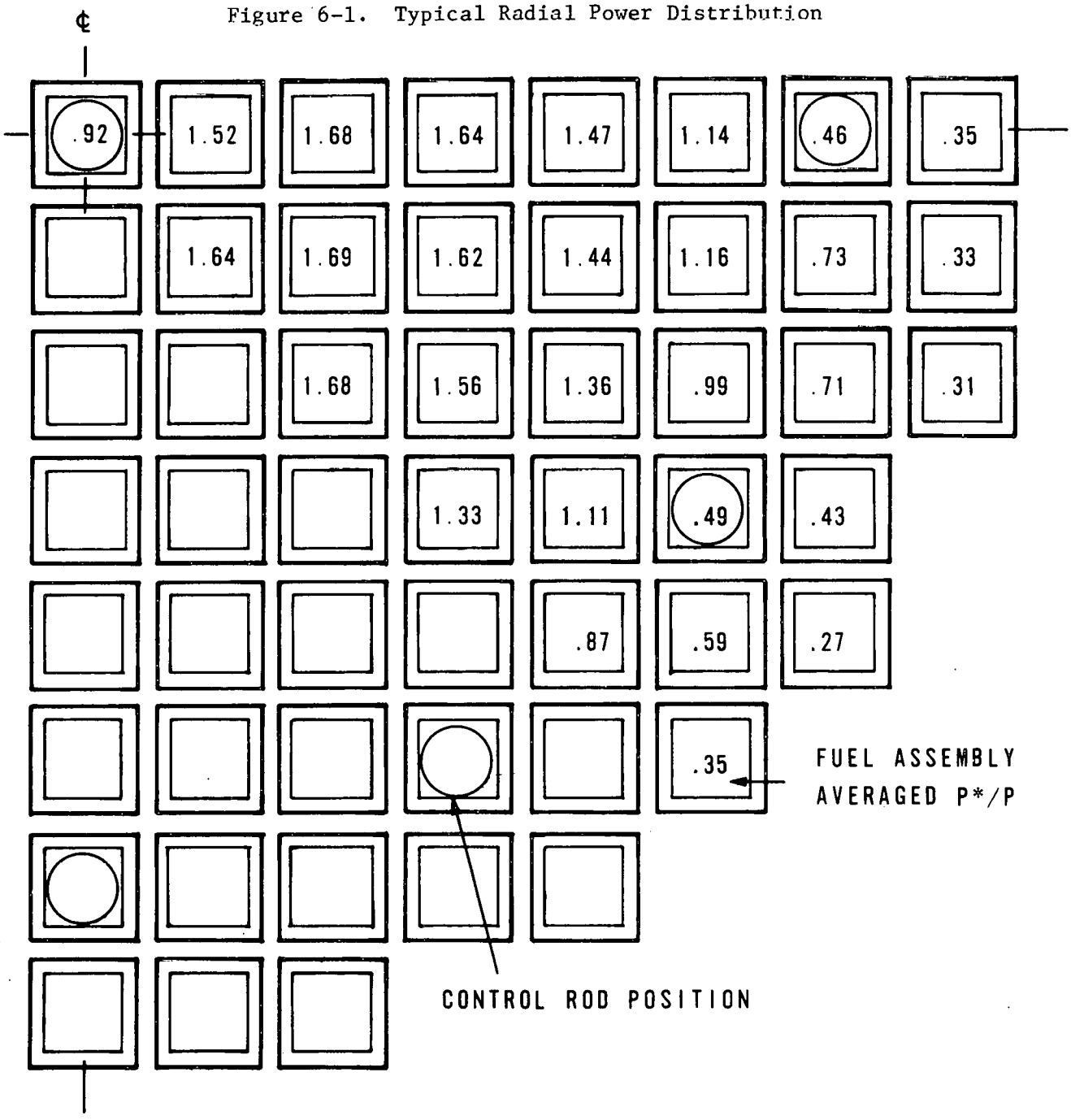

Figure 6-2. Maximum Fuel Rod Power Peaks

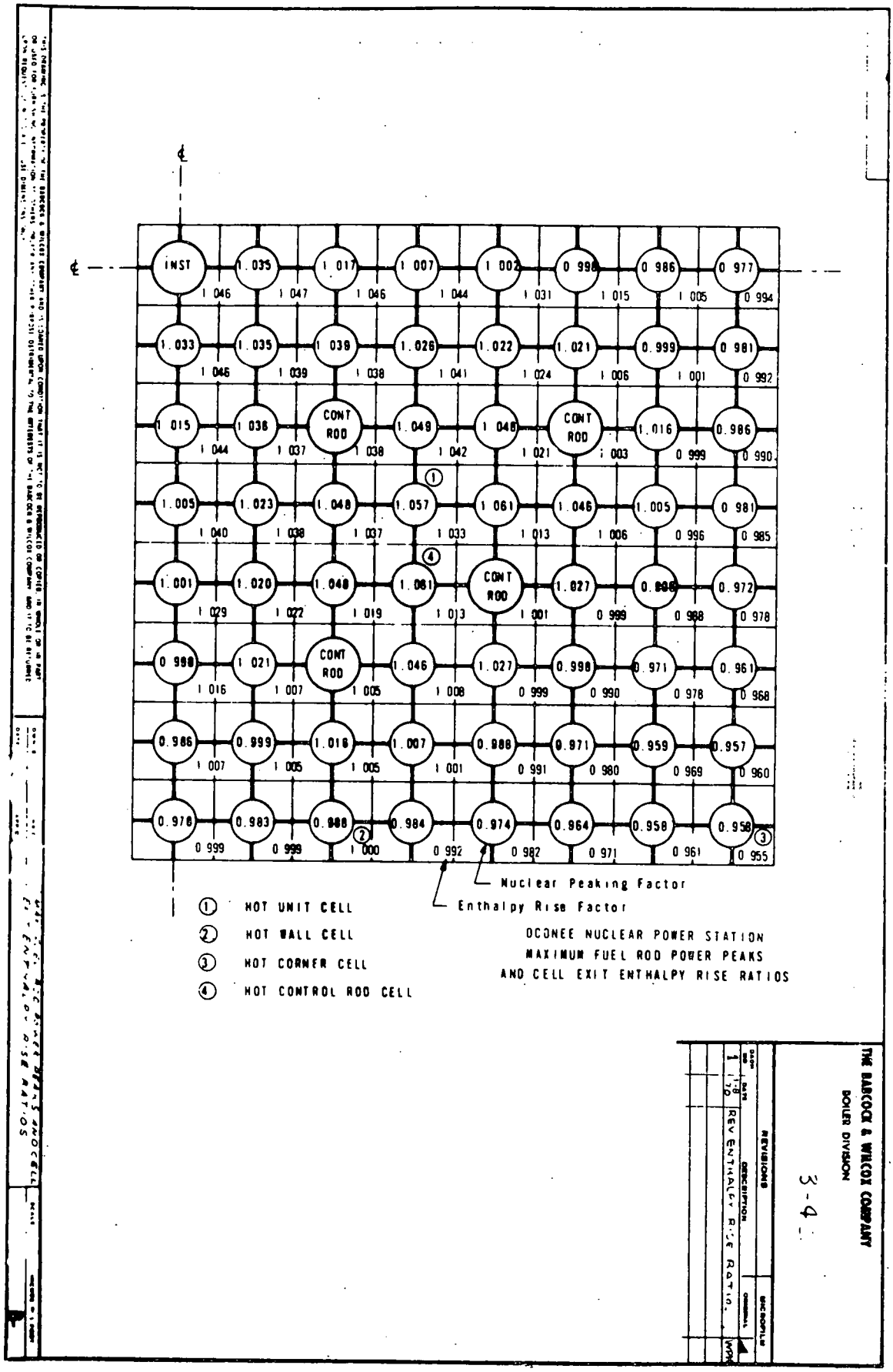

Figure 6-3. The Effects of Fuel Densification on the 1.5 Cosine Reference Design Axial Flux Shape

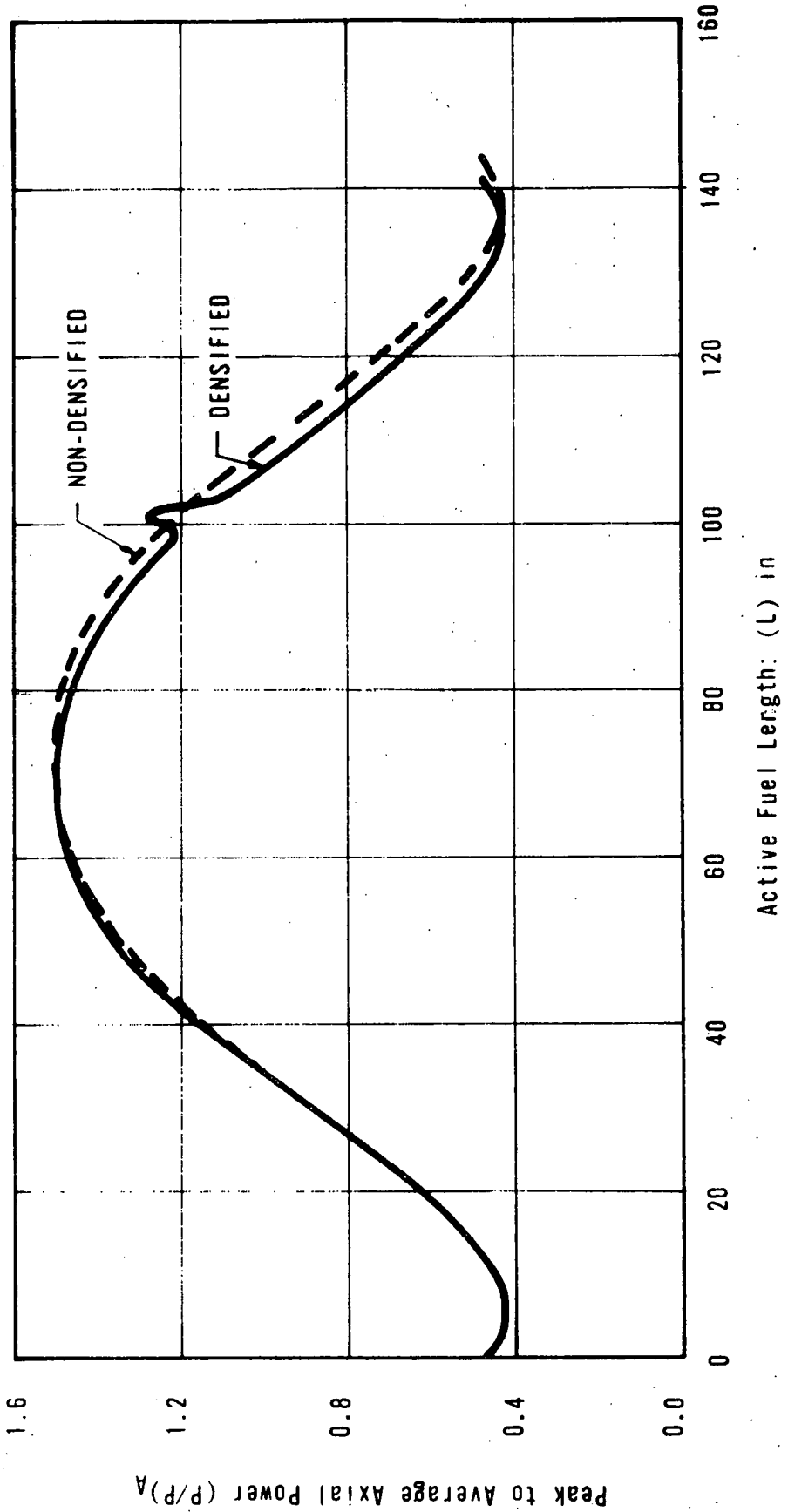

Figure 6-4. The Effects of Densification on the 1.833 $(P/\overline{P})_A$ Axial Flux Shape

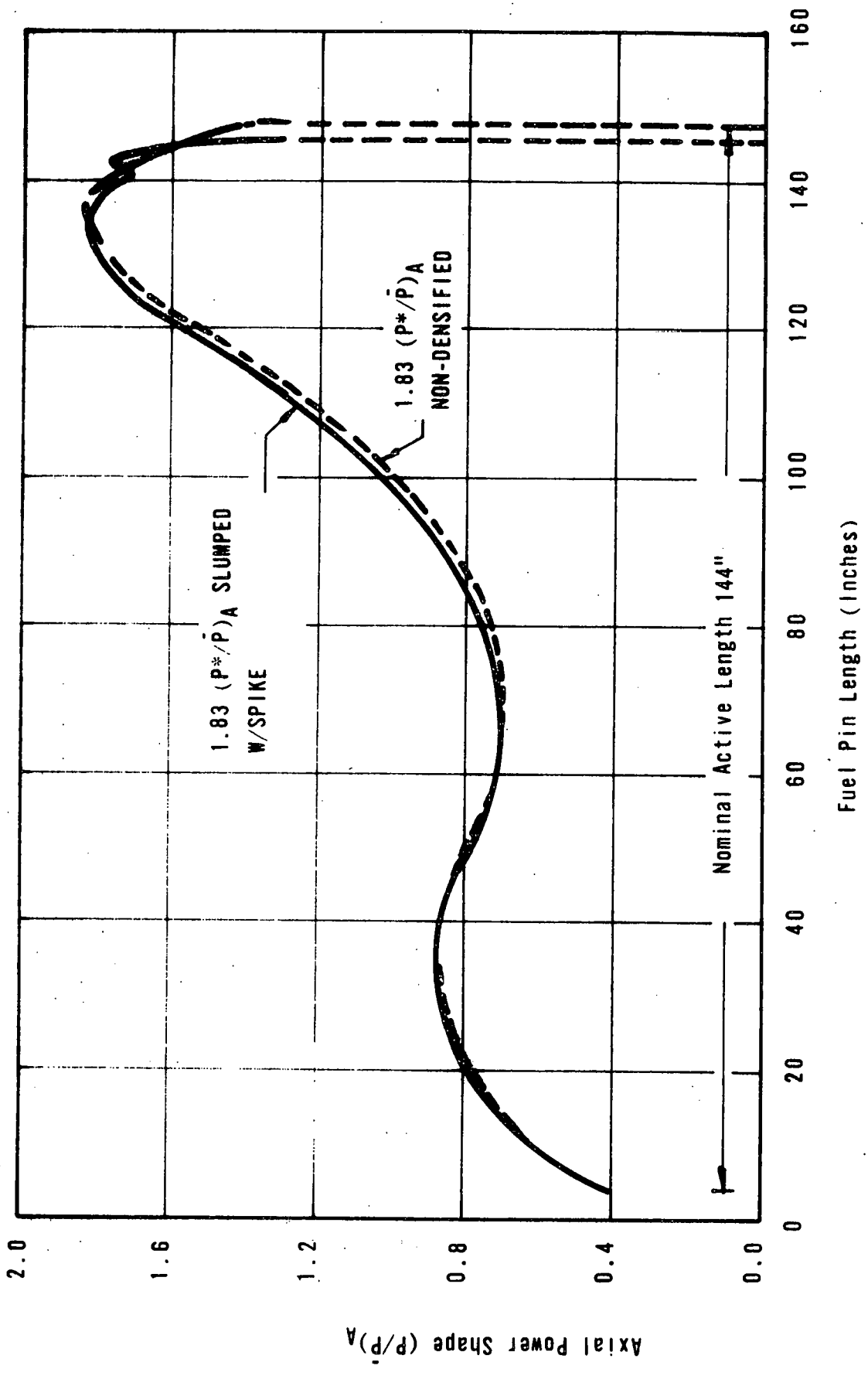

Figure 6-5. Power Spike Factor Vs. Axial Position, Oconee 1

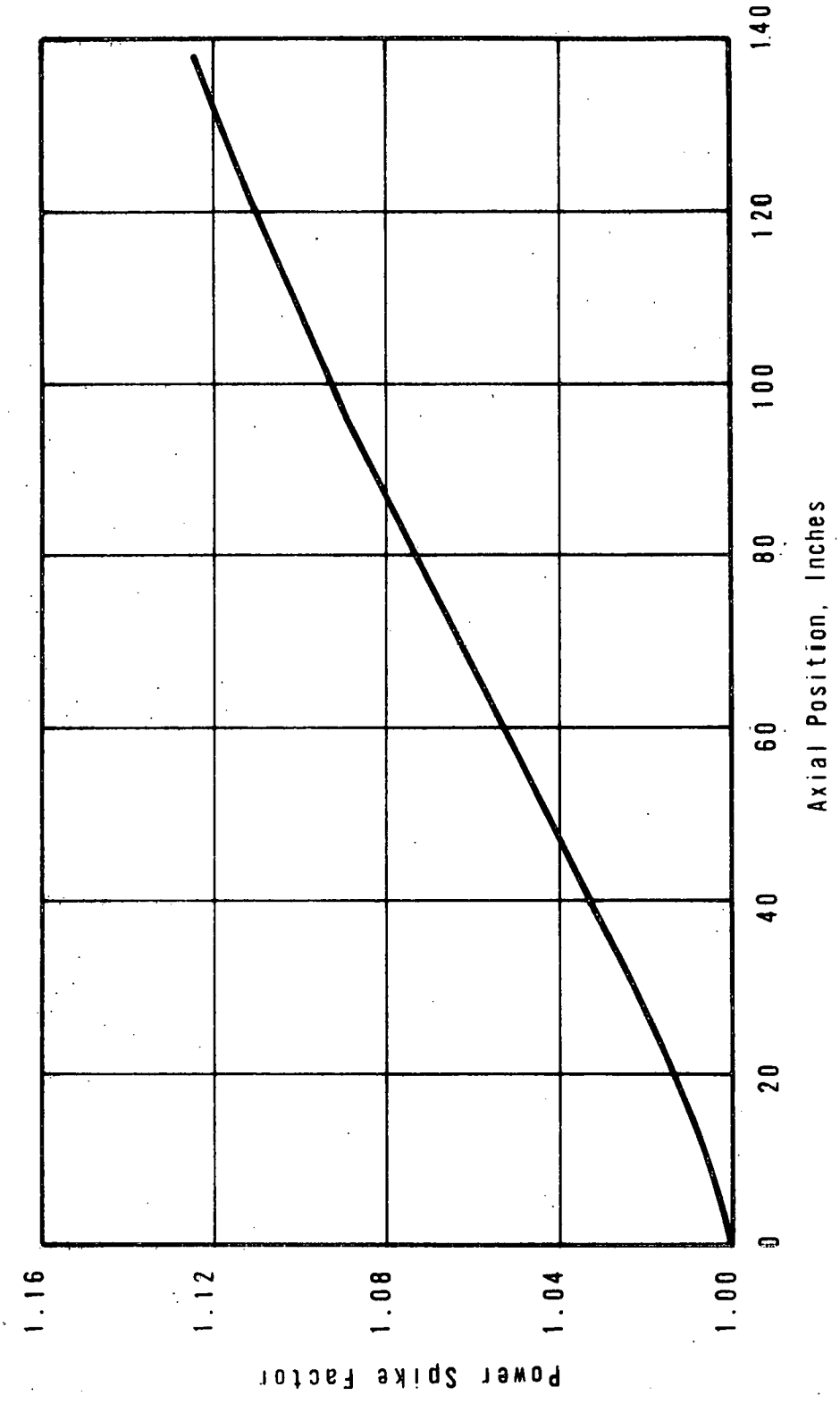

Question 7

Provide an analysis of the (1) loss of flow transient and (2) locked rotor accident for Oconee 1 without and with the assumption of densified fuel. The information provided should include the following:

a. Nuclear power decay.

b. Core coolant flow decay.

c. Core inlet pressure.

d. DNBR vs. time.

e. Peak clad temperature vs. time.

f. Peak fuel centerline temperature vs. time.

g. Average heat flux vs. time.

h. Gap conductance vs. time.

i. Clad to coolant heat transfer coefficient.

Response

1. The loss of flow transient is included in the revised version of BAW-1387.

2. Locked Rotor Accident

An analysis has been performed for the locked rotor accident with the assumptions outlined in Table 10-1 of the rod ejection section. The power distribution was assumed to be a 1.5 cosine with a power spike located at the point of minimum DNBR. Figure 7-1 shows the power, hot channel mass velocity, and calculated heat flux.

The pressure was assumed to be constant at 2135 psig. The initial power level for this accident was 102% of 2568 MW. Trip occurs at about 0.9 seconds after which the power decays to a value of about 20% at about 10 seconds. Figure 7-2 shows the maximum fuel temperature and the film heat transfer coefficient at the point of maximum fuel temperature versus time. The fuel temperature is affected very little since the power rises only slightly. Figure 7-3 shows the maximum cladding temperature, the DNBR and the film coefficient at the point of maximum cladding temperature. It is seen that the DNBR reaches the cri-

terion value of 1.3 at about 1.0 seconds after which the cladding temperature increases to a value of 1300F which occurs 4.5 seconds after the initiation of the accident.

Figure 7-1. Oconee 1 Locked Rotor

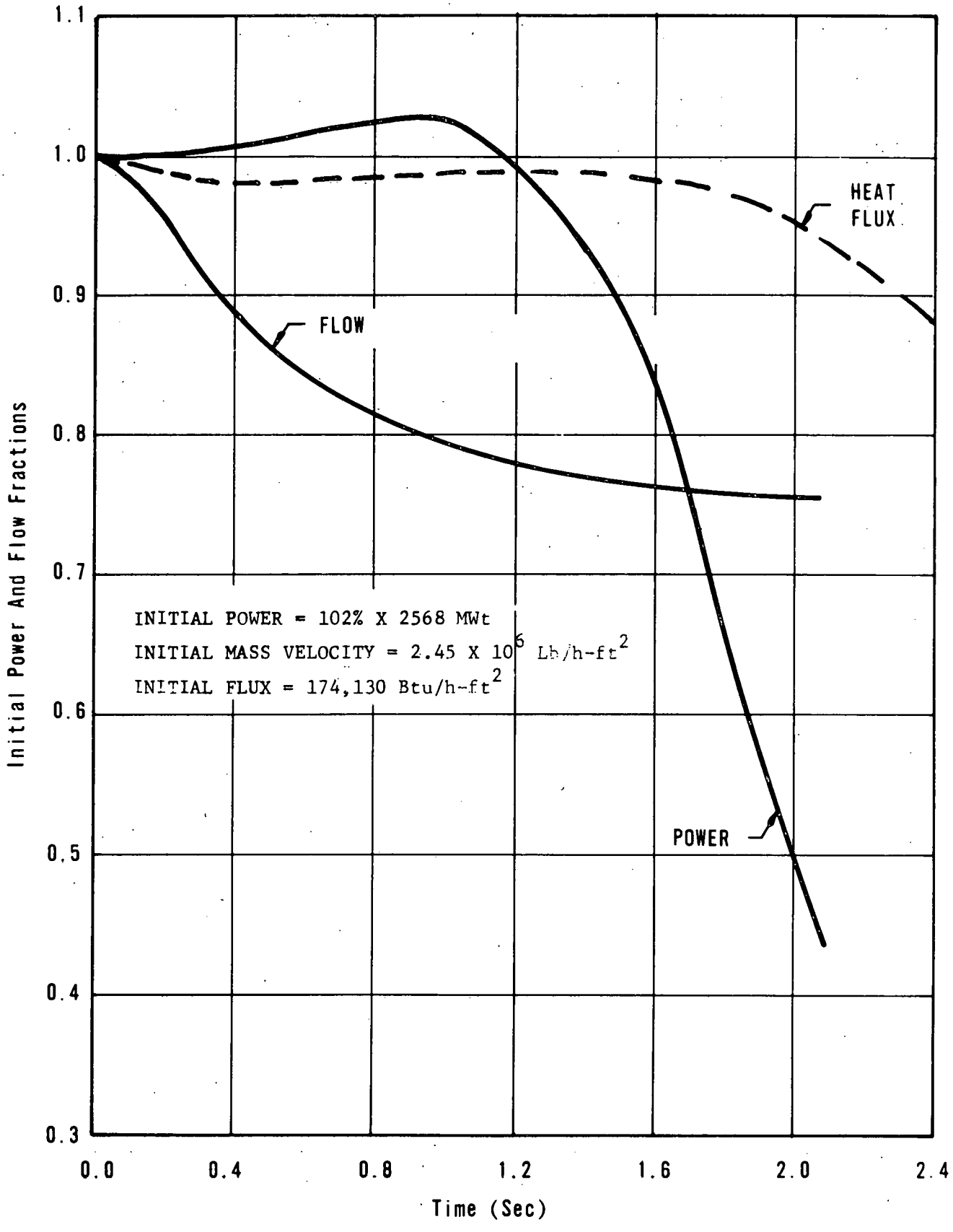

Figure 7-2. Maximum Fuel Temperature and Film Coefficient Versus Time for a Locked Rotor Accident

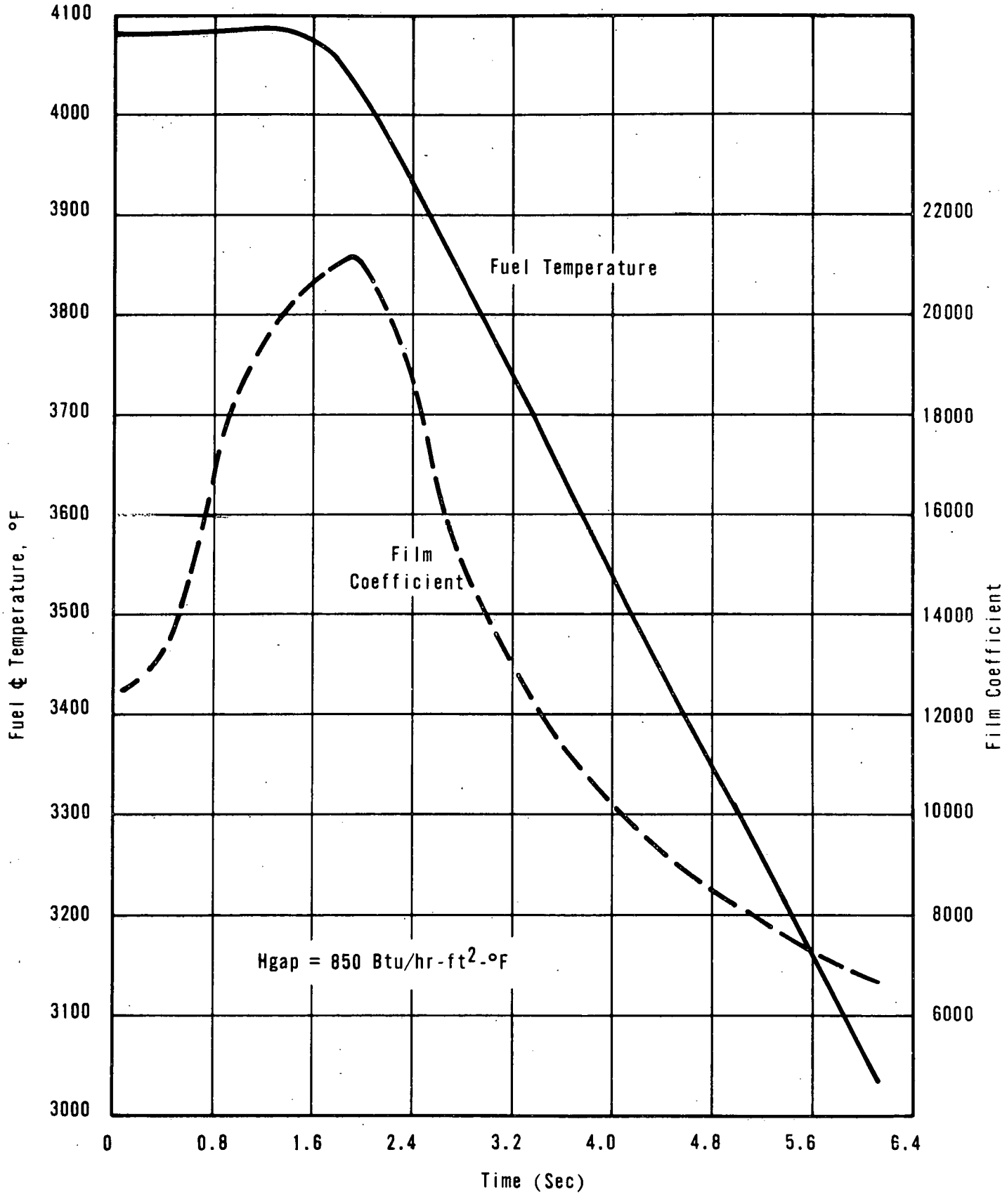

Figure 7-3. Maximum Clad Temperature, DNB Ratio, and Film Coefficient for a Locked Rotor Accident. H_{gap} = 850 Btu/h-ft^2-F

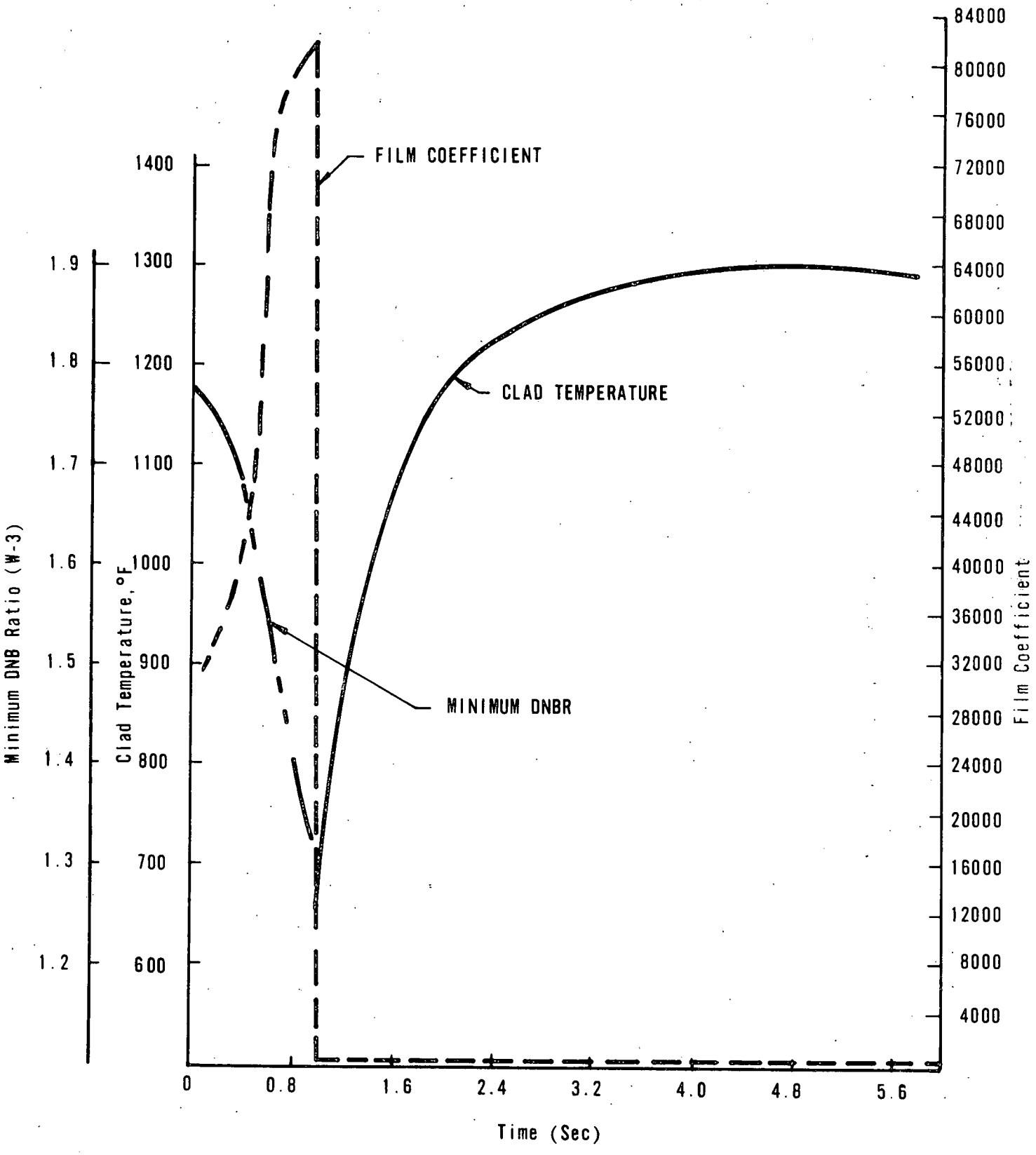

Question 8

Provide the technical bases and supporting analyses for your conclusion that the 8.55 ft^2 split break would remain the worst break for a loss-of-coolant accident within the break spectrum considering the effects of fuel densification. For the worst break provide curves showing:

a. Hot rod axial flux distribution for the steady state condition.

b. Maximum clad temperature and local rod heat transfer coefficient as a function of time.

c. Hot channel flow rate as a function to time.

Response

Densified fuel affects the CRAFT runs only to the extent that higher core average temperatures tend to cause slightly lower core flows during a loss-of-coolant accident. CRAFT is used to represent the average core conditions and the average core temperature experiences a very small change in temperature in going from 92.5% to 96.5% density during densification. The results presented in BAW-10034 were based on an average core temperature equivalent to or greater than those existing with densified fuel. Therefore, all of the CRAFT results presented in BAW-10034 are appropriate for densified fuel.

As the core hydrodynamics and fluid condition presented in BAW-10034 are appropriate for each break size, the break which resulted in the highest cladding temperature without the power spike is the break size which yields the highest temperature when the power spike is included. Since this spike is not dependent on break size, the worst break size presented in BAW-10034 is the worst break size when a power spike is assumed to exist.

The hot rod axial power distribution for a 4-day maneuvering transient, maximum clad temperature during the loss-of-coolant accident, local hot spot heat transfer coefficient, and hot channel mass flux are shown in Figures 8-1 through 8-4.

As stated in this report, the radial peaking factor was varied until the maximum linear power density consistent with the Interim Acceptance Criteria was obtained. The cladding temperature shown in Figure 8-2 is for beginning of life conditions with a maximum linear heat rate of 19.8 kW/ft.

Figure 8-1. Axial Power Shape

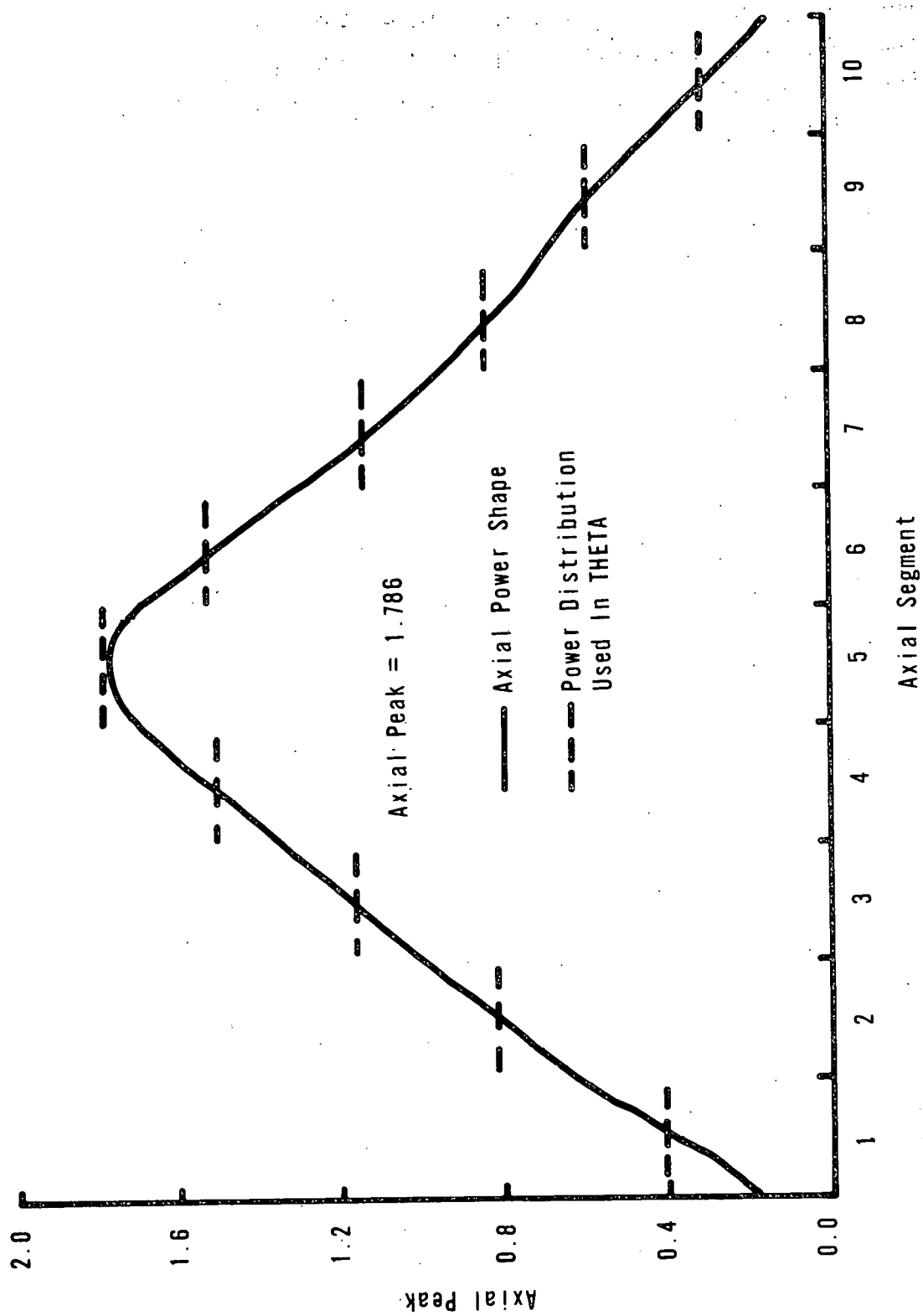

Figure 8-2. Hot Spot Cladding Temperature for 8.55 ft^2 Cold Leg Break

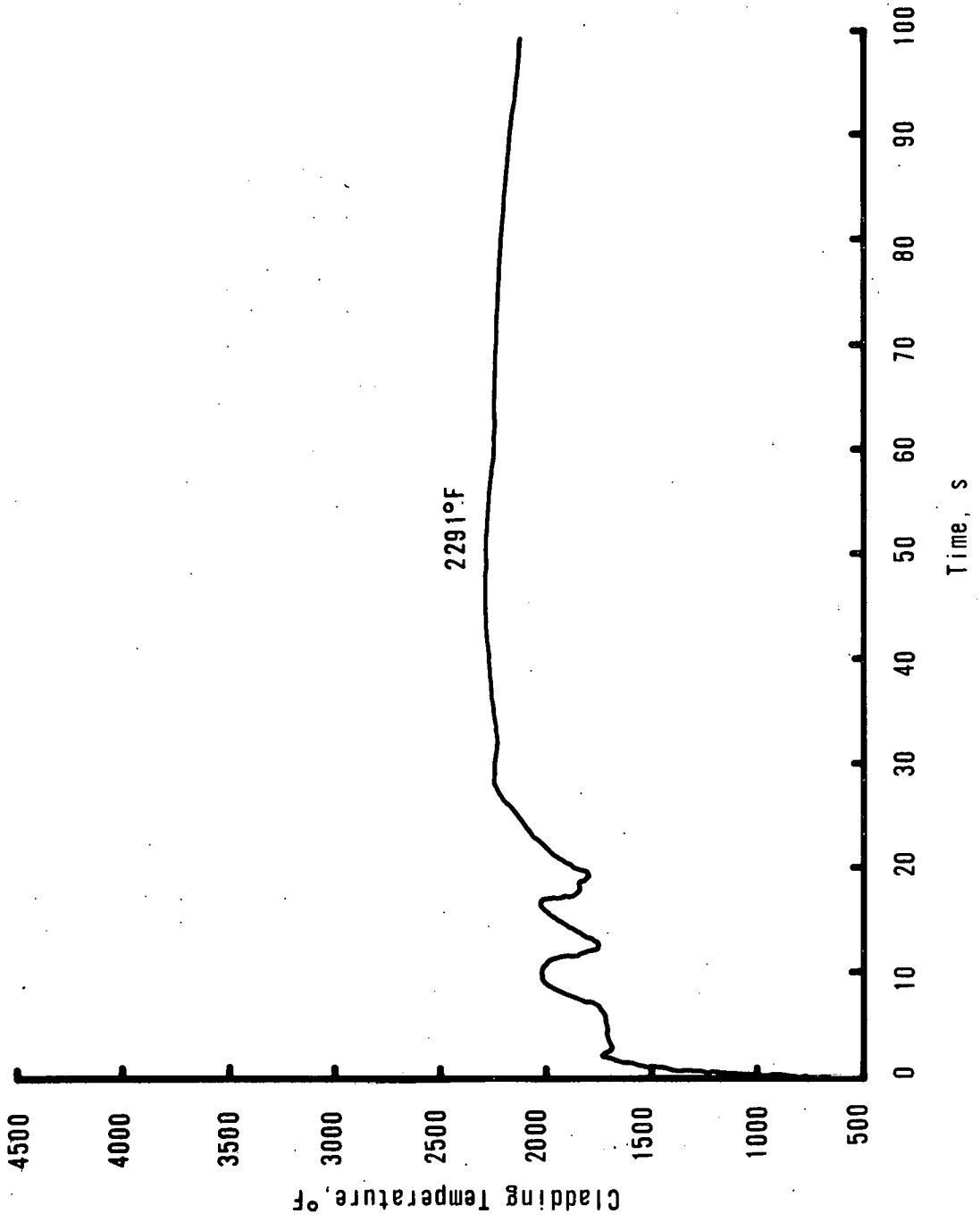

Figure 8-3. Hot Spot Heat Transfer Coefficient for 8.55 ft^2 Cold Leg Break

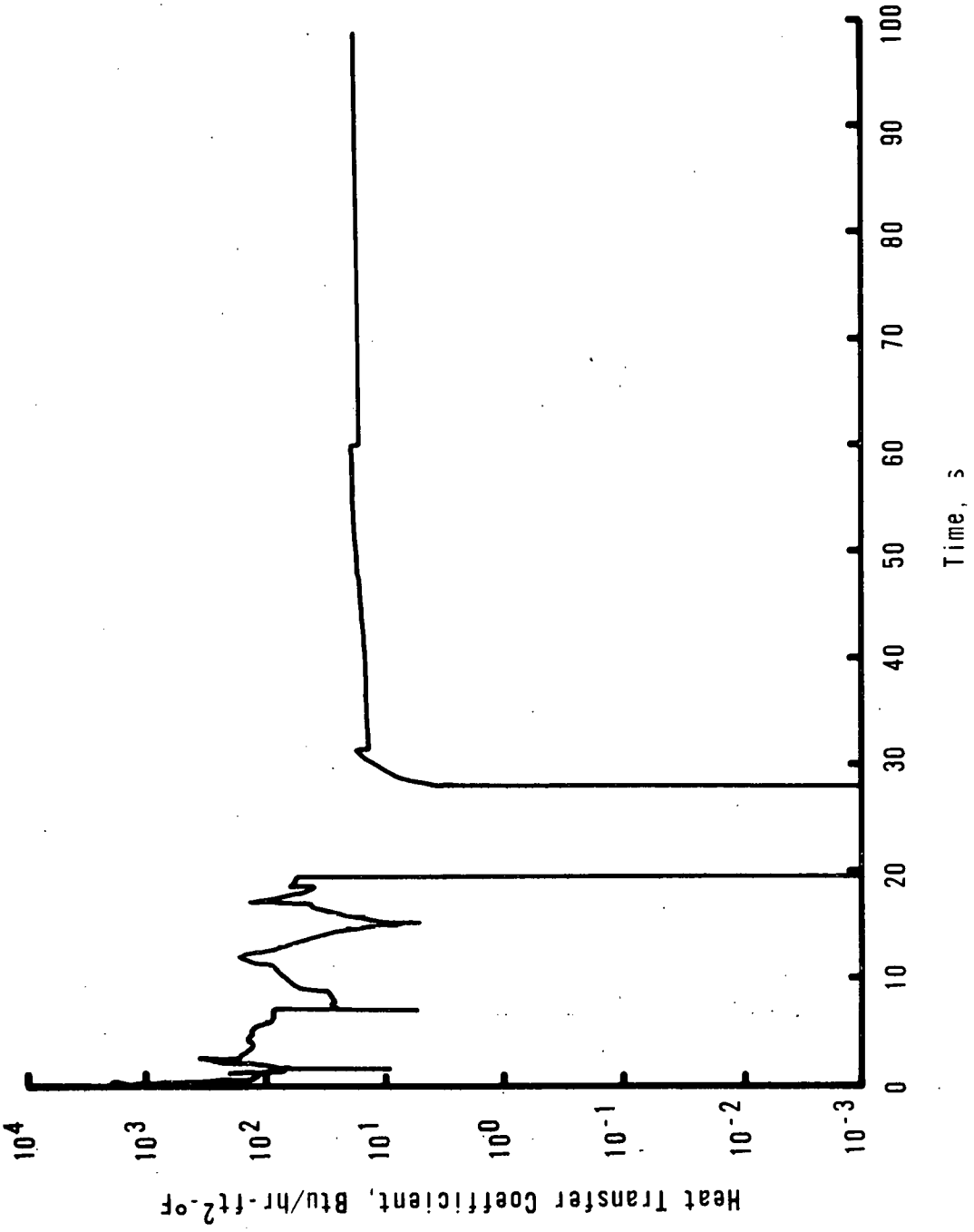

Figure 8-4. Hot Spot Mass Flux for 8.55 ft^2 Cold Leg Break

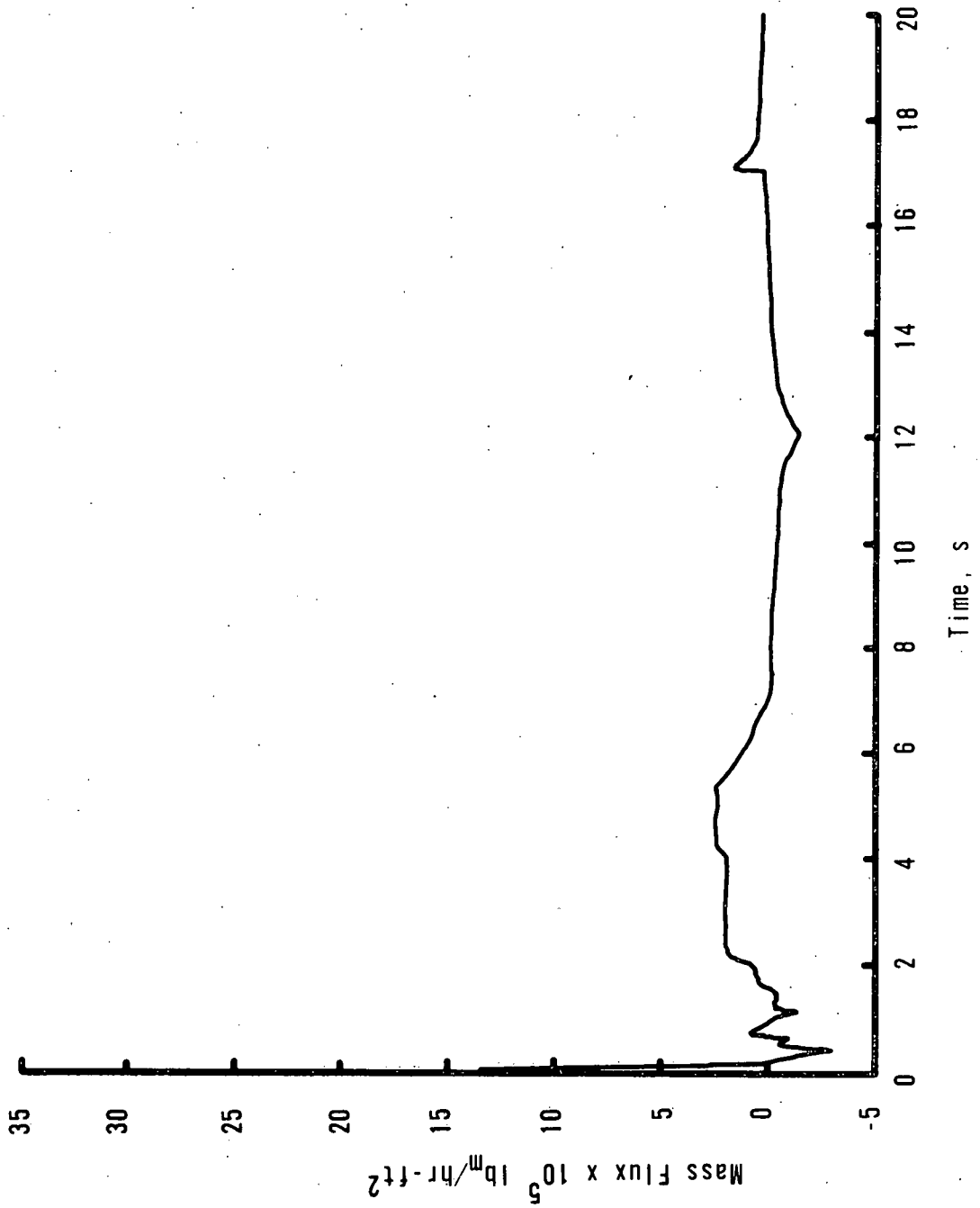

Question 9

Provide details of the assumptions and justification for establishing the design transient 100-30-100% power as the limiting transient. Discuss the axial xenon oscillations that are included in the design transient analysis.

Response

A number of power transients were examined. These included variations in the range, e.g. 100-50-100; and variations in the rate of power recovery. The range of power reduction and the rate of power recovery affect the amount of inserted rod worth prior to power reduction and the rod insertion for xenon undershoot reactivity. The 100-30-100% power transient, with recovery at time of peak xenon at the rate of 10% power/minute, combine the effects of maximum xenon undershoot and maximum rod insertion. Hence, the resulting power peaks from this transient (design power transient) are the most limiting.

The transient xenon effects on power distributions are included in the nuclear analysis. The design power transient studies include: (1) peak xenon buildup during reduced power, (2) rapid xenon depletion and xenon undershoot at full power, and (3) xenon redistribution (axial oscillations). The reactivity effects and axial power shifts caused by transient xenon conditions are controlled by control rod motion and APSR positioning.

Design power transients with the resulting xenon redistributions were examined throughout core lifetime. The hot channel power peaks are shown in Tables 3.3-3 through 3.3-8 of this report.

Question 10

Discuss, in detail, and justify how the effects of fuel densification are included in the rod ejection accident analysis and compare this analysis to the one in the FSAR without fuel densification. In particular, for full power cases, provide the initial peaking factors and their relationship to the power spike model and to design limits in the Technical Specifications for Oconee Unit 1. Describe how the initial pellet density variation has been accounted for if other than by a 2 σ variation on heat flux and gap increase. Provide the peak fuel temperature (average and centerline) and clad temperature as a function of time during the accident. Indicate the number of fuel rods that experience DNB and will fail during the course of the accident.

Response

An analysis of the ejection of the maximum Technical Specification value of rod worth from the core with the effects of fuel densification included has been performed. Due to the small changes in fuel geometry and heat transfer characteristics, it was expected that no changes in the basic kinetic response of the core would occur and the calculations have verified this expectation. The basic assumptions for the calculations of the plant parameters are the same as presented in the Oconee 1 FSAR. Figure 10-1 shows the neutron power and pressure for the ejection of a 0.5%Δk/k control rod at beginning of core life. The neutron power reaches about 320% prior to inward rod motion which occurs at about 0.6 seconds after which the power decays to a value of about 30%. The pressure increases to about 2320 psia due to the increased energy transfer to the coolant then decreases later on in the transient. Figure 10-2 shows the fuel temperature and the heat transfer coefficient at the point of maximum fuel temperature during the transient. It is seen that the maximum temperature occurs about 1.0 second after the peak neutron power and reaches a maximum value of about 4480F which is well below the assumed beginning of life melting point of 5080F. The gap coefficient used was 850 Btu/h-ft^2-F; this value was chosen to match the TAFY steady state fuel temperature and it is conservative with respect to centerline fuel temperature. Table 10-1 shows the important assumptions for the ther-

mal analysis. Figure 10-3 shows the assumed axial power distribution for the thermal analysis.

Figure 10-4 shows the cladding temperature, clad-to-moderator heat transfer coefficient and DNBR as a function of time. The DNBR reached 1.3 at about 0.6 seconds after which the maximum cladding temperature reached was 1305F, a value well below the assumed limit of 2300F.

It can be seen from the plot of film coefficient versus time that the film boiling heat transfer coefficient reaches a low value of 435 Btu/h-ft^2-F at about 0.7 seconds and remains low for several seconds; however, the clad temperature decreases after about 2.5 seconds due to the decreased neutron power.

A parameter study was performed to determine the percentage of fuel pins that would experience a DNBR less than or equal to 1.3. It was determined that for the rod worth analyzed (0.5%Δk/k) about 13% of the pins would exhibit a DNBR of 1.3 or lower.

Table 10-1. Assumptions For Thermal Analysis

Active fuel length, in.	141.8
Pellet diameter, in.	0.365
Cladding thickness, in.	0.0265
Gap coefficient	850 Btu/h-ft^2-F
Film coefficient	Variable*
Hot Channel Factors	
Overall power factor (F_q)	1.0107
Local heat flux factor (F''_q)	1.0137
Flow area reduction factor	0.98
Assumed DNB	1.30
DNB correlation used	W-3
Flow (vent valve open)	95.4% of design flow
Errors	
Tinlet, F	+2
Pressure, psi	-65
Flux trip setpoint,%	+6.5

* After a DNBR of 1.3 the Bishop, Sandburg, Tong correlations were used for both transition and film boiling.

Figure 10-1. Pressure and Neutron Power Vs. Time for Rod Ejection Accident (0.5%Δk/k) for Oconee 1

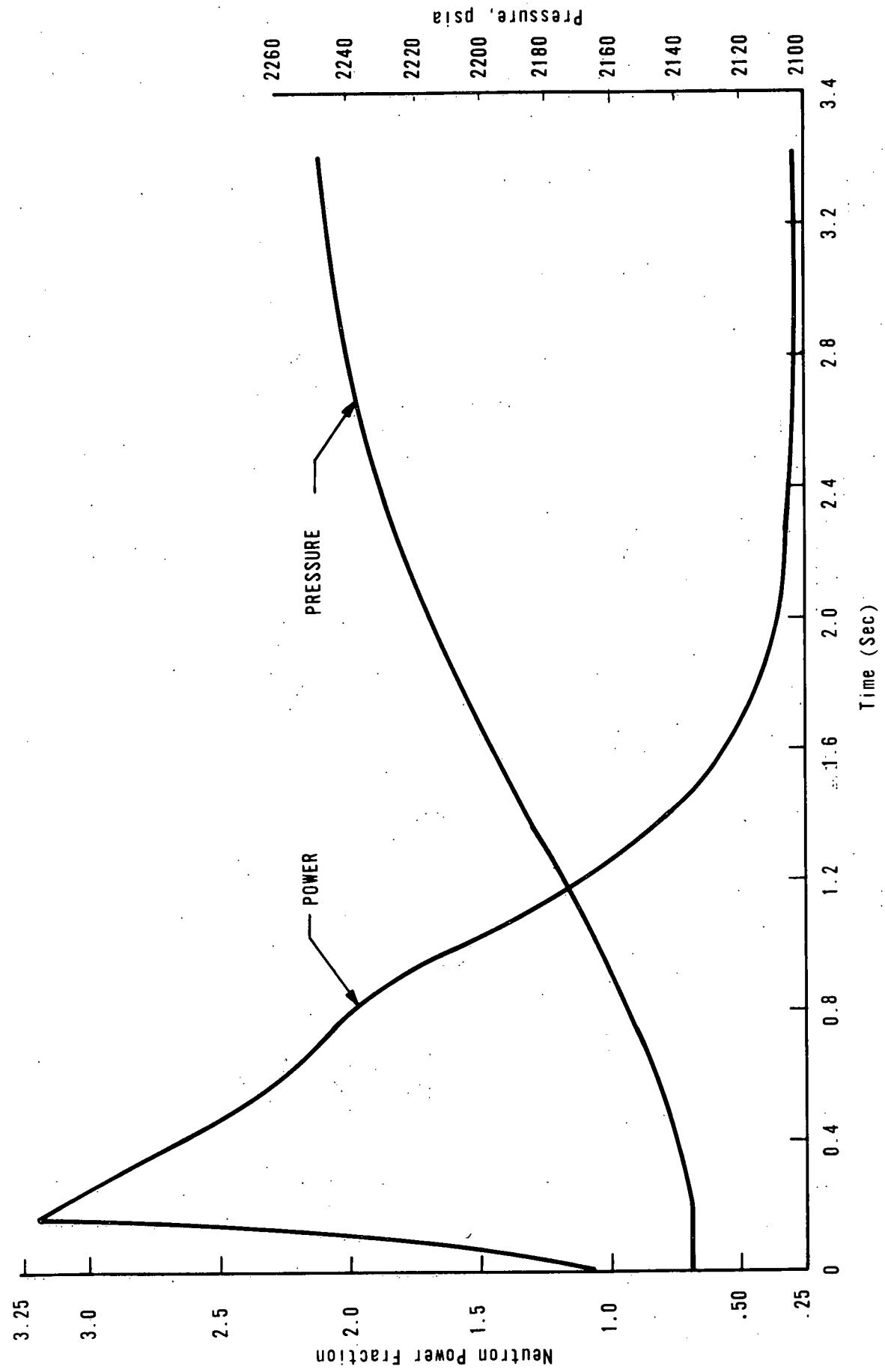

Babcock & Wilcox

Figure 10-2. Maximum Fuel Temp Vs. Time and Water Clad Heat Transfer Coefficient Vs. Time (at Max Fuel Temp) for Rod Ejection Accident Max Design Conditions

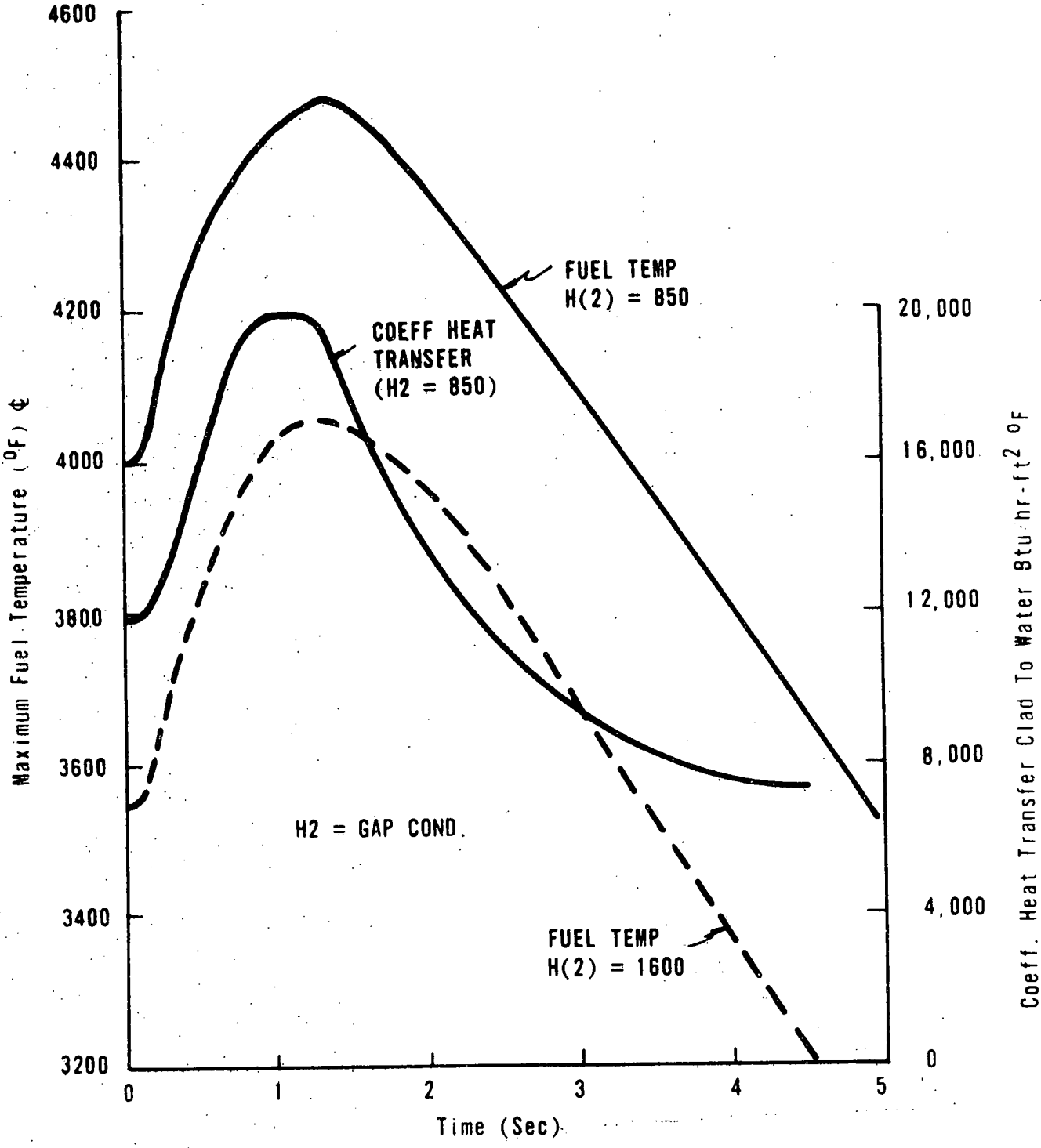

Figure 10-3. Slumped and Spiked Axial Flux - Oconee 1

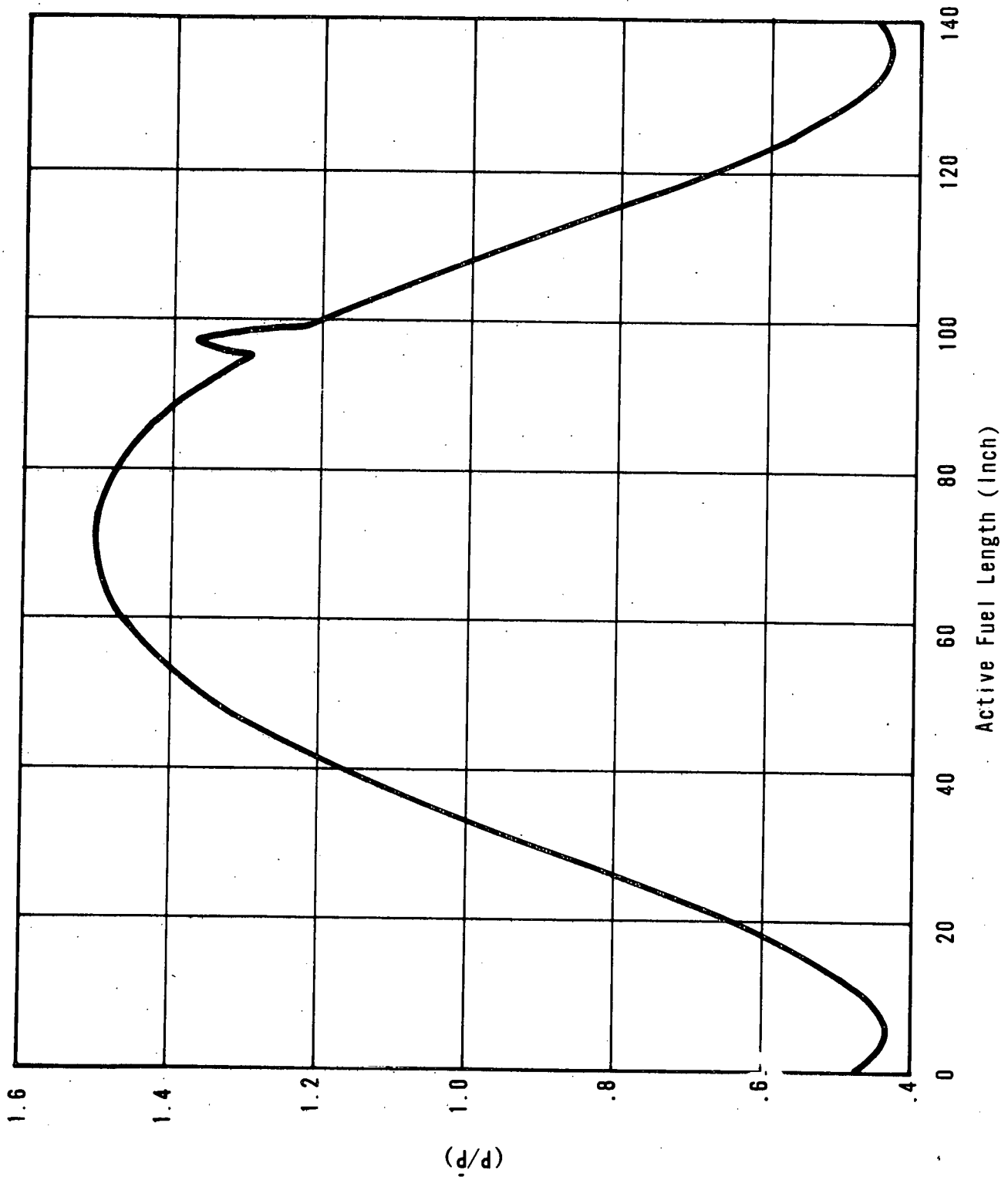

Figure 10-4. Clad Temp and Clad-Water Heat Transfer Coefficient (at Max Cladding Temp) for Rod Ejection Accident, Oconee 1

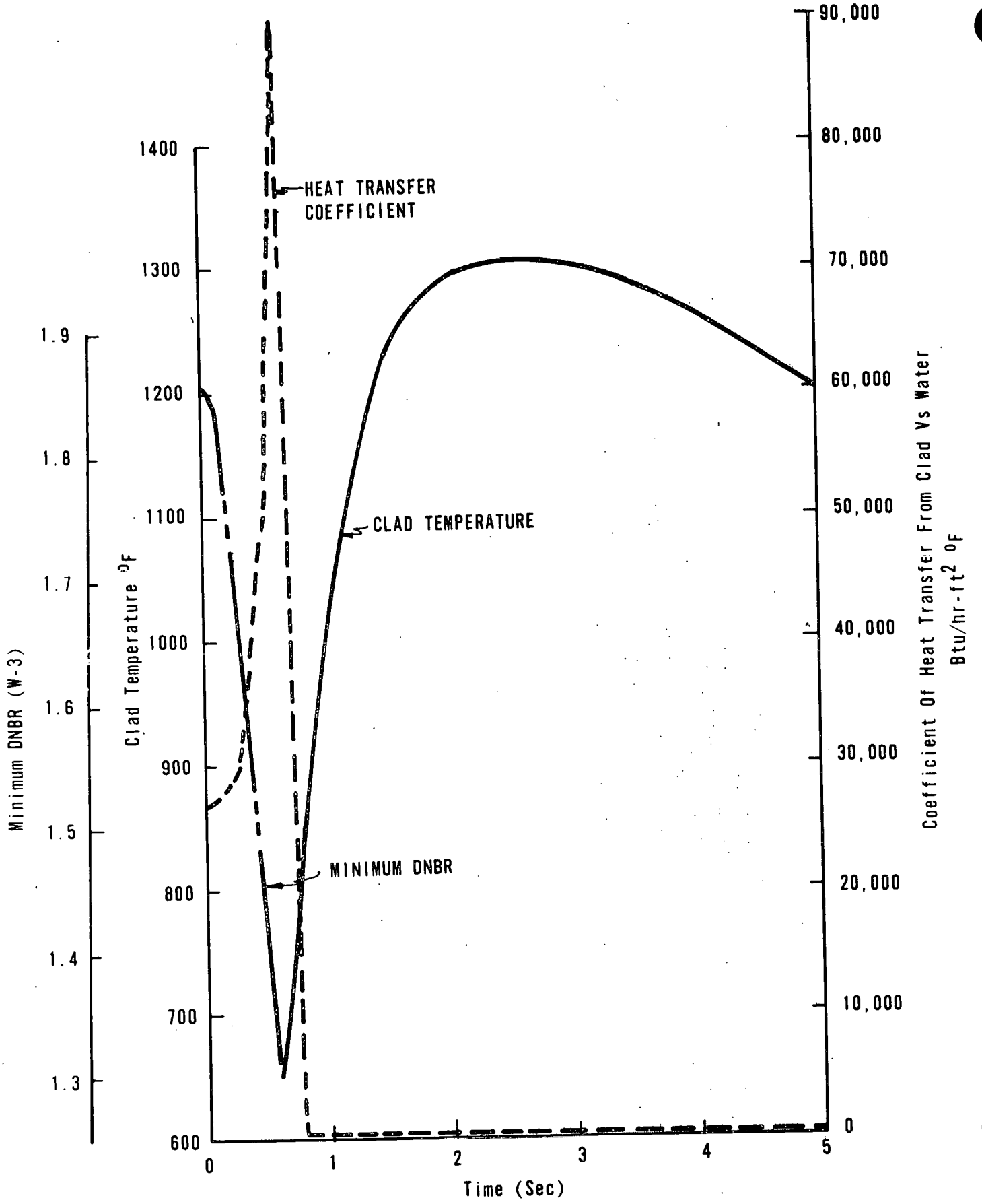

Babcock & Wilcox